

Nucleobase catalysts for the enzymatic activation of 8-oxoguanine DNA glycosylase 1

Emily C. Hank,^{1, #} Nicholas D. D'Arcy-Evans,¹ Emma Rose Scaletti,² Carlos Benítez-Buelga,^{3, 4} Olov Wallner,¹ Florian Ortis,¹ Kaixin Zhou,¹ Liuzhen Meng,¹ Alicia del Prado,⁵ Patricia Calvo,⁵ Ingrid Almlöf,¹ Elisée Wiita,¹ Karen Nierlin,¹ Sara Košenina,² Andreas Krämer,⁶ Alice Eddershaw,^{1, 10} Mario Kehler,¹ Maeve Long,¹ Ann-Sofie Jemth,¹ Holly Dawson,¹ Josephine Stewart,¹ Adam Dickey,¹ Mikhael E. Astorga,¹ Marek Varga,¹ Evert J. Homan,¹ Martin Scobie,¹ Stefan Knapp,⁶ Leandro Sastre,^{3, 7} Pål Stenmark,^{2, 8} Miguel de Vega,⁵ Thomas Helleday,^{1, 9} Maurice Michel^{1, 10 *}

AUTHOR ADDRESS

1 Science for Life Laboratory, Department of Oncology-Pathology, Karolinska Institutet, Stockholm, Sweden

2 Department of Biochemistry and Biophysics, Stockholm University, Stockholm, Sweden

3 Instituto de Investigaciones Biomédicas Alberto Sols CSIC/UAM, Madrid, Spain

4 Molecular Genetics Unit, Instituto de Investigación de Enfermedades Raras (IER), Instituto de Salud Carlos III (ISCIII), Madrid, Spain.

5 Centro de Biología Molecular 'Severo Ochoa' (CSIC-UAM), Madrid, Spain

6 Institute of Pharmaceutical Chemistry & Structural Genomics Consortium (SGC), Goethe University, Frankfurt, Germany

7 Centro de Investigación Biomédica en Red de Enfermedades Raras (CIBERER). Instituto de Salud Carlos III. C., Madrid, Spain

8 Department of Experimental Medical Science, Lund University, Lund, Sweden

9 Weston Park Cancer Centre and Division of Clinical Medicine, School of Medicine and Population Health, University of Sheffield, Sheffield, United Kingdom

10 Center for Molecular Medicine, Karolinska Institute and Karolinska Hospital, Stockholm, Sweden

Current Address: Department of Pharmacy, Ludwig-Maximilians-Universität Munich, Germany

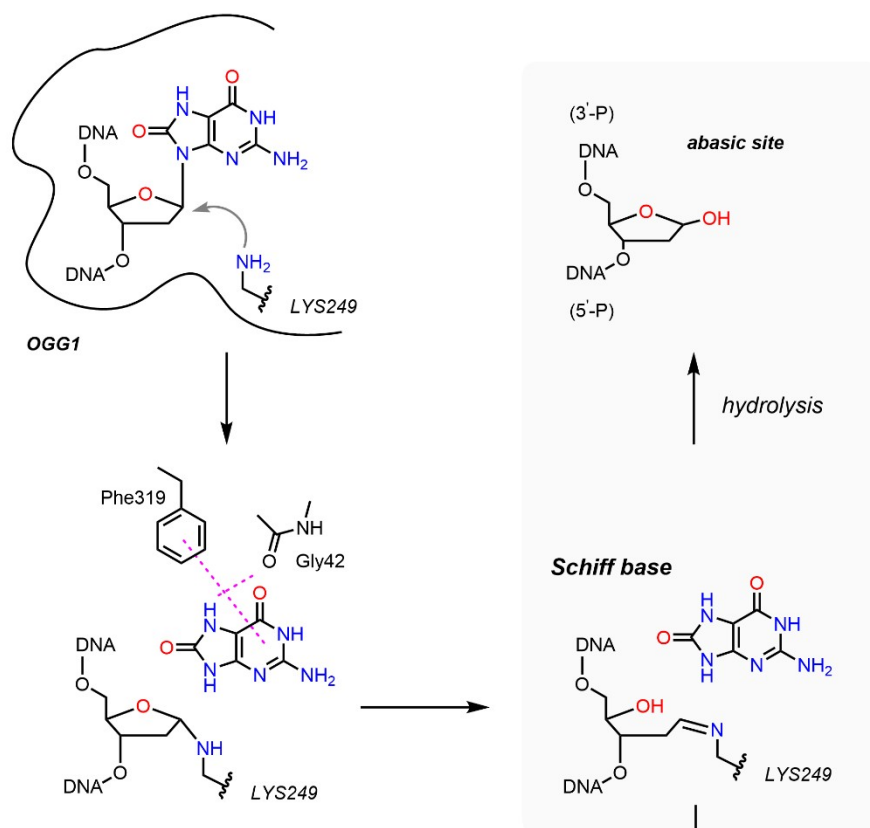
Supporting Data

Scheme S1: Possible mode of action of OGG1 biochemistry:

Glycosylase activity: OGG1 searches DNA for 8oxoG residues. The enzyme establishes additional affinity to the substrate through H-bonding with Gly42 and π -stacking with Phe319. Lys249 attacks the anomeric position and removes the oxidized base, forming a Schiff Base in the process. The Schiff Base is a masked abasic site which is the reaction product of OGG1's glycosylase activity. OGG1 requires APE1 to be removed from the Schiff Base, a process which requires some time in cells. OGG1's roles in transcription are mediated by the stability of this complex.

Lyase activity: 8oxoG may catalyze a low number of incision events by proton abstraction on the α -carbon of the Schiff Base, an event followed by elimination of the 3' DNA strand, called β -elimination, resulting in formation of 3'-phosphate unsaturated aldehyde (3'-PUA). Due to the limited physicochemical properties of 8oxoG, incision events following this abstraction are slow *in vitro* and absent in cells. Previously, TH10785 was developed which exploits identical amino acid interactions and has a suitable pKa to rapidly abstract protons from the Schiff Base. The result is a rapid accumulation of 3'-PUA and further δ -elimination, yielding both free 3'- and 5'-phosphates of the now detached DNA strand. This study examines the chemical space of nucleobases capable of promoting either β - or β,δ -eliminations.

Glycosylase activity



Lyase activity

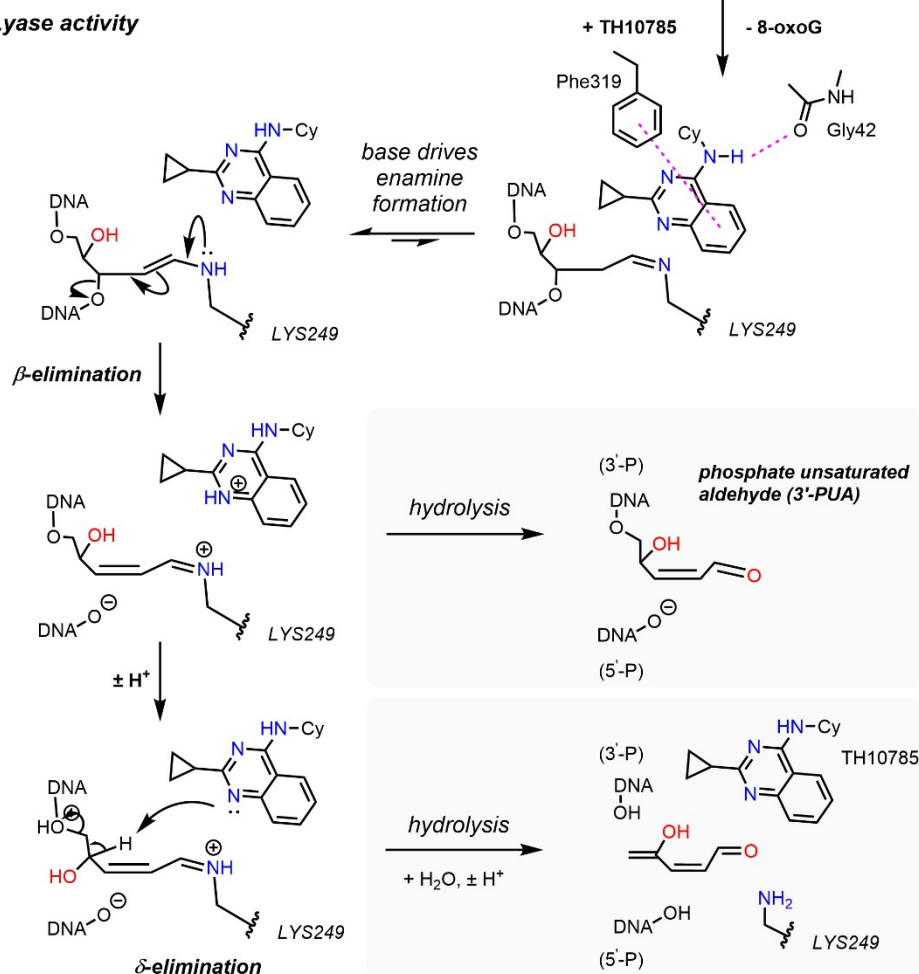
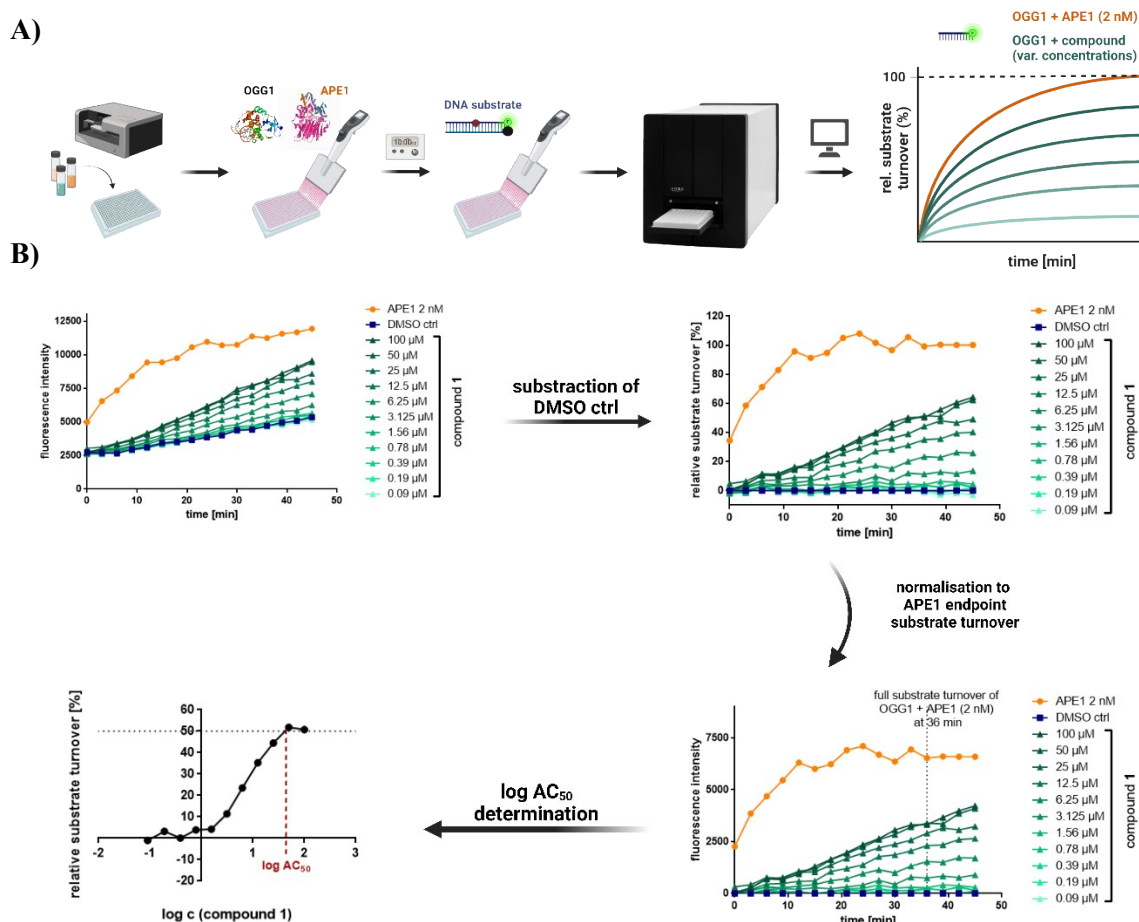


Figure S1: Biochemical assay and AC₅₀ calculation scheme and visualised raw data of the focused screen. A) Workflow of the biochemical assay as described in Materials and Methods. After the kinetic readout, fluorescence values for the DMSO control are subtracted from the fluorescence values of each compound concentration and the data is normalised to the full turnover fluorescence in the coupled APE (2 nM) control. Created in BioRender.com. B) Example of the raw data processing and AC₅₀ calculation for compound **1** (structure depicted in Figure 1). Created in BioRender.com. C) Assay data of the screened compounds at 100 µM concentration presented as fluorescence intensity after background (DMSO control) subtraction, data at t = 0 min (start) and t = 36 min (endpoint, full turnover in the APE control), data are the mean ± S.E.M., *n* = 2. Structures of the compounds depicted in Figure 1, Table 1 and Figure S2.



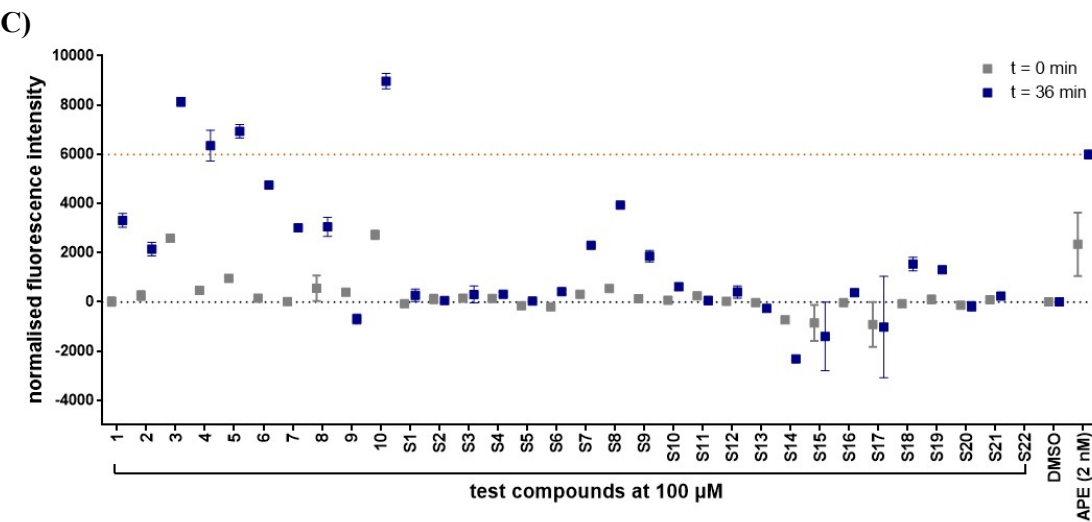


Figure S2: Summary of a focused screen to identify OGG1 organocatalytic switches. Assay performed as described in Material and Method section. Compounds were screened at 100 μ M.

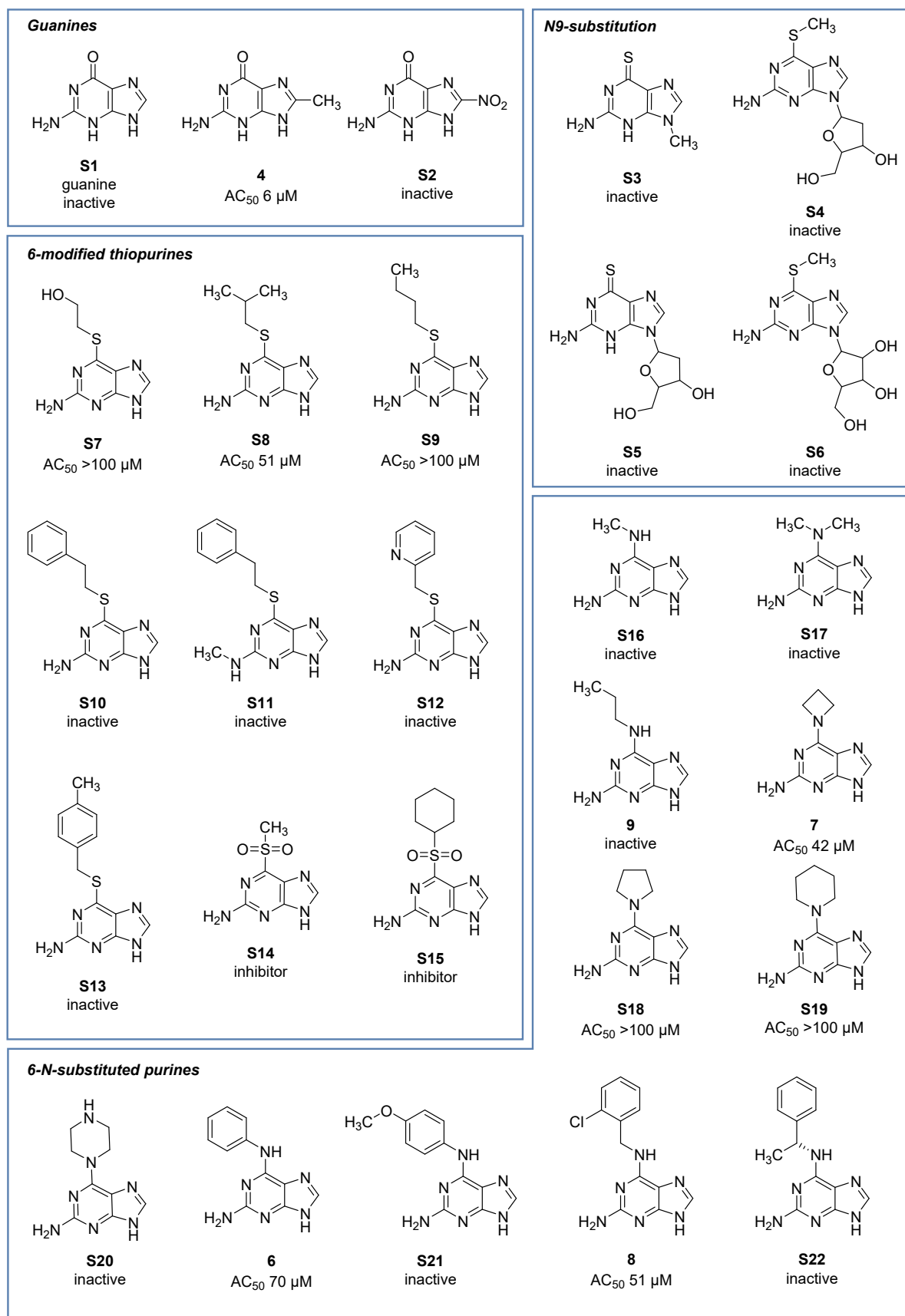
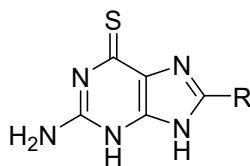


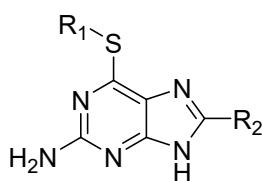
Table S1: Thioguanines are potent OGG1 organocatalytic switches. A) Investigation of effect of 8-substitution, B) Investigation of effect of combinations of 6- and 8-substitution; AC₅₀ in μM , CI95% confidence interval 95% in μM . Assay Details in Methods and Material.

A)



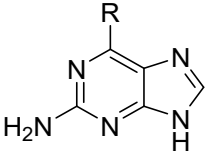
#	R	AC ₅₀ (CI 95)
1	-H	>100
3	-Me	0.32 (0.27 - 0.39)
10	-CH ₂ CH ₂ CH ₃	0.55 (0.26 - 1.2)
S23	-NH ₂	1.1 (0.68 - 1.9)
S24	-SMe	0.47 (0.19 - 1.2)
S25	-CH ₂ NH ₂	21.1 (17.6 – 25.3)
S26	-CH ₂ NHBoc	inactive

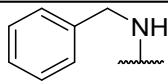
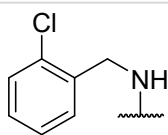
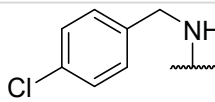
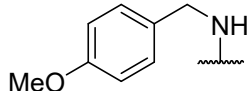
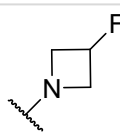
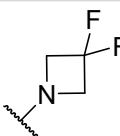
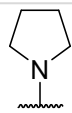
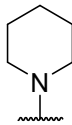
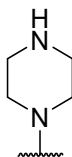
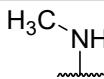
B)



#	R ¹	R ²	AC ₅₀ (CI 95)
S27	Me	H	>100
S28	-CH ₂ CH ₃	H	12.8 (11.2 – 14.8)
S29	<i>i</i> -Pr	H	14.3 (9.6 – 21.2)
S30	-CH ₂ CH ₂ CH ₃	H	20.5 (12.5 – 33.6)
S31	-CH ₂ CH=CH ₂	H	23.9 (15.7 – 36.4)
S32	Me, <i>N</i> -9 Me	H	Inactive
S33	Me	Me	3.1 (2.3 – 4.1)
S34	Me	NH ₂	>100
S35	Me	-SMe	7.3 (3.6 – 15.2)
S14	-SO ₂ Me	H	Inactive
S15	-SO ₂ Cy	H	Inactive
S36	-SCy	H	>100
S37		H	>100
S38	-SPh	H	Inactive
S39	(3,4-Dichloro)thiophenyl	H	>100

Table S2: Investigation of 6-amino purine analogues. AC₅₀ in μM , CI95 confidence interval 95% in μM . Assay Details in Methods and Material.



#	R	AC ₅₀ (CI 95)
S40		> 100
8		>100
S41		>100
S21		>100
S42		59.2 (53.6 – 65.4)
S43		29.1 (13.2 – 64.1)
S18		> 100
S19		>100
S20		inactive
S16		inactive

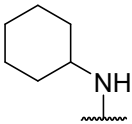
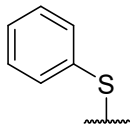
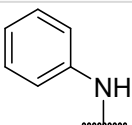
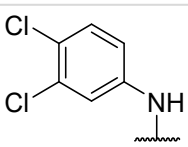
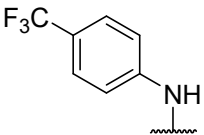
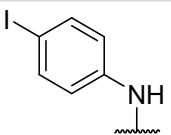
13		>100
S38		inactive
6		62.2 (44.1 – 87.6)
11		12.5*
S44		inactive
S45		> 100

Figure S3: Fluorescence readout of the biochemical assay for OGG1 activation with compound 11 in different concentrations: The compound follows a bell-shaped activation profile and does not reach the half-maximal substrate turnover of APE1 in order to determine an AC₅₀. Assay performed as described in Material and Method section. Structure of compound **11** depicted in Table 1.

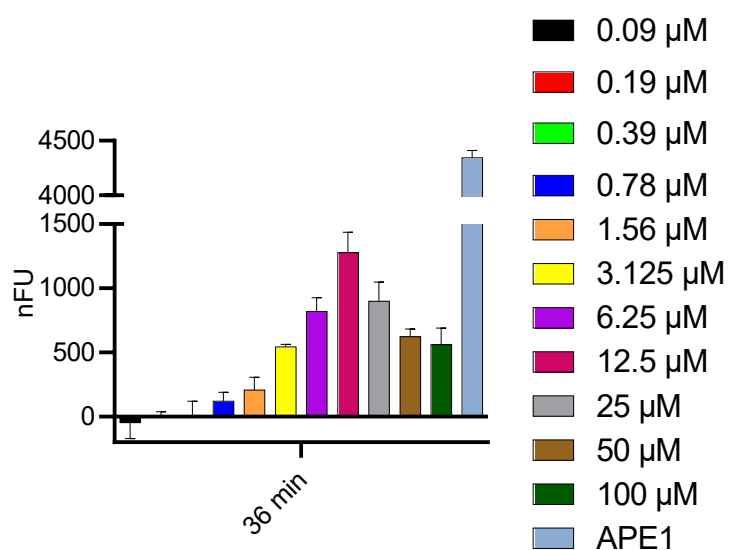
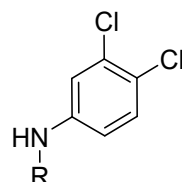


Table S3. 6-substituted pyrazolo-[3,4-*d*]-pyrimidine are organocatalytic switches of OGG1: A) Scaffolds other than guanine are investigated and reveal a fused pyrazolo ring to enhance potency of both guanine and adenine analogues; B) Matched-pair analysis of guanine and pyrazolo-[3,4-*d*]-pyrimidine derivatives confirm the superior performance of the latter scaffold; AC₅₀ in μM , CI95 confidence interval 95% in μM ; * compound only reaches AC₃₅ following a bell-shape activity curve.

A)



	R	AC ₅₀ (CI 95)
11		12.5*
12		13.1 (2.3 – 75.1)
S46		inactive
S47		6.2 (4.7 – 8.2)
S48		inactive
S49		inactive

B)

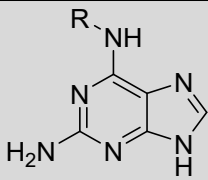
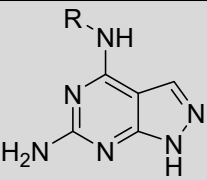
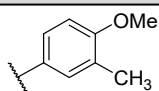
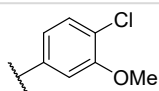
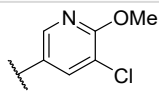
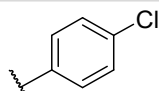
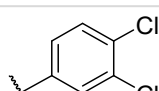
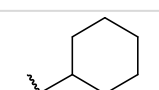
				
R	#	AC₅₀ (CI 95)	#	AC₅₀ (CI 95)
	S50	>100	S51	14.0 (11.4 – 17.3)
	S52	>100	S53	40.0 (23.7 – 67.5)
	S54	autofluorescence	15	28.2 (10.0–79.8)
	S55	>100	S56	5.4 (1.6 – 18.5)
	11	12.5*	12	13.1 (2.3-75.1)
	13	>100	14	11.7 (5.5 – 24.9)

Figure S4. The recognition of ligands by mouse OGG1: Amino acids contributing to ligand binding are depicted as sticks; C atoms are coloured blue, O atoms red, N atoms dark blue and S atoms gold. The ligands **14** (A), **3** (B), **10** (C) and **15** (D) are presented as stick models; C atoms coloured yellow, N atoms coloured dark blue, O atoms coloured red, Cl atoms coloured green and S atoms coloured gold. Hydrogen bond interactions are shown as dashed lines. Water molecules are shown as red spheres. The 2Fo-Fc electron density maps around the ligands are contoured at 1.0 σ (blue) and the Fo-Fc electron density maps are contoured at - 3.5 σ (red) and +3.5 σ (green). Structures of compounds **3**, **10**, **14** and **15** depicted in Table 1.

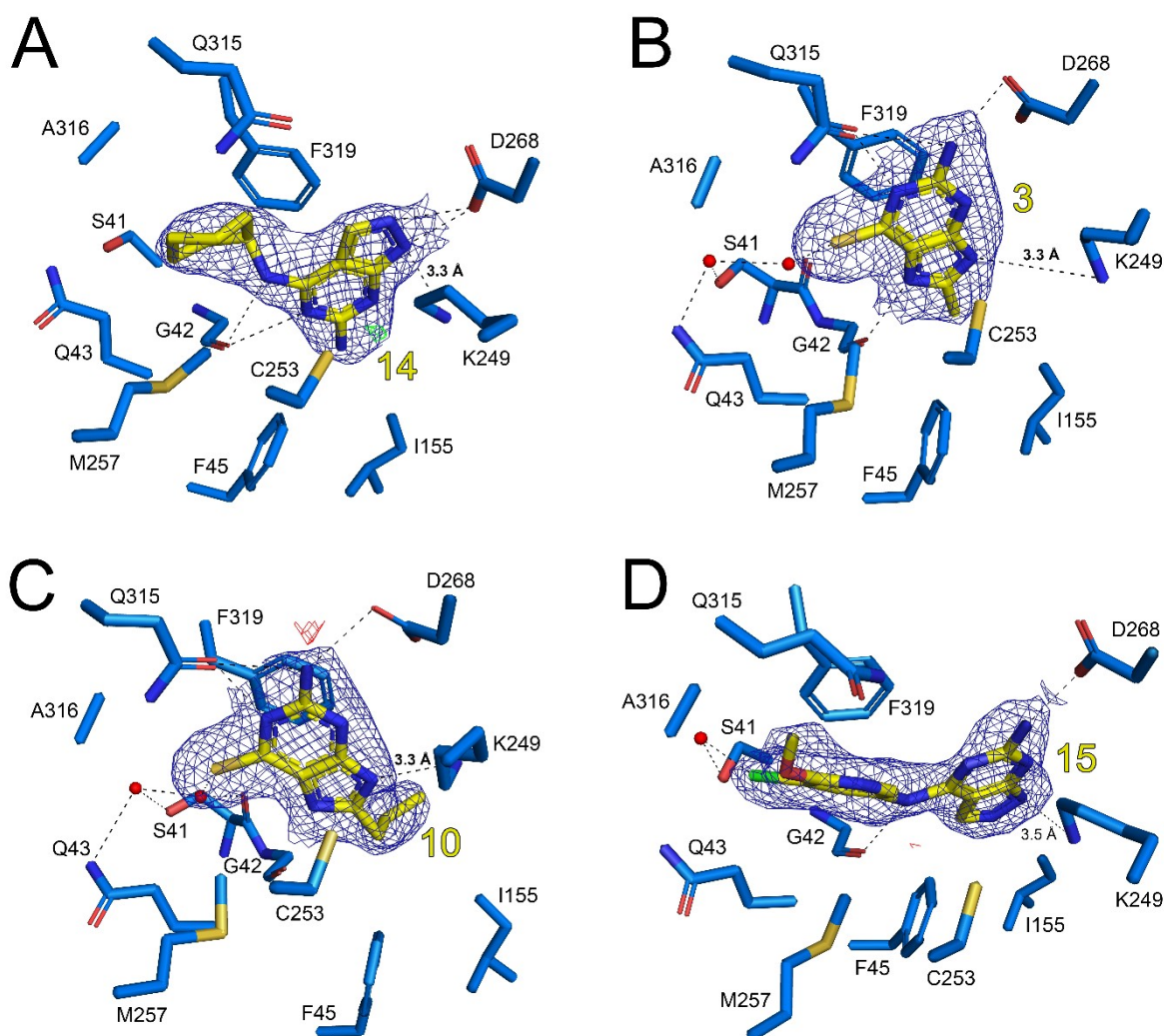


Figure S5: Position of Ser326 in OGG1 structure: Superposition of mouse OGG1 bound **3** (green), human OGG1 bound DNA-8-oxoG (magenta, PDB ID: 1HU0) and the human OGG1 AlphaFold model (grey, AF-015527-F1-v4) monomers. DNA from the 8-oxoG complex is coloured light orange. Ligands are depicted as sticks; C atoms are coloured green (**3**) or magenta (8-oxoG), O atoms red, and N atoms dark blue. The position of Ser326 from the AlphaFold model is highlighted. The computational model was used here as this residue is not ordered in any experimental hOGG1 or mOGG1 structures to date in the Protein Data Bank (PDB).

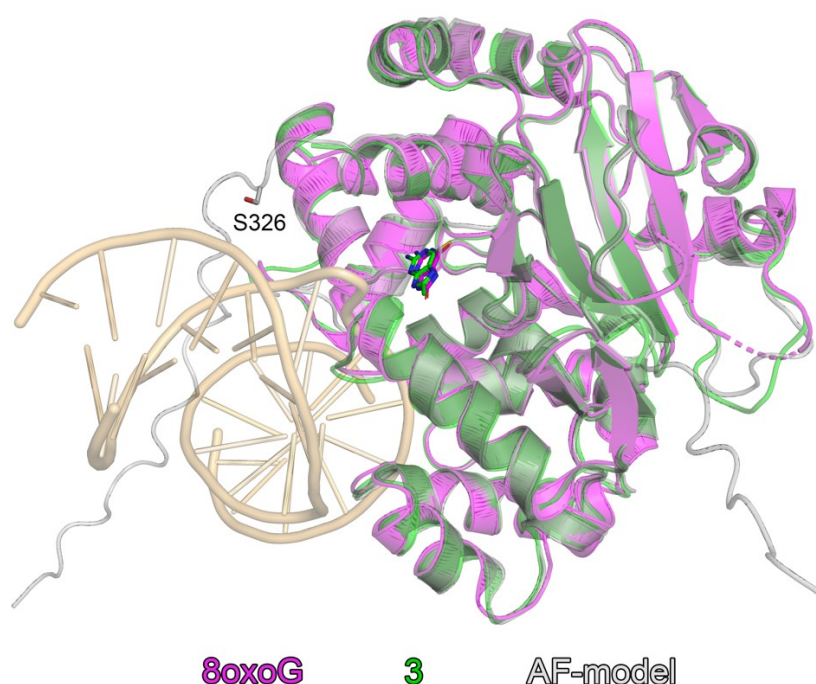
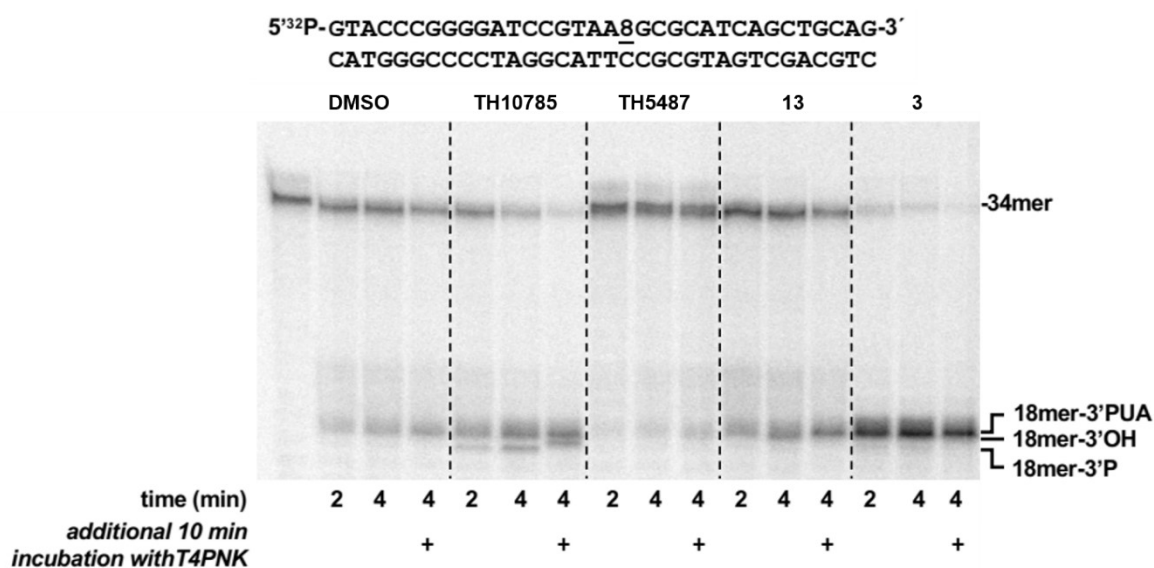


Figure S6. Effect of the compounds on the AP-lyase activity of *hOGG1* on 8-oxoG:C-containing DNA over a 2- and 4- minute (top) or 30- and 60-min (down) timespan respectively. The assay was performed as described in Materials and Methods using 2 nM of the indicated [32 P]5'-labeled 8-oxoG-containing substrate, in the presence of 10 nM *hOGG1*, 20 mM EDTA and either 10% DMSO or 6.25 μ M for TH10785, **13** and **3**; 50 μ M for TH5487. After incubation for the indicated times at 37°C, reactions were either stopped or further incubated 10 min in the presence of T4 PNK (+). Thereafter, samples were analyzed by 7M urea-20% PAGE and autoradiography. Position of products is indicated. DMSO and TH10785 serve as controls of β - and β,δ -elimination respectively. Structures of compounds **3** and **13** depicted in Table 1, structure of TH10785 depicted in Figure 1.



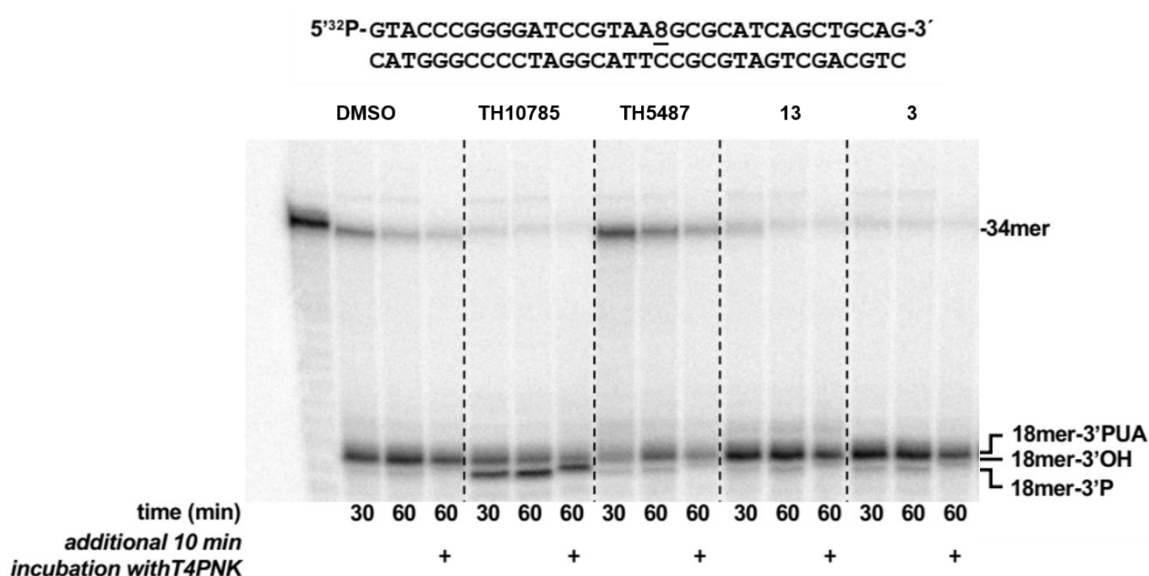


Table S4: Nano-DSF confirms OGG1 protein stability to be influenced by pH and compound binding: **A)** Light scattering was monitored to assess the degree of protein aggregation due to protein denaturation; **B)** OGG1 binder increase scattering in distinct pH environments; **C)** The melting temperature (T_m) of OGG1 in the presence of compound confirms OGG1 stabilization, indicating that the observed activity boost in Figure 2B can be partly attributed to protection against pH induced denaturation. Nano-DSF as performed in Materials and Methods. Protein was used at 25 μ M concentration and compound at 200 μ M.

A)	pH 6.7	pH 7.5	pH 7.7	pH 8.0	pH 8.3
Upper limit (Scattering, AU) for wtOGG1	88.5	87.4	88.7	91.6	90.1
Lower limit (Scattering, AU) for wtOGG1	85	87.4	85.5	88.7	89.0
Average (Scattering, AU) for wtOGG1	86.8	87.4	87.1	90.2	89.6

B)	pH 6.7	pH 7.5	pH 7.7	pH 8.0	pH 8.3
wtOGG1 + TH 10785 (AU)	102.0	100	117	116.0	106
wtOGG1 + 14 (AU)	85	86	87	87.5	90.0
wtOGG1 + 3 (AU)	87	89	91	90	85
wtOGG1 (AU)	86.8	87.5	87.1	90.1	89.6

c)	pH 6.7	pH 7.5	pH 7.7	pH 8.0	pH 8.3
T _m for wtOGG1 (°C)	48.2	46.8	48.4	47.2	46.4
T _m for wtOGG1 + TH10785 (°C)	55.0	55.6	56.4	55.8	55.8
T _m for wtOGG1 + 14 (°C)	49.5	50.3	50.3	52.1	51.6
T _m for wtOGG1 + 3 (°C)	51.5	51.4	50.6	49.8	49.9

Figure S7: Performing the incision assay in deuterated solvent confirms the role of proton transfer and nitrogen basicity in the action of organocatalytic switches. Assay was performed in water or deuterated water using 8-oxoA:C as substrate. Compounds were used at their best performing concentration and at three pH environments; a) pH 6.8; b) pH 7.5; c) pH 8.2. The general ratio of incision events remains similar compared to Figure 2B but is significantly reduced for the deuterated environment. Assay performed as described in Materials and Methods. Structures of compounds **3** and **13** depicted in Table 1, structure of TH10785 depicted in Figure 1.

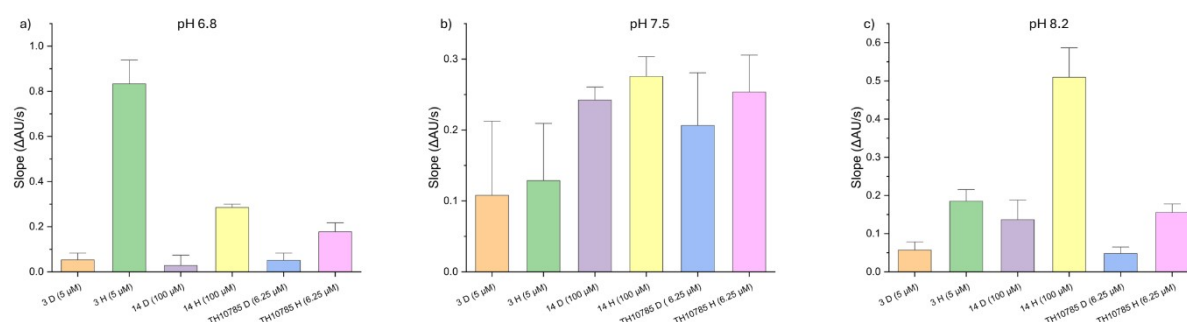
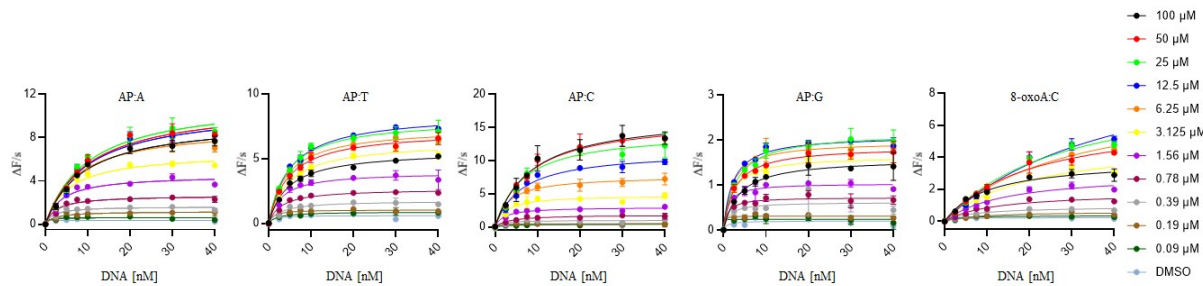
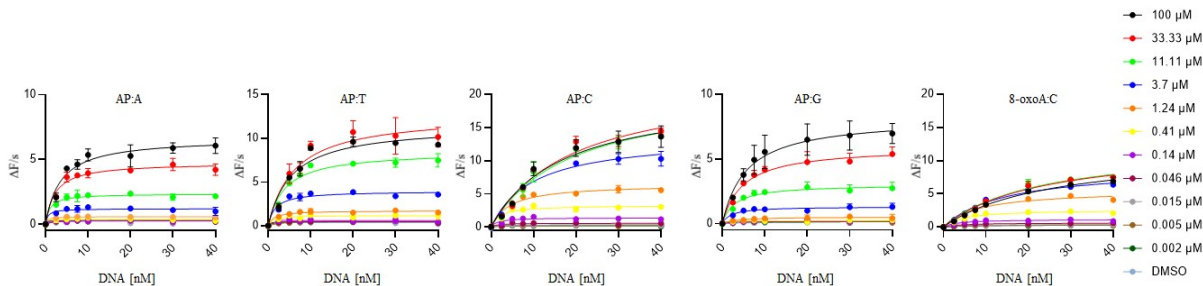


Figure S8: Rate of substrate turnover for OGG1 with TH10785 and **3 against a number of AP site substrates in the fluorescence-based biochemical assay:** A) TH10785 activates OGG1 on AP sites opposite any canonical nucleobase; B) **3** follows a similar pattern and all AP sites are more efficiently converted than 8-oxo substrates. v_0 of reaction measured within the initial linear slope of the reaction. Details described in Materials and Methods. C) Kinetic control experiments for compounds **3** and **14** without OGG1 enzyme demonstrate no significant acceleration of strand cleavage by the compounds independent of OGG1. D) Baseline activity (cleavage rate of AP site:C substrates in RFU/min) of the OGG1 mutants at 10 nM (100 nM for F319A) in reference to wt-OGG1. Structures of compounds **3** and TH10785 depicted in Figure 1, structure of compound **14** depicted in Table 1.

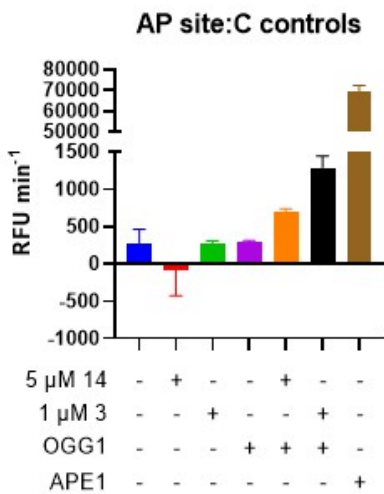
A)



B)



C)



D)

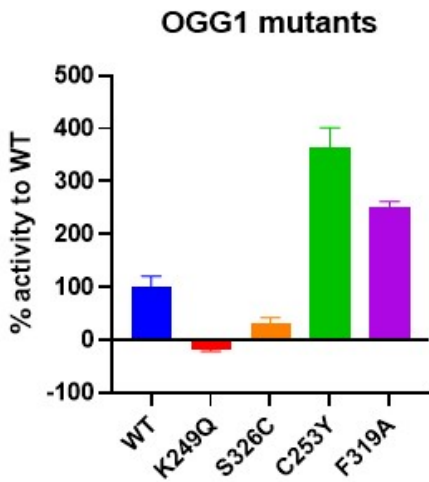


Table S5: X-ray crystallography data collection and refinement statistics

	mOGG1-14	mOGG1-3	mOGG1-10	mOGG1-15
Data collection				
PDB code	8BQ7	9F8U	9F8V	9F8Z
Station	MAXIV-BioMAX	DLS-I03	DLS-I03	DLS-I03
Space group	P2 ₁ 2 ₁ 2 ₁	P2 ₁ 2 ₁ 2 ₁	P2 ₁ 2 ₁ 2 ₁	P2 ₁ 2 ₁ 2 ₁
Cell dimensions:				
a, b, c (Å)	80.7, 82.1, 169.5	81.3, 81.7, 169.9	81.5, 81.6, 170.3	80.6, 82.3, 171.9
α , β , γ (°)	90, 90, 90	90, 90, 90	90, 90, 90	90, 90, 90
Resolution (Å)	72.9-2.6 (2.72-2.60)	58.7-2.5 (2.60-2.50)	58.9-2.4 (2.48-2.40)	85.9-2.50 (2.71-2.50)
Total reflections	474075 (58223)	552287 (63840)	603093 (52882)	427533 (23269)
Unique reflections	35462 (4247)	40082 (4445)	45246 (4343)	31051 (1553)
R_{merge}	14.0 (279.6)	7.5 (212.8)	8.6 (105.9)	11.8 (241.6)
R_{pim}	5.6 (112.1)	3.0 (83.4)	3.5 (45.9)	3.7 (91.8)
CC _{1/2} (%)	99.8 (58.9)	100 (59.7)	99.9 (77.4)	100 (70.5)
I/σ	11.4 (1.2)	19.8 (1.4)	16.9 (2.1)	13.9 (1.4)
Completeness	100 (100)	100 (100)	100 (100)	94.1 (71.2)
Redundancy	13.4 (13.7)	13.8 (14.4)	13.3 (12.2)	13.8 (15.0)
Refinement				
$R_{\text{work}}/R_{\text{free}}$ (%)	25.5/30.6	23.7/29.0	23.0/28.1	22.5/27.7
<i>B</i> -factors:				
Protein (all atoms) ^a	67.5/84.8/100.5	71.4/91.3/117.4	53.1/78.9/99.2	68.9/64.6/78.1
Ligand ^a	85.0/x/x	53.0/x/x	41.5/64.2/90.6	66.2/58.0/x
Water	64.9	67.5	49.5	41.1
R.m.s. deviations:				
Bond lengths (Å)	0.035	0.012	0.010	0.010
Bond angles (°)	1.18	0.98	1.43	1.27
Ramachandran statistics:				
Favoured (%)	99.9	99.8	99.2	99.5
Outliers (%)	0.1	0.2	0.8	0.5

Values in parentheses are for the highest-resolution shell. ^a Values for each monomer (A, B and C) of the asymmetric unit. An x indicates that a ligand is not bound in that specific monomer.

Table S6: Results from the DSF-based selectivity screening against a curated kinase library. The assay was performed as described in Materials and Methods using compounds **3**, **10**, **14** and TH10785 in a concentration of 10 μ M. n.d. = not determined.

Kinase	ΔT_m [K]				Reference		
	compd 3	compd 14	compd 10	TH10785	Reference substance	Δ T_m [K]	IC_{50}/K_D [nM]
MAP3K5	-0.1	3.5	-0.2	-0,2	Staurosporine	16	24
RSK1_b	-0.1	2.6	-0.6	n.d.	Staurosporine	3	0.1
BIKE	0.3	2.6	0.1	-0,1	Staurosporine	18	1
ULK3	-0.1	2.3	-0.3	-0,2	Staurosporine	17	1.5
GAK	0.3	2.1	-0.5	-1,3	Staurosporine	9	17
AAK1	-1.2	2.1	-1.6	0,0	Staurosporine	15	1.2
ABL1	0.1	2.0	0.3	0,1	Staurosporine	9	60
AURKB	0.4	1.9	1.6	n.d.	Staurosporine	8	5
AurA	-0.8	1.9	-1.1	-0,1	Staurosporine	17	1.5
CLK1	-0.5	1.7	-0.4	0,0	Staurosporine	16	4
BMPR2	-0.2	1.7	0.1	0,3	Staurosporine	3	670
TAF1	0.1	1.4	1.2	0,6	Bromosporine	7	n.d.
DMPK1	0.1	1.3	1.0	0,0	Staurosporine	9	22.7
CDK2	-1.6	1.2	-1.8	-0,3	Staurosporine	15	1.3
MEK4	-0.8	1.1	-1.6	0,1	Staurosporine	11	1
FLT1	-0.5	0.9	-0.8	-0,7	Staurosporine	12	11
PCTAIRE1	-0.3	0.9	-0.3	0,6	Staurosporine	9	14
PAK4	0.2	0.8	-0.2	2,4	Staurosporine	12	6.3
MARK3	-0.6	0.8	-0.9	0,2	Staurosporine	18	0.5
BRD4	0.1	0.7	0.3	0,5	JQ1	7	60
BRAF	0.3	0.7	0.2	0,1	Dabrafenib	27	0.7
MARK4	0.1	0.7	0.0	0,8	Staurosporine	14	0.5
PLK4	-0.3	0.7	-0.1	-0,1	Staurosporine	18	4
BMX	-0.5	0.6	-1.3	0,2	Staurosporine	7	170
ULK1	-0.5	0.6	-0.4	0,3	Staurosporine	12	n.d.
DYRK2	-0.5	0.5	-1.5	0,2	Staurosporine	7	280
CASK	-0.2	0.5	-0.4	-0,2	Staurosporine	5	19

CAMK1G	-0.7	0.5	-0.5	n.d.	Staurosporine	9	23
MAPK15	0.0	0.4	0.0	n.d.	Staurosporine	14	5.5
CHK2	-0.4	0.4	0.4	0,1	Staurosporine	17	0.1
NEK1	0.2	0.3	0.5	-0,5	-	-	-
MAP2K6	0.0	0.3	-0.2	-0,2	Staurosporine	11	1
MST1	-1.3	0.3	-2.9	n.d.	Staurosporine	16	1
SRC	-0.2	0.3	0.0	-0,2	Staurosporine	5	2.3
DAPK3	0.5	0.2	-0.7	0,4	Staurosporine	16	1
CAMK2B	-0.5	0.2	-1.2	0,6	Staurosporine	11	0.1
CLK3	-0.5	0.2	-0.7	-0,2	CLK-T3	15	110
MST2	-3.1	0.2	-4.4	1,2	Staurosporine	13	0.18
CAMK1D	-0.1	0.2	-0.4	0,2	Staurosporine	9	0.4
JNK1	-0.8	0.2	-1.0	-1,8	Staurosporine	8	220
MRCKa	0.0	0.2	-0.1	-0,7	Staurosporine	n.d.	10.3
EPHA7	-0.6	0.2	-0.4	-0,2	Staurosporine	11	30.4
EphA2	-0.7	0.2	-0.8	0,1	Staurosporine	7	53
p38d	0.3	0.2	-0.2	0,3	Doramapimod	n.d.	1
MELK	0.1	0.1	0.3	0,3	Staurosporine	13	0.7
SLK	-1.0	0.1	-1.7	0,1	Staurosporine	17	3.9
DRAK2	-1.7	0.1	-3.0	-1,2	Staurosporine	11	21
CK1d	0.4	0.1	0.1	0,2	PF-670462	9	8
Haspin	-0.9	0.1	-0.7	-0,4	Staurosporine	9	50
PIM3	-0.6	0.1	-1.9	0,2	Staurosporine	19	0.1
CDKL1	-0.6	0.1	-1.5	0,2	CEP-32496	7	n.d.
FGFR1	-0.1	0.1	-0.3	-0,2	Staurosporine	6	3.2
WNK1	-0.3	0.1	-0.5	0,0	-	5	n.d.
EPHA4	-1.1	0.0	-0.1	n.d.	Staurosporine	5	7.4
STLK3	-0.1	0.0	-0.3	0,2	Staurosporine	11	22
TTK	0.1	0.0	-0.7	-0,4	Staurosporine	9	61
JNK3	-0.7	0.0	-2.5	0,1	CEP-32496	9	n.d.
CK2a1	-0.1	0.0	-0.4	-0,3	Similtasertib	15	1
MAP2K1	-0.3	0.0	-0.7	0,1	Staurosporine	3	24
DAPK1	0.2	0.0	-0.6	-0,6	Staurosporine	9	4
MAPKAPK2	-0.6	0.0	-0.7	n.d.	Staurosporine	4	196

PIM1	-0.7	-0.1	-1.0	n.d.	Staurosporine	12	3
JNK2	-0.9	-0.1	-1.8	0,8	SBI-0069279	9	n.d.
CSNK1E	-0.1	-0.1	0.0		PF-670462	8	14
MSSK1	-0.4	-0.1	-0.3	-0,4	-	-	-
EPHB1	0.2	-0.1	-0.3	n.d.	Staurosporine	6	25
GPRK5	-0.3	-0.1	-2.6	0,1	Staurosporine	6	150
Erk2	0.0	-0.1	0.3	-0,2	GDC-0994	8	1
OSR1	-0.1	-0.1	-1.7	0,0	Staurosporine	6	91
HIPK2	-0.9	-0.1	-0.9	n.d.	Staurosporine	4	791
CK2a2	-0.2	-0.1	-0.6	0,1	Similtasertib	16	1
AKT3	-0.3	-0.1	0.1	0,0	Staurosporine	7	5
CAMK2D	0.4	-0.2	-1.2	0,2	Staurosporine	16	0.5
SRPK1	-0.6	-0.2	-1.0	-0,4	Staurosporine	7	120
FGFR2	-0.2	-0.2	-0.2	-0,4	Staurosporine	8	3.3
FES	-1.1	-0.3	-1.5	0,1	Staurosporine	8	1.7
MYT1	-1.0	-0.3	-2.9	n.d.	Dasatinib	5	130
EPHA5	-0.8	-0.3	-0.9	0,3	Staurosporine	7	19
NEK7	-0.6	-0.3	-0.9	-0,2	-	-	-
PAK1	-1.6	-0.3	-2.1	-0,2	Staurosporine	7	0.3
VRK1	-0.7	-0.3	-0.6	-0,3	-	5	n.d.
p38a	-1.2	-0.3	-2.1	-0,2	Doramapimod	20	1
TIF1	-6.8	-0.3	-2.0	0,6	-	6	222
BRPF1	-1.0	-0.4	-3.0	n.d.	GSK6853	14	20
LOK	-2.5	-0.4	-2.7	n.d.	Staurosporine	24	0.03
DYRK1A	-1.4	-0.5	-2.3	n.d.	Staurosporine	10	4
NQO2	-0.4	-0.5	1.1	n.d.	Imatinib	n.d.	43
PHKg2	-1.5	-0.5	-2.0	-0,2	Staurosporine	21	0.1
CAMK4	-0.8	-0.6	-0.1	n.d.	Staurosporine	8	141
MER	-0.7	-0.6	-0.9	0,1	Staurosporine	6	6.4
DRAK1	-1.2	-0.7	-1.0	-0,3	Staurosporine	8	14
MST4	-2.1	-0.7	-1.5	0,3	Staurosporine	6	6.7
MAP2K7	0.1	-0.7	-0.3	n.d.	Staurosporine	7	440
NDR2	-1.0	-0.9	-1.8	0,2	Staurosporine	12	1.4
TLK1	-1.7	-1.0	-2.0	n.d.	Staurosporine	9	44

MST3	-3.1	-1.0	-2.5	-0,7	Staurosporine	6	120
DCAMKL1	-1.6	-1.0	-1.1	-1,4	Staurosporine	11	120
EPHB3	-2.1	-1.0	-1.2	0,2	Staurosporine	6	825
NEK2	-1.9	-1.1	-0.6	-0,4	Staurosporine	4	650
MSK1_b	-0.2	-1.1	1.0	n.d.	Staurosporine	16	5

Figure S9. Results from the DSF-based selectivity screening against a curated kinase library. The assay was performed as described in Materials and Methods using compounds **3**, **10**, **14** and TH10785 in a concentration of 10 μ M. Heatmap indicating stabilization or destabilization of the kinase set through compounds used, white = not determined.

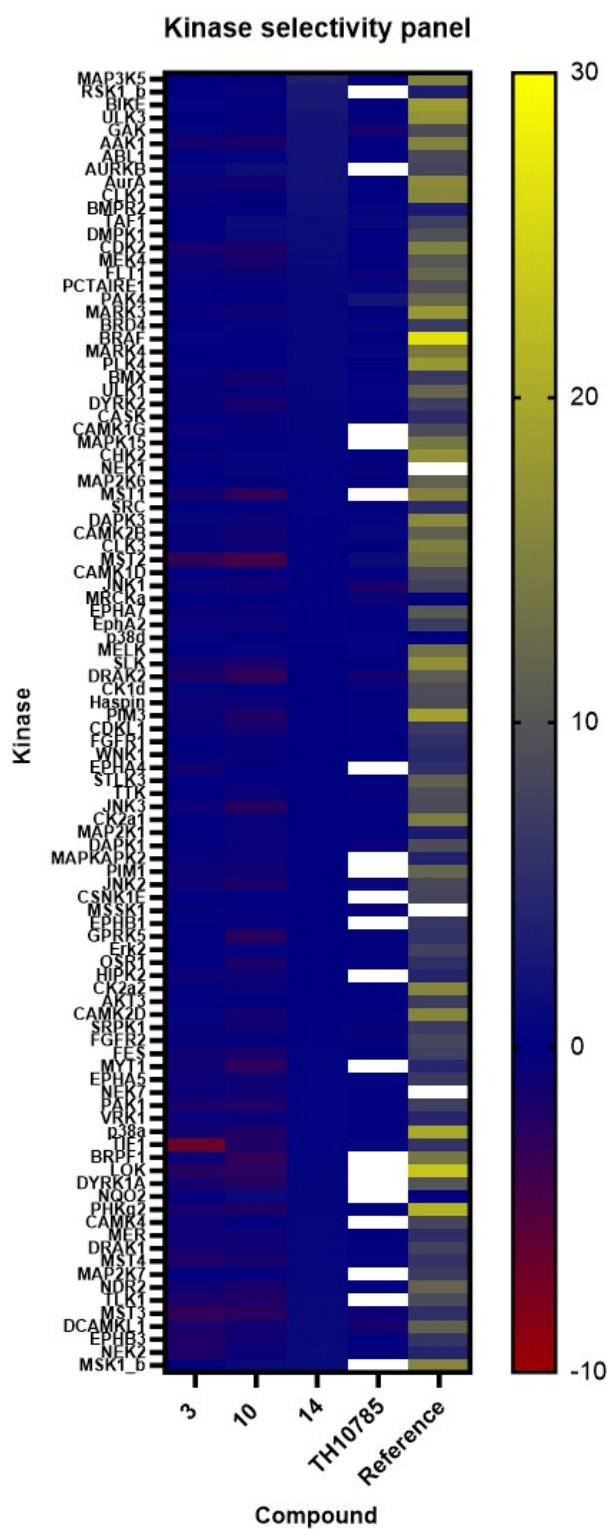


Table S7: Results from selectivity experiments on other DNA glycosylases and NUDIX protein family members. The assay was performed as described in Materials and Methods using compounds **3**, **10**, **12** and **14** in a concentration of 99 μ M. X* is an AP site targeting PAINS (pan-assay interference compound), that stalls AP site.

entry	3	10	14	12	TH010785	reference	
Glycosylase or NUDIX	inhibition%					inhibition%	substance
APE1	-10.38	-8.07	-5.61	-8.81	3.26	92.99	X*
MPG	-38.05	-36.95	4.13	22.11	20.84	88.01	X*
NEIL1	-6.92	-5.09	-6.86	25.00	14.71	90.30	X*
NTHL1	-6.32	-14.56	-0.71	24.19	28.50	70.89	X*
NUDT5	-9.74	-15.86	-7.45	1.62	2.08	99.31	TH005427
NUDT15	5.23	-0.01	-5.55	3.80	3.38	96.48	TH001760
NUDT22	-16.15	-11.12	-7.97	-8.54	3.66	92.93	TH008525
SMUG1	-21.97	-17.81	-30.10	12.70	-15.36	76.37	X*
TDG	-5.51	-10.87	5.73	35.39	14.09	83.00	X*
UNG	-11.06	-13.72	5.42	39.24	48.6	94.93	X*

Figure S10: Results from selectivity experiments on other DNA glycosylases and NUDIX protein family members. The assay was performed as described in Materials and Methods using compounds **3**, **10**, **12** and **14** in a concentration of 99 μ M.

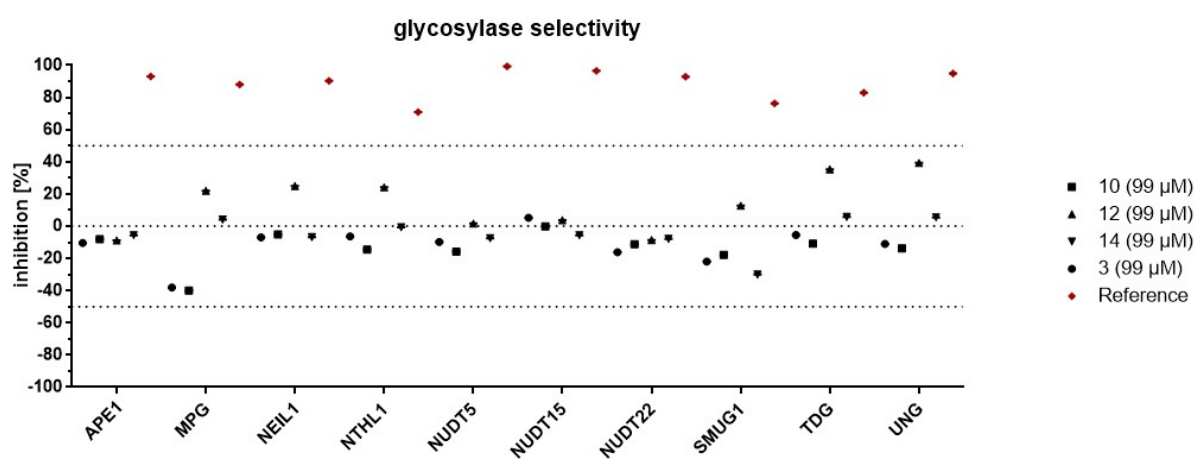
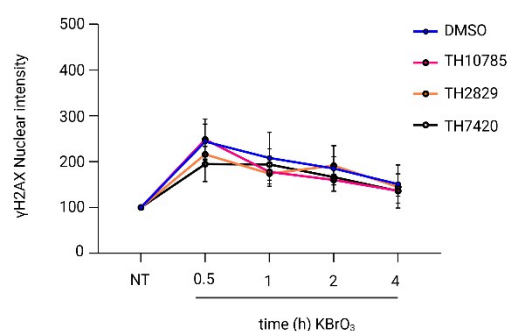


Table S8: Cell viability dose-response of compounds 3, 10, 12 and 14 in BJ-hTERT and BJ-hTERT SV40RAS cell lines. The assay was performed as described in Materials and Methods. TH000287C, an MTH1 inhibitor, served as reference.

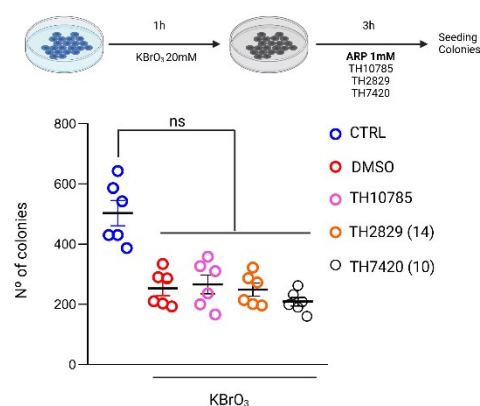
Entry		3	10	14	12	Reference: TH000287C
IC50 [μ M]	BJ-hTERT	>100	>100	>100	57.7	6.27
	BJ-hTERT SV40RAS	>100	>100	>100	35.0	2.35

Figure S11: A) Quantification of nuclear γ H2AX levels across different time points in U2OS cells exposed to organocatalytic switches or DMSO, under oxidative stress conditions (20 mM of KBrO_3 for 1h). Each bar represents the mean \pm SEM. Data are the average of three independent experiments. For each experiment, 25 fields and around 1000 cells were captured per condition. Statistical significance was calculated using two-way ANOVA for multiple comparisons. Nonsignificant differences were found **B) Clonogenic survival of U2OS cells to KBrO_3 in the presence of activators.** The cancer cell line U2OS was first exposed to an acute dose of KBrO_3 (20mM for 1h) and incubated overnight in the presence of activators (10 μ M) or DMSO, and replaced with fresh media to allow the formation of colonies. After 10 days, colonies were counted. Data are average \pm SD values of three biological replicates of two independent experiments. Statistical significance was calculated using an unpaired two-tailed Student's t-test. ns, nonsignificant

A)



B)



Materials and Methods

Biochemical assay (Fluorescence)

Enzymes were purified as below and the biochemical assay including materials used was based on the publication by Visnes *et al.*^[1] and “EUBOPEN” protocols (<https://www.eubopen.org/protocols-reagents>) and adapted where mentioned. OGG1 (10 nM) activation on 10 nM substrate was monitored in a kinetic mode and a time resolved curve was obtained for each compound concentration in triplicates except where stated otherwise. Initial slopes were taken of the linear part of these curves to determine rates and kinetics. Fluorescence values of each compound concentration were normalised by the DMSO control values and calculated as % activation of the full turnover fluorescence of the APE (2 nM) control. The median activation concentration (AC₅₀) for each compound was calculated from the % activation of all tested concentrations and refers to the compound concentration which activates the reaction to 50% of the substrate turnover reached in the assay control coupled to APE1 (2 nM) as described before.^[2] In the screening, primary hits were defined as compounds with an AC₅₀ of below 100 µM. A schematic representation of the assay and AC₅₀ determination can be found in Figure S2.

Proteins and reagents

Enzymes (APE1, UNG2, TDG, SMUG1, MPG, NEIL1, NTHL1, NUDT15, NUDT22, NUDT5) and mutants were produced as reported previously.^[1–4] 8-oxoG-containing oligonucleotide (see sequence below) was radiolabelled at the 5' end with [³²P]-ATP (Perkin-Elmer Life Sciences) and T4 polynucleotide kinase (T4PNK) from New England Biolabs.

Oligonucleotides

For PAGE analysis: Oligonucleotide 5'-GTACCCGGGGATCCGTAA8GCGCATCAGCTGCAG (Integrated DNA Technologies), where 8 stands for 8oxodG, was 5'-labeled and further hybridized to the complementary oligonucleotide 5'-CAGCAGCTGATGCGCCTTACGGATCCCCGGGTAC in the presence of 60 mM Tris-HCl (pH 7.5) and 0.2 M NaCl by heating to 80 °C for 5 min before slowly cooling to room temperature overnight.

For standard biochemical assay: Complementary strands containing FAM and DAB were ordered from ATD BIO. Sequence were 5'-FAM-TCTG CCA XCA CTG CGT CGA CCT G-3' and 5'-CAG GTC GAC GCA GTG YTG GCA GT-Dab-3' where X is a lesion such as uracil, thymine glycol, 8-oxoA, AP-site analogue, inosine, hydroxymethyl cytosine and Y is the corresponding required complementary base.

hOGG1 activity assay on 8oxodG-containing substrates (PAGE)

To analyse the AP lyase activity of *hOGG1* on 8-oxoG containing substrates, 2 nM of the indicated 34 mer [³²P]5'-labeled 8oxoG-containing substrate was incubated with 10 nM *hOGG1* and either 10% DMSO or 6.25 µM for TH10785, **13** and **3**; 50 µM for TH5487 in the presence of 30 mM Hepes, pH

7.5, 4% glycerol and 20 mM EDTA. Samples were incubated at 37 °C for the indicated times. When specified, samples were further incubated 10 min in the presence of 0.2 U of T4PNK. The reaction products were stabilized by incubation with 30 mM of freshly prepared NaBH₄ and further incubation for 20 min on ice. DNA products were analyzed by 7 M urea-20% PAGE and autoradiography.

pKa prediction

pKa predictions were carried out within the Schrödinger Suite 2023-2 using the Epik module. States were predicted for aqueous conditions with a pH of 7 ± 2 , tautomers were generated where applicable and the number of output structures was limited to 16. Position corresponding to basic positions able to abstract the α -proton are reported.

Crystallization

Purified mOGG1 (22 mg/mL) was pre-incubated with 6.25 mM ligand (3, 10, 14 or 15) and crystallized via sitting drop vapor diffusion in conditions from the Morpheus Screen (Molecular Dimensions). This included 0.12 M Monosaccharides, 0.1 M bicine/Trizma base pH 8.5, 50 % GOL_P4K (mOGG1-14 and mOGG1-10), 0.09 M NPS, 0.1 M imidazole/MES pH 6.5, 50 % MPD_P1K_P3350 (mOGG1-3) or 0.12 M Ethylene Glycols, 0.1 M sodium HEPES/MOPS pH 7.5, 50 % GOL_P4K (mOGG1-15) at 18 °C. Protein crystals were fished without additional cryoprotectant and flash frozen in liquid nitrogen.

Data collection, structure determination, and refinement

For the mOGG1-14 complex, X-ray diffraction data was collected at BioMAX (Lund, Sweden) equipped with an EIGER X 16M detector. A complete dataset was collected on a single crystal at 100 K. The dataset was processed and scaled with DIALS^[5] and AIMLESS^[6] within the CCP4 suite^[7]. For the mOGG1-3, mOGG1-10 and mOGG1-15 complexes, X-ray diffraction data were collected at station I03 of the Diamond Light Source (Oxford, UK) equipped with a PILATUS-6M detector. Complete datasets were collected on single crystals at 100 K. The datasets were processed with DIALS^[5] or XDS^[8] and scaled with AIMLESS^[6] or STARANISO. Molecular replacement was performed in Phaser^[9] or MOLREP^[10] using the structure of mouse OGG1 (PDB ID: 6G3Y) with all ligands and waters removed, as the search model. Several rounds of manual model building and refinement were performed using COOT^[11] and REFMAC5^[12] during which waters and ligands were incorporated into the structures.

NanoDSF

Buffer (HEPES 200 mM + NaCl 300 mM + Glycerol 30%) and pH solution was prepared for pH 6.7, 7.5, 7.7, 8 and 8.3. Protein solution was prepared at protein stock solution (42.5 uM) + 9.3 uL reaction buffer at desired pH. DMSO controls were included. The reaction solutions were taken up by capillary

tubes and melted in a process with constant increment of 2.5°C from 0°C to 90°C in a Prometheus (Nano Temper Technologies). The scattering of protein from the melting process was plotted, as well as the first derivatives of the scatterings.

DSF-based selectivity screening against OGG1 and a curated kinase library

The assay was performed as previously described.^[13,14] Briefly, protein kinase domains at a concentration of 2 µM were mixed with 10 µM compound in a buffer containing 20 mM HEPES, pH 7.5, and 500 mM NaCl. Conditions for OGG1 were as reported previously.^[15] SYPRO Orange (5000×, Invitrogen) was added as a fluorescence probe (1 µl per mL). Subsequently, temperature-dependent protein unfolding profiles were measured using the QuantStudio™ 5 Realtime PCR machine (Thermo Fisher). Excitation and emission filters were set to 465 nm and 590 nm, respectively. The temperature was raised with a step rate of 3°C per minute. Data points were analysed with the internal software (Thermal Shift Software™ Version 1.4, Thermo Fisher) using the Boltzmann equation to determine the inflection point of the transition curve.

Selectivity screen against other glycosylases and NUDIX enzymes

The compounds were tested at a concentration of 99 µM in biochemical assays following a similar protocol as for the OGG1 biochemical readout, using the respective enzyme and the labelled enzyme substrate. Glycosylase inhibition was monitored in a kinetic mode and calculated in percent in relation to the DMSO control. The experiment was performed in duplicates for each compound. For NUDT5, NUDT15 and NUDT22, a malachite green assay was conducted, using a previously described protocol.^[16–18]

Resazurin cell viability assay with BJ-hTERT and BJ-hTERT SV40RAS cells for toxicity testing in a dose-response manner

Prior to cell-seeding, compounds **3**, **10**, **12** and **14** were dispensed in 384-well cell culture plates using an Echo acoustic liquid handler. Dose response curves were dispensed in duplicates from 100 µM to 0.09 µM. BJ-hTERT and BJ-hTERT SV40RAS cells were cultured in DMEM Glutamax + 10% FBS + 50U/50 µg/mL Penicillin/Streptomycin and were seeded in the cell culture plates containing the nano-dispensed compounds to concentrations of 1200 cells/well (BJ-hTERT) and 600 cells/well (BJ-hTERT SV40RAS) using a Multidrop Combi reagent dispenser. After incubation for 72 hours at 37°C, Resazurin (59 µg/mL in PBS/ 10 µL/well) was added and the plates were incubated for a further 4-7 hours at 37°C before performing a fluorescence readout on a Hidex Sense microplate reader.

Immunofluorescence analysis (γH2AX and 8-OxoG)

Cells were seeded on coverslips in 24-well plates (25,000 cells per well). After the treatments, cells were fixed with 3.7% PFA for 10 min. Permeabilization was performed by incubation with 0.5% Triton X-100 in PBS for 15 min. Cells were washed with PBS twice and blocked for 1 hour at room temperature

with a blocking solution (3% BSA complemented with 0.1% Tween-20 in PBS). Cells were incubated overnight with the primary antibody in a blocking solution (γ H2AX: 05-636; Millipore). Cells were washed three times with PBS-Tween 20 (0.1%) and incubated with a secondary antibody diluted in a blocking solution for 1 hour at room temperature in the dark. Cells were washed three times with PBS-Tween 20 (0.1%), and nuclei were stained with 0.5 μ g/mL DAPI. Coverslips were washed three times (10 min in PBS each time) and mounted. Image acquisition was performed with a Zeiss Axio Observer / Cell Observer. Coverslips were scanned, and 25 fields were acquired at 20X. The nuclear fluorescence signal of γ H2AX was determined using Cell Profiler [®].

Relative AP-site quantification by FACS

A total of 100,000 cells were seeded in a p35 petri dish. Cells were exposed to 40 mM of KBrO₃ for 1 hour in the presence of compounds or vehicle (DMSO). Afterward, fresh media containing compounds or DMSO was added. ARP (N-(aminooxyacetyl)-N'-(D-Biotinoyl) hydrazine (ref: A10550) was then added in a concentration of 1 mM, for a period of 3 hours. The cells were fixed and permeabilized using eBioscience™ Foxp3 / Transcription Factor Staining Buffer Set according to the manufacturer's instructions (00-5523-00). The cells were then incubated with Streptavidin-PE Conjugate antibody (1:500) or Vari Fluor 555-Streptavidin. Labeled cells were analyzed in a FACS Canto II cytometer and each condition was run in biological triplicates. FloJo software analysis was used to calculate the ARP-Streptavidin-FITC geometrical mean signal intensity. Graphs were plotted using Graphpad Prism.

Colony formation assays

The U2OS cell line was seeded and grew in 80% subconfluence in a p100. Cells were treated with 40 mM of KBrO₃ for 1 hour, or not (control). Cells were trypsinized, counted, and seeded in p35 plates at 400 cells per well and incubated overnight with TH10785, **14**, **10** or DMSO. After that, cells were allowed to grow in fresh media until colony size surpassed 50 cells in the control, followed by medium removal and the addition of 4% (w/v) methylene blue in methanol. Following washing with tap water and air drying, colonies with >50 cells were counted.

Statistics

Unless stated otherwise, all biochemical assays were performed in three independent replicates with triplicates in each experiment. In cell biology experiments, each bar represents the mean \pm SD. Data are the average of three biological replicates. Statistical significance was calculated using an unpaired two-tailed Student's t-test. ns, nonsignificant; *P < 0.05; **P < 0.01; ***P < 0.001. ****P < 0.0001

General Information Chemical Synthesis

All reagents and solvents were purchased from commercial vendors and used without further purification. Unless otherwise stated, reactions were performed without care to exclude air or moisture. Analytical thin-layer chromatography was performed on silica gel 60 Å F-254 plates (E. Merck) and visualized under a UV lamp. Flash column chromatography was performed in a Biotage® SP1 MPLC system using Fisher Chemical silica gel 60 Å. ¹H and ¹³C NMR spectra were recorded on Bruker DRX-400 MHz or Bruker Ascend 400 MHz spectrometers. Chemical shifts are expressed in parts per million (ppm) and referenced to the residual solvent peak (¹H: δ 7.26 for CDCl₃, δ 2.50 for DMSO-*d*₆, δ 3.31 for methanol-*d*₄; ¹³C: δ 29.84 for CDCl₃, δ 39.52 for DMSO-*d*₆, δ 49.00 for methanol-*d*₄). Analytical LC-MS were performed either on an Agilent MSD mass spectrometer connected to an Agilent 1100 system or an Agilent 1260 infinity II with a G6125B mass spectrometer. Columns used were ACE 3 C8 (50 x 3.0 mm); H₂O (+ 0.1% TFA) and MeCN were used as mobile phases at a flow rate of 1 mL/min, or Xterra MSC18 (50 x 3.0 mm) column where H₂O (10 mM NH₄HCO₃; pH = 10) and MeCN were used as mobile phases at a flow rate of 1 mL/min. For LC-MS, detection was made by UV and MS (ESI+). Preparative LC was performed on a Gilson system using Waters C18 OBD 5 μm column (30 x 75 mm) with water buffer (50 mM NH₄HCO₃ at pH 10) and MeCN as mobile phases using a flow rate of 45 mL/min or ACE 5 C8 (100 x 21.2 mm) column with water buffer (0.1 % TFA) and MeCN as mobile phases using a flow rate of 30 mL/min. All final compounds were assessed to be >95% pure by LC-MS analysis. Compounds in our nucleobase/nucleoside/nucleotide and prior art screening set were not resynthesized and no characterization was performed. Compounds available through NCI DTP were not resynthesized and no characterization was performed. High-resolution mass spectra (HRMS) were measured with EI or ESI ionization. A chromatographic purification was performed before each measurement. The Thermo Q-Exactive plus device for ESI-mass spectra was coupled to a binary UHPLC system. For EI-measurement, a GC-system was coupled to the Thermo Q-Exactive GC device.

General procedure A for the nucleophilic substitution with anilines or pyridine-3-amines

In a 10 mL reaction tube, the appropriate chloride and 1 – 2 equiv. of the corresponding aniline or pyridine-3-amine were dissolved in 1 – 2 mL of 2,2,2-trifluoroethanol (TFE). To the stirred solution, 1 – 2 equiv. of trifluoroacetic acid (TFA) were added dropwise. The reaction tube was flushed with N₂ and the reaction mixture was stirred at 80 °C for 2 – 48 h. After completion, the reaction was quenched with the respective amount of *N,N*-diisopropylethylamine (DIPEA; 1 equiv. per 1 equiv. of TFA), the solvent was removed under reduced pressure and the product was purified as stated in the descriptions below.

General procedure B for the nucleophilic substitution with amines

In a 10 mL reaction tube, the appropriate chloride and 1 – 2 equiv. of the corresponding amine were dissolved in 1-2 mL of *N,N*-dimethylformamide (DMF). To the stirred solution, 1 – 2 equiv. of DIPEA were added and the reaction mixture was stirred at 80 – 100 °C for 12 – 48 h. After completion, the

solvent was removed under reduced pressure, and the product was purified as stated in the description below.

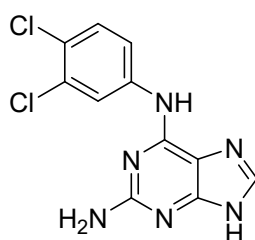
General procedure C for the nucleophilic substitution with thiols

In a 10 mL reaction tube, the appropriate chloride and 1 – 2 equiv. of the thiol were dissolved in 1 – 2 mL of DMF. 1 – 2 equiv. of K_2CO_3 were added, the tube was flushed with N_2 , and the reaction mixture was stirred at 80 – 100 °C for 12 – 48 h. After completion, the remaining solids were filtered off, the solvent was evaporated under reduced pressure and the residue was purified as stated in the description below.

General procedure D for the alkylation of 2-amino-6-chloropurine.

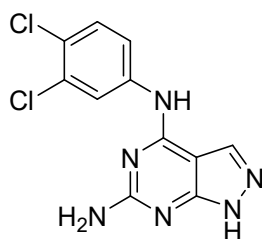
Step 1: A mixture of the corresponding carboxylic acid (1.5 mmol), 4-dimethylaminopyridine (DMAP; 1.8 mg, 0.015 mmol), N-hydroxyphthalimide (240 mg, 1.5 mmol), and diisopropylcarbodiimide (0.23 mL, 1.5 mmol) were dissolved in DMSO (2.0 mL). N_2 was then bubbled through the solution for 2 – 3 min. The vial was closed, and the mixture was stirred at 20 °C for 16 h. The mixture was used in the next step without purification.

Step 2: In a 10 mL vial, 2-amino-6-chloropurine (170 mg, 1.0 mmol), 4CzIPN (7.9 mg, 0.010 mmol), and TFA (0.076 mL, 1.0 mmol) were dissolved in DMSO (2.0 mL), then the DMSO solution of the corresponding phthalimide carboxylate from step 1 was added. After this, N_2 was violently bubbled through the mixture for 5 min. The vial was sealed and illuminated (365 nm, 50 W) for 16 h under stirring. The reaction mixture was poured into aq. $NaHCO_3$ (10 mL) and was subsequently extracted with DCM (10 mL \times 3). The combined organics were concentrated and purified by silica gel chromatography.



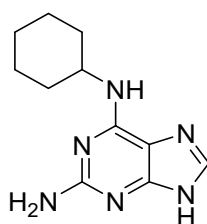
(11): *N6-(3,4-dichlorophenyl)-9H-purin-2,6-diamine*

The compound was synthesised according to General procedure A from 2-amino-6-chloro-9H-purine (20 mg, 0.12 mmol) and 3-methoxyaniline (20 mg, 0.12 mmol). Recrystallisation from methanol yielded the product as a white solid (27 mg, 75%). LCMS $[M+H]^+$ 295. 1H -NMR (400 MHz, $DMSO-d_6$) δ 8.39 (d, J = 2.5 Hz, 1H), 8.06 (dd, J = 8.9, 2.6 Hz, 1H), 7.48 (d, J = 8.9 Hz, 1H), 7.31 (s, 1H), 7.18 (s, 1H), 7.05 (s, 1H). ^{13}C NMR (151 MHz, $DMSO-d_6$ + 4% H_2SO_4) δ 154.3, 150.2, 148.6, 142.4, 138.4, 131.4, 130.8, 126.2, 122.3, 121.2, 106.2. HRMS (ESI+): m/z calculated 295.0260 for $C_{11}H_9N_6Cl_2$, found 295.0259 ($[M+H]^+$).



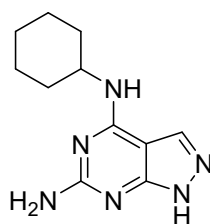
(12): *N4-(3,4-dichlorophenyl)-1H-pyrazolo[3,4-d]pyrimidin-4,6-diamine*

The compound was synthesised according to General procedure A from 4-chloro-1*H*-pyrazolo[3,4-*d*]pyrimidin-6-amine (17 mg, 0.10 mmol) and 3,4-dichloroaniline (22 mg, 0.14 mmol). Recrystallisation from methanol yielded the product as a yellowish solid (8 mg, 27%). LCMS $[M+H]^+$ 295. 1H -NMR (400 MHz, DMSO- d_6) δ 8.34 (s, 1H), 7.99 (d, J = 9.5 Hz, 1H), 7.64 (d, J = 8.9 Hz, 2H). ^{13}C NMR (151 MHz, DMSO- d_6 + 4% H_2SO_4) δ 156.7, 156.2, 149.4, 138.1, 131.2, 130.6, 128.5, 126.7, 123.5, 122.2, 97.4. HRMS (ESI $^+$): m/z calculated 295.0260 for $C_{11}H_9N_6Cl_2$, found 295.0258 ($[M+H]^+$).

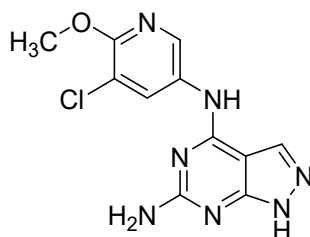


(13): *N6-cyclohexyl-9H-purin-2,6-diamine*

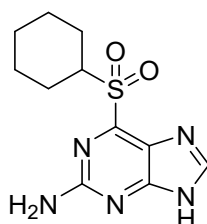
The compound was synthesised according to General procedure B from 2-amino-6-chloro-9*H*-purine (20 mg, 0.12 mmol) and cyclohexylamine (23 μ L, 0.20 mmol). Purification by preparative HPLC (0.1% TFA in water/ acetonitrile) yielded the product as a white solid (6 mg, 14%). LCMS $[M+H]^+$ 233. 1H -NMR (400 MHz, DMSO- d_6) δ 8.51 (s, 1H), 8.13 (s, 1H), 7.49 (s, 1H), 4.06 (s, 1H), 1.97 – 1.87 (m, 1H), 1.82 – 1.71 (m, 3H), 1.66 – 1.58 (m, 1H), 1.39 – 1.17 (m, 6H). ^{13}C NMR (151 MHz, DMSO- d_6 + 4% H_2SO_4) δ 154.1, 151.4, 147.3, 141.7, 105.3, 49.8, 32.2, 25.3, 24.8. HRMS (ESI $^+$): m/z calculated 233.1509 for $C_{11}H_{16}N_6$, found 233.1500 ($[M+H]^+$).

**(14):** *N4-cyclohexyl-1H-pyrazolo[3,4-d]pyrimidin-4,6-diamine*

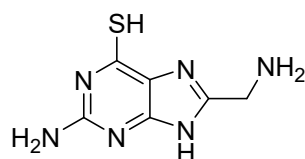
The compound was synthesised according to General procedure B from 4-chloro-1*H*-pyrazolo[3,4-*d*]pyrimidin-6-amine (18 mg, 0.10 mmol) and cyclohexylamine (23 μ L, 0.20 mmol). Purification by preparative HPLC (50 mM NH_4HCO_3 pH 10/ acetonitrile) yielded the product as a white solid (3 mg, 14%). LCMS $[\text{M}+\text{H}]^+$ 233. ^1H -NMR (400 MHz, CDCl_3) δ 7.68 (s, 1H), 2.02 – 1.92 (m, 3H), 1.76 – 1.68 (m, 3H), 1.66 – 1.58 (m, 2H), 1.38 – 1.13 (m, 3H). ^{13}C NMR (151 MHz, $\text{DMSO}-d_6$ + 4% H_2SO_4) δ 157.3, 156.3, 149.4, 128.2, 96.7, 50.0, 32.1, 25.3, 25.1. HRMS (ESI $^+$): m/z calculated 233.1509 for $\text{C}_{11}\text{H}_{16}\text{N}_6$, found 233.1523 ($[\text{M}+\text{H}]^+$).

**(15)** *N4-(5-chloro-6-methoxypyridin-3-yl)-1H-pyrazolo[3,4-d]pyrimidine-4,6-diamine*

The compound was synthesised according to General procedure A from 4-chloro-1*H*-pyrazolo[3,4-*d*]pyrimidin-6-amine (18 mg, 0.10 mmol) and 5-chloro-6-methoxy-pyridin-3-amine (23 mg, 0.14 mmol). Purification by preparative HPLC (50 mM NH_4HCO_3 pH 10/ acetonitrile) yielded the product as a white solid (16 mg, 56%). LCMS $[\text{M}+\text{H}]^+$ 292. ^1H -NMR (400 MHz, $\text{DMSO}-d_6$) δ 12.63 (s, 1H), 9.65 (s, 1H), 8.72 (d, $J = 2.4$ Hz, 1H), 8.40 (d, $J = 2.4$ Hz, 1H), 7.95 (s, 2H), 6.38 (s, 1H), 3.93 (s, 3H). ^{13}C NMR (176 MHz, $\text{DMSO}-d_6$) δ 161.9, 157.6, 154.2, 153.9, 136.4, 132.2, 131.9, 131.2, 115.8, 95.3, 54.0. HRMS (ESI $^+$): m/z calculated 292.0708 for $\text{C}_{11}\text{H}_{10}\text{ClN}_7\text{O}$, found 292.0711 ($[\text{M}+\text{H}]^+$).

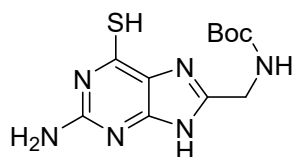
**(S15)** *6-(Cyclohexylsulfonyl)-9H-purin-2-amine*

A mixture of 6-(cyclohexylthio)-9*H*-purin-2-amine (0.10 mmol) and mCPBA (0.20 mmol) was stirred in DCM (2.0 mL) for 3 hours at room temperature. The reaction mixture was then purified by silica gel chromatography using a gradient of MeOH (0 – 15%) in DCM which afforded 4 mg (14%) of the title compound. LCMS $[M+H]^+$ 282. $^1\text{H-NMR}$ (400 MHz, $\text{DMSO-}d_6$) δ 11.95 (br. s., 3H), 8.45 (s, 1H), 6.09 – 8.10 (m, 1H), 3.75 (tt, $J = 3.3, 11.9$ Hz, 1H), 1.88 – 1.96 (m, 2H), 1.75 – 1.85 (m, 2H), 1.58 – 1.67 (m, 1H), 1.47 (dd, $J = 2.9, 12.2$ Hz, 1H), 1.40 (dd, $J = 3.1, 12.2$ Hz, 1H), 1.09 – 1.32 (m, 3H). $^{13}\text{C NMR}$ (176 MHz, $\text{DMSO-}d_6$) δ 159.85, 157.40, 152.31, 143.67, 121.93, 59.68, 24.84, 24.40, 24.11. HRMS (ESI $^+$): m/z calculated 282.1019 for $\text{C}_{11}\text{H}_{15}\text{N}_5\text{O}_2\text{S}$ found 282.1017 ($[M+H]^+$).



(S25): 2-Amino-8-(aminomethyl)-6,9-dihydro-3*H*-purine-6-thione

Tert-butyl *N*-[(2-amino-6-sulfanylidene-6,9-dihydro-3*H*-purin-8-yl)methyl]carbamate (**S26**, 25 mg, 0.084 mmol) was suspended in DCM (1 mL), then TFA (1 mL) was added. After 1 hours the solvents were evaporated and the crude compound was triturated using EtOH. The title compound was collected by filtration, no further purification was done. Yield 12 mg (72%). LCMS $[M+H]^+$ 197. $^1\text{H-NMR}$ (400 MHz, $\text{DMSO-}d_6$) δ 12.05 (br. s., 1H), 8.53 (br. s., 3H), 6.70 (br. s., 2H), 4.16 (br. s., 2H). $^{13}\text{C NMR}$ (176 MHz, $\text{DMSO-}d_6$) δ 158.26, 158.08, 153.25, 118.02, 116.32, 36.27. HRMS (ESI $^+$): m/z calculated 197.0604 for $\text{C}_6\text{H}_8\text{N}_6\text{S}$ found 197.0610 ($[M+H]^+$).

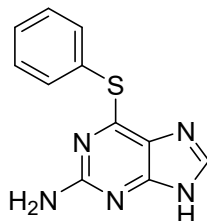


(S26): Tert-butyl *N*-[(2-amino-6-sulfanylidene-6,9-dihydro-3*H*-purin-8-yl)methyl]carbamate

Step 1. tert-butyl *N*-[(2-amino-6-chloro-9*H*-purin-8-yl)methyl]carbamate was synthesized according to General procedure D from *N*-Boc glycine which afforded 100 mg (33%). LCMS $[M+H]^+$ 299. $^1\text{H-NMR}$ (400 MHz, $\text{DMSO-}d_6$) δ 12.70 (s, 1H), 7.35 (br. s., 1H), 6.70 (s, 2H), 4.25 (d, $J = 5.6$ Hz, 2H), 1.41 (s, 9H).

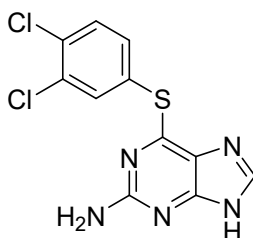
Step 2: A mixture of tert-butyl *N*-[(2-amino-6-chloro-9*H*-purin-8-yl)methyl]carbamate (45 mg, 0.15 mmol), thiourea (45 mg, 0.60 mmol), and formic acid (0.015 mL, 0.39 mmol) was stirred in EtOH (1.0 mL) at reflux for 3 h. After cooling, the precipitate was collected by filtration and washed with aq. ethanolic solution (70 %). No further purification was done. Yield 25 mg (56%). LCMS $[M+H]^+$ 297. $^1\text{H-NMR}$ (400 MHz, $\text{DMSO-}d_6$) δ 12.42 (br. s., 1H), 11.81 (br. s., 1H), 7.27 (br. s., 1H), 6.63 (br. s.,

1H), 6.45 (br. s., 1H), 4.12 – 4.27 (m, 2H), 1.39 (br. s., 9H). HRMS (ESI+): m/z calculated 297.1128 for $C_{11}H_{16}N_6O_2S$ found 297.1149 ($[M+H]^+$).



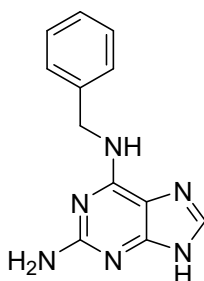
(S38) 6-(phenylthio)-9H-purin-2-amine

The title compound was synthesized according to Huang, *et. al.* Tetrahedron 2007, 63, 5323–5327.



(S39) 6-(3,4-dichlorophenyl)sulfanyl-9H-purin-2-amine

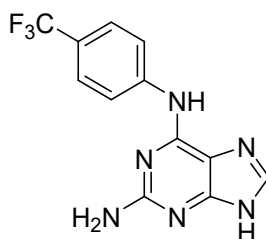
The compound was synthesised according to General procedure C from 2-amino-6-chloro-9H-purine (84 mg, 0.50 mmol) and 3,4-dichlorothiophenol (90 mg, 0.50 mmol). Purification on silica (DCM/MeOH gradient method) yielded the product as a white solid (21 mg, 13%). LCMS $[M+H]^+$ 312. 1H -NMR (400 MHz, DMSO- d_6) δ 12.61 (s, 1H), 7.96 (s, 1H), 7.88 (d, J = 2.1 Hz, 1H), 7.70 (d, J = 8.4 Hz, 1H), 7.59 (dd, J = 8.4, 2.1 Hz, 1H), 6.30 (s, 2H). ^{13}C NMR (151 MHz, DMSO- d_6) δ 159.74, 156.50, 152.56, 139.71, 135.85, 134.91, 131.86, 131.39, 130.92, 129.19, 123.53. HRMS (ESI+): m/z calculated 311.9872 for $C_{11}H_7Cl_2N_5S$ found 311.9870 ($[M+H]^+$).



(S40) N6-benzyl-9H-purin-2,6-diamine

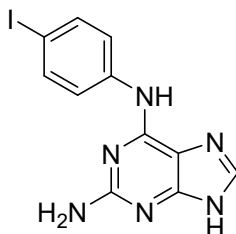
The compound was synthesised according to General procedure B from 2-amino-6-chloro-9H-purine (34 mg, 0.20 mmol) and benzylamine (55 μ L, 0.40 mmol). Purification by preparative HPLC (0.1% TFA in water/ acetonitrile) yielded the product as a white solid (13 mg, 19%). LCMS $[M+H]^+$ 241. 1H -

NMR (400 MHz, Methanol- d_4) δ 8.03 (s, 1H), 7.43 – 7.39 (m, 2H), 7.38 – 7.33 (m, 2H), 7.32 – 7.27 (m, 1H), 4.82 (s, 2H). ^{13}C NMR (176 MHz, DMSO- d_6) δ 160.16, 140.70, 135.24, 128.67, 128.61, 128.33, 128.08, 127.26, 126.44, 42.55. HRMS (ESI $^{+}$): m/z calculated 241.1196 for $\text{C}_{12}\text{H}_{12}\text{N}_6$ found 241.1182 ($[\text{M}+\text{H}]^{+}$).



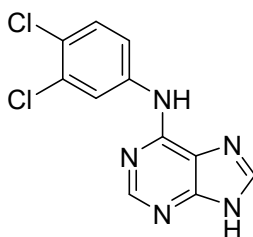
(S44): *N6-[4-(trifluoromethyl)phenyl]-9H-purin-2,6-diamine*

The compound was synthesised according to General procedure A from 2-amino-6-chloro-9H-purine (20 mg, 0.12 mmol) and 4-trifluoromethylaniline hydrochloride (25 mg, 0.13 mmol). Purification by preparative HPLC (0.1% TFA in water/acetonitrile) yielded the product as a white solid (19 mg, 53%). LCMS $[\text{M}+\text{H}]^{+}$ 295. ^1H -NMR (400 MHz, DMSO- d_6) δ 11.45 (s, 1H), 8.38 (s, 1H), 8.23 (d, $J = 8.3$ Hz, 2H), 7.73 (d, $J = 8.1$ Hz, 2H). ^{13}C -NMR (176 MHz, DMSO- d_6) δ 154.45, 150.04, 148.88, 141.98, 126.61, 125.96, 125.94, 125.06, 124.11, 123.52, 120.75. HRMS (ESI $^{+}$): m/z calculated 295.0914 for $\text{C}_{12}\text{H}_9\text{F}_3\text{N}_6$ found 295.0917 ($[\text{M}+\text{H}]^{+}$).



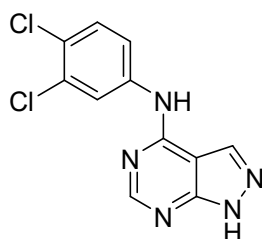
(S45): *N6-(4-iodophenyl)-9H-purin-2,6-diamine*

The compound was synthesised according to General procedure A from 2-amino-6-chloro-9H-purine (26 mg, 0.16 mmol) and 4-iodoaniline (45 mg, 0.20 mmol). Recrystallisation from methanol yielded the product as a white solid (19 mg, 25%). LCMS $[\text{M}+\text{H}]^{+}$ 353. ^1H -NMR (400 MHz, DMSO- d_6) δ 12.44 (br. s., 1H), 9.61 (br. s., 1H), 7.79 – 8.00 (m, 3H), 7.60 (d, $J = 8.5$ Hz, 2H), 6.21 (br. s., 2H). ^{13}C NMR (151 MHz, DMSO- d_6 + 4% H_2SO_4) δ 154.4, 150.5, 148.6, 142.7, 138.3, 138.0, 124.0, 106.4, 89.3. HRMS (ESI $^{+}$): m/z calculated 351.9928 for $\text{C}_{11}\text{H}_9\text{IN}_6$ found 353.0016 ($[\text{M}+\text{H}]^{+}$).



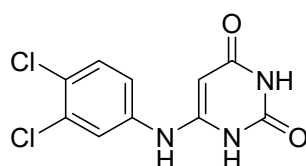
(S46) *N*-(3,4-dichlorophenyl)-9*H*-purin-6-amine

The title compound was synthesized according to Grotzfeld, Robert M.; Patel, Hitesh K.; Mehta, Shamal A.; Milanov, Zdravko V.; Lai, Andiliy G.; et al United States, US20050153989.



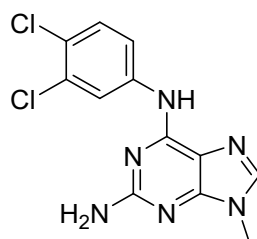
(S47) *N*-(3,4-dichlorophenyl)-1*H*-pyrazolo[3,4-*d*]pyrimidin-4-amine

The title compound was synthesized from 4-chloro-1*H*-pyrazolo[3,4-*d*]pyrimidine (16 mg, 0.10 mmol) and 3,4-dichloroaniline (23 mg, 0.14 mmol) according to General procedure A affording 10 mg (35%). LCMS $[M+H]^+$ 281. $^1\text{H-NMR}$ (400 MHz, $\text{DMSO-}d_6$) δ 13.76 (br. s., 1H), 10.23 (s, 1H), 8.49 (s, 1H), 8.39 (d, $J = 2.4$ Hz, 1H), 8.33 (s, 1H), 7.83 (dd, $J = 2.4, 8.8$ Hz, 1H), 7.67 (d, $J = 8.8$ Hz, 1H). $^{13}\text{C NMR}$ (176 MHz, $\text{DMSO-}d_6$) δ 155.02, 154.67, 153.75, 139.64, 132.28, 130.85, 130.54, 124.27, 121.61, 120.43, 100.82. HRMS (ESI $^+$): m/z calculated 280.0149 for $\text{C}_{11}\text{H}_8\text{N}_5\text{Cl}_2$, found 280.0151 ($[M+H]^+$).



(S48) 6-((3,4-dichlorophenyl)amino)pyrimidine-2,4(1*H*,3*H*)-dione

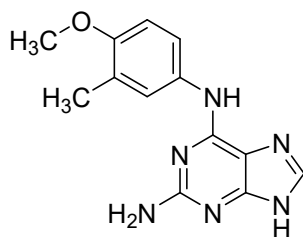
The title compound was synthesized according to J.M. Wilson, *et. al.*, Bioorg. Med. Chem. 15 (1) (2007) 77-86.



(S49) *N*6-(3,4-dichlorophenyl)-9-methyl-9*H*-purine-2,6-diamine

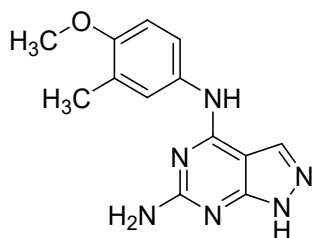
The title compound was synthesized from 6-chloro-9-methyl-9*H*-purin-2-amine (18 mg, 0.10 mmol) and 3,4-dichloroaniline (23 mg, 0.14 mmol) according to General procedure A. Purification by preparative HPLC (50 mM NH_4HCO_3 pH 10/ acetonitrile) yielded the product as a white solid (33%). $^1\text{H-NMR}$ (400 MHz, $\text{DMSO-}d_6$) δ 9.72 (s, 1H), 8.38 (d, $J = 2.1$ Hz, 1H), 8.07 (dd, $J = 2.3, 8.9$ Hz, 1H), 7.85 (s, 1H), 7.47 (d, $J = 8.9$ Hz, 1H), 6.28 (br. s., 2H), 3.60 (s, 3H). $^{13}\text{C NMR}$ (151 MHz, $\text{DMSO-}d_6$ +

4% H₂SO₄) δ 155.9, 151.5, 145.3, 139.9, 138.4, 131.2, 130.7, 126.0, 123.1, 121.9, 110.2, 31.2. HRMS (ESI⁺): m/z calculated 309.0417 for C₁₂H₁₀Cl₂N₆, found 309.0426 ([M+H]⁺).



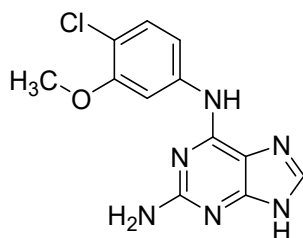
(S50): *N6-(4-methoxy-3-methylphenyl)-9H-purin-2,6-diamine*

The compound was synthesised according to General procedure A from 2-amino-6-chloro-9H-purine (18 mg, 0.11 mmol) and 4-methoxy-3-methylaniline (16 mg, 0.12 mmol). Purification by preparative HPLC (50 mM NH₄HCO₃ pH 10/ acetonitrile) yielded the product as a white solid (12 mg, 40%). LCMS [M+H]⁺ 271. ¹H NMR (400 MHz, DMSO-*d*₆) δ 12.20 (br. s., 1H), 8.97 (s, 1H), 7.68 – 7.79 (m, 3H), 6.83 (d, *J* = 8.5 Hz, 1H), 5.88 (br. s., 2H), 3.76 (s, 3H), 2.16 (s, 3H). ¹³C NMR (151 MHz, DMSO-*d*₆ + 4% H₂SO₄) δ 155.1, 154.0, 150.3, 148.0, 142.4, 130.3, 126.4, 124.9, 121.1, 110.7, 106.0, 55.8, 16.5. HRMS (ESI⁺): m/z calculated 271.1302 for C₁₃H₁₄N₆O, found 271.1331 ([M+H]⁺).

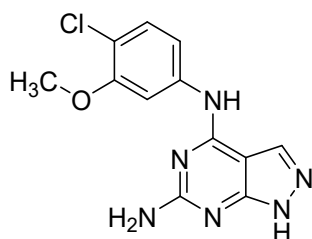


(S51) *N4-(4-methoxy-3-methylphenyl)-1H-pyrazolo[3,4-d]pyrimidin-4,6-diamine*

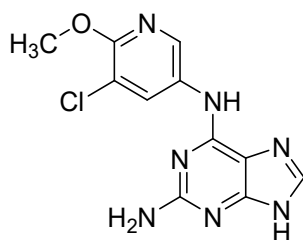
The compound was synthesised according to General procedure A from 4-chloro-1H-pyrazolo[3,4-d]pyrimidin-6-amine (17 mg, 0.10 mmol) and 4-methoxy-3-methylaniline (23 mg, 0.17 mmol). Purification by preparative HPLC (50 mM NH₄HCO₃ pH 10/ acetonitrile) yielded the product as a white solid (8 mg, 31%). LCMS [M+H]⁺ 271. ¹H-NMR (400 MHz, DMSO-*d*₆) δ 12.51 (s, 1H), 9.23 (s, 1H), 7.78 (s, 1H), 7.62 – 7.56 (m, 2H), 6.88 (d, *J* = 8.8 Hz, 1H), 6.14 (s, 2H), 3.78 (s, 3H), 2.17 (s, 3H). ¹³C-NMR (101 MHz, DMSO-*d*₆) δ 156.6, 156.5 (overlap), 155.3, 149.4, 130.5, 128.4, 126.2, 125.5, 121.9, 110.6, 97.5, 55.9, 16.6. HRMS (ESI⁺): m/z calculated 271.1302 for C₁₃H₁₅N₆O, found 271.1300 ([M+H]⁺).

**(S52):** *N6-(4-chloro-3-methoxyphenyl)-9H-purin-2,6-diamine*

The compound was synthesised according to General procedure A from 19.7 mg 2-amino-6-chloro-9H-purine (20 mg, 0.12 mmol) and 4-chloro-3-methoxyaniline (21 mg, 0.14 mmol). Recrystallisation from methanol yielded the product as a white solid (33 mg, 95%). LCMS $[M+H]^+$ 291. $^1\text{H-NMR}$ (400 MHz, $\text{DMSO-}d_6$) δ 7.93 (s, 1H), 7.57 (dd, $J = 8.7, 2.4$ Hz, 1H), 7.32 (d, $J = 8.6$ Hz, 1H), 7.29 (s, 1H), 7.16 (s, 1H), 7.03 (s, 1H), 3.88 (s, 3H). $^{13}\text{C NMR}$ (151 MHz, $\text{DMSO-}d_6 + 4\% \text{H}_2\text{SO}_4$) δ 154.7, 154.2, 150.2, 148.4, 142.3, 138.3, 129.9, 116.6, 114.0, 106.1, 56.4. HRMS (ESI $^+$): m/z calculated 291.0756 for $\text{C}_{12}\text{H}_{12}\text{N}_6\text{OCl}$, found 291.0754 ($[M+H]^+$).

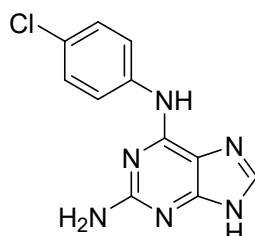
**(S53):** *N4-(4-chloro-3-methoxyphenyl)-1H-pyrazolo[3,4-d]pyrimidin-4,6-diamine*

The compound was synthesised according to General procedure A from 4-chloro-1H-pyrazolo[3,4-d]pyrimidin-6-amine (18 mg, 0.10 mmol) and 4-chloro-3-methoxyaniline (25 mg, 0.16 mmol). Recrystallisation from methanol yielded the product as a yellowish solid (11 mg, 37%). LCMS $[M+H]^+$ 291. $^1\text{H-NMR}$ (400 MHz, $\text{DMSO-}d_6$) δ 11.27 (s, 1H), 8.81 (s, 1H), 8.13 – 7.70 (m, 2H), 7.56 – 7.35 (m, 2H), 6.52 (s, 1H), 3.91 (s, 3H). $^{13}\text{C-NMR}$ (101 MHz, $\text{DMSO-}d_6$) δ 156.9, 156.7, 154.8, 149.7, 138.4, 130.0, 128.8, 117.3, 115.4, 107.6, 97.8, 56.7. HRMS (ESI $^+$): m/z calculated 291.0756 for $\text{C}_{12}\text{H}_{12}\text{N}_6\text{OCl}$, found 291.0755 ($[M+H]^+$).

**(S54):** *N6-(5-chloro-6-methoxypyridin-3-yl)-9H-purine-2,6-diamine*

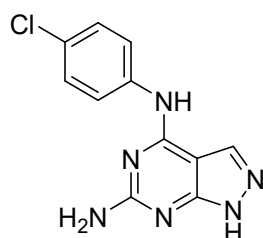
The compound was synthesised according to General procedure A from 2-amino-6-chloro-9H-purine (22 mg, 0.13 mmol) and 5-chloro-6-methoxy-pyridin-3-amine (20 mg, 0.13 mmol). Recrystallisation

from methanol yielded the product as a white solid (20 mg, 53%). LCMS $[M+H]^+$ 292. $^1\text{H-NMR}$ (400 MHz, $\text{DMSO-}d_6$) δ 8.79 (d, $J = 2.5$ Hz, 1H), 8.42 (d, $J = 2.4$ Hz, 1H), 8.05 (s, 1H), 6.78 (s, 2H), 3.93 (s, 3H). $^{13}\text{C NMR}$ (151 MHz, $\text{DMSO-}d_6 + 4\% \text{H}_2\text{SO}_4$) δ 155.5, 154.1, 150.3, 148.1, 142.2, 137.7, 132.1, 129.8, 116.4, 106.3, 54.4. HRMS (ESI $^+$): m/z calculated 292.0708 for $\text{C}_{11}\text{H}_{10}\text{ClN}_7\text{O}$, found 292.0714 ($[M+H]^+$).



(S55): *N6-(4-chlorophenyl)-9H-purin-2,6-diamine*

The compound was synthesised according to General procedure A from 2-amino-6-chloro-9H-purine (21 mg, 0.12 mmol) and 4-chloroaniline (17 mg, 0.13 mmol). Recrystallisation from methanol yielded the product as a white solid (24 mg, 76%). LCMS $[M+H]^+$ 261. $^1\text{H-NMR}$ (400 MHz, $\text{DMSO-}d_6$) δ 12.42 (s, 1H), 9.58 (s, 1H), 8.06 (d, $J = 9.0$ Hz, 2H), 7.86 (s, 1H), 7.30 (d, $J = 9.0$ Hz, 2H), 6.15 (s, 2H). $^{13}\text{C NMR}$ (176 MHz, $\text{DMSO-}d_6$) δ 159.18, 152.57, 151.52, 139.33, 137.10, 128.12, 125.37, 121.51, 112.41. HRMS (ESI $^+$): m/z calculated 261.0650 for $\text{C}_{11}\text{H}_9\text{ClN}_6$, found 261.0662 ($[M+H]^+$).

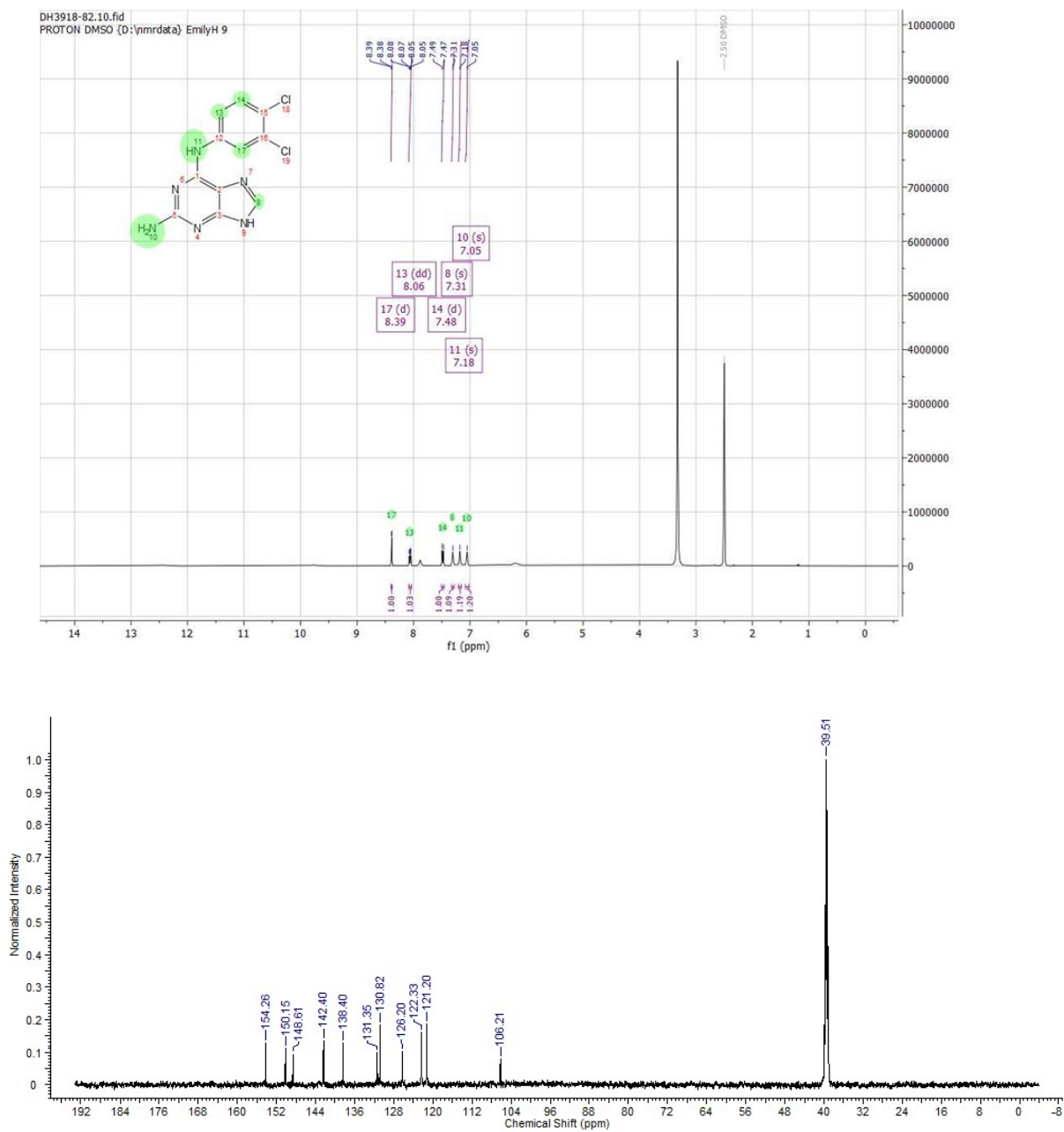


(S56): *N4-(4-chlorophenyl)-1H-pyrazolo[3,4-d]pyrimidin-4,6-diamine*

The compound was synthesised according to General procedure A from 4-chloro-1H-pyrazolo[3,4-d]pyrimidin-6-amine (18 mg, 0.11 mmol) and 4-chloroaniline (16 mg, 0.12 mmol). Recrystallisation from methanol yielded the product as a yellow solid (8 mg, 28%). LCMS $[M+H]^+$ 261. $^1\text{H-NMR}$ (400 MHz, $\text{DMSO-}d_6$) δ 12.65 (s, 1H), 9.63 (s, 1H), 8.02 – 7.94 (m, 3H), 7.40 – 7.31 (m, 2H), 6.35 (s, 2H). $^{13}\text{C-NMR}$ (101 MHz, $\text{DMSO-}d_6$) δ 156.9, 156.7, 149.6, 137.4, 129.2, 129.0, 124.4, 97.7. HRMS (ESI $^+$): m/z calculated 261.0650 for $\text{C}_{11}\text{H}_{10}\text{N}_6\text{Cl}$, found 261.0647 ($[M+H]^+$).

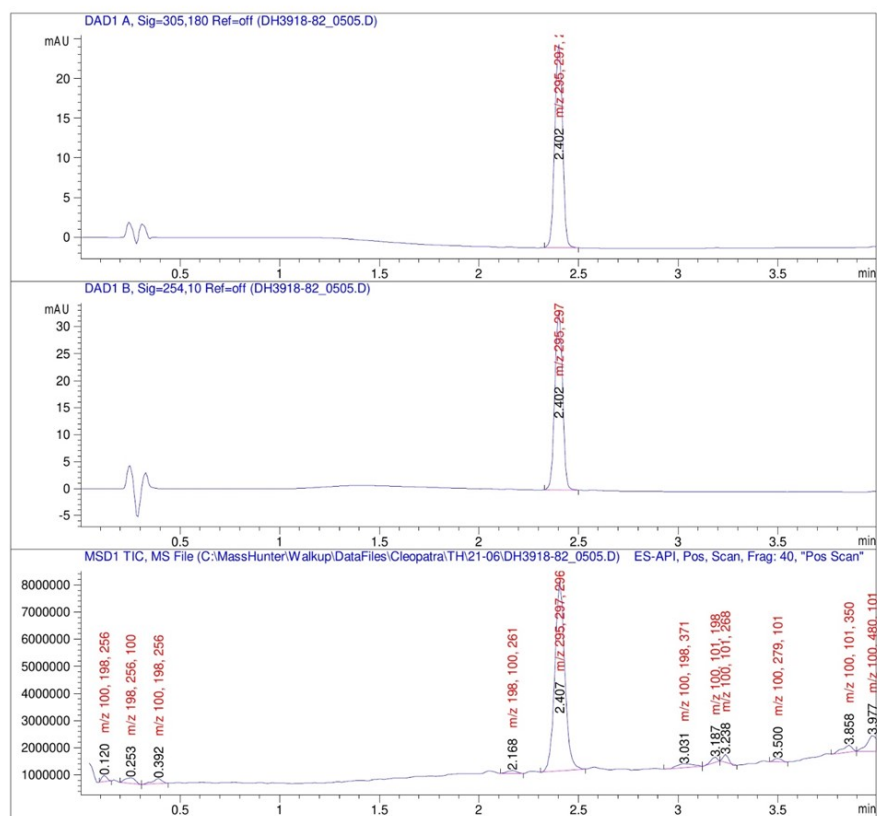
NMR Spectra and LC-UV purity:

Compound (11):

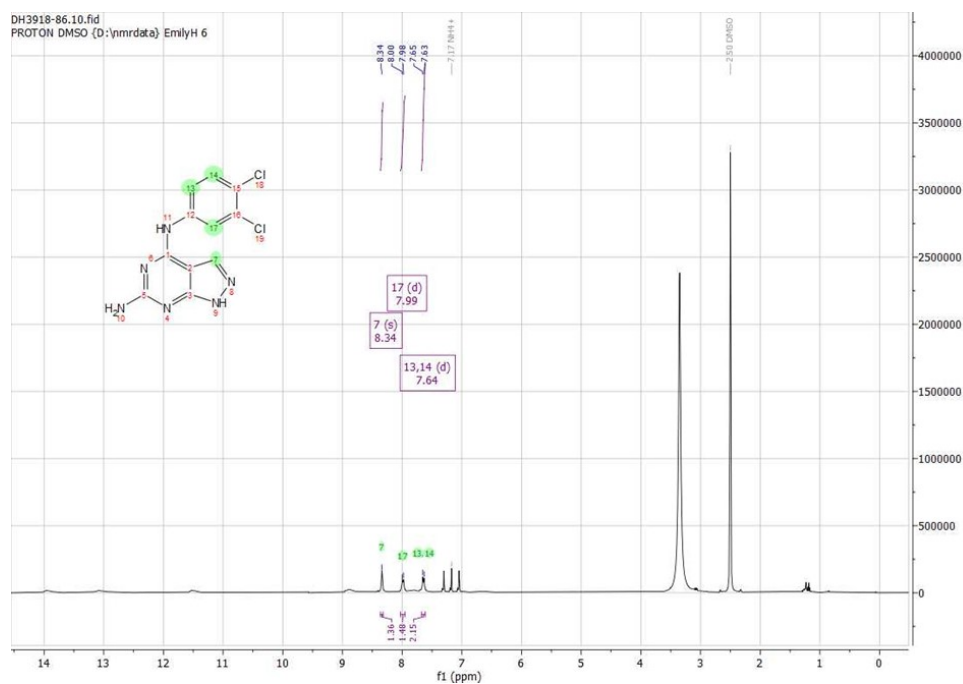


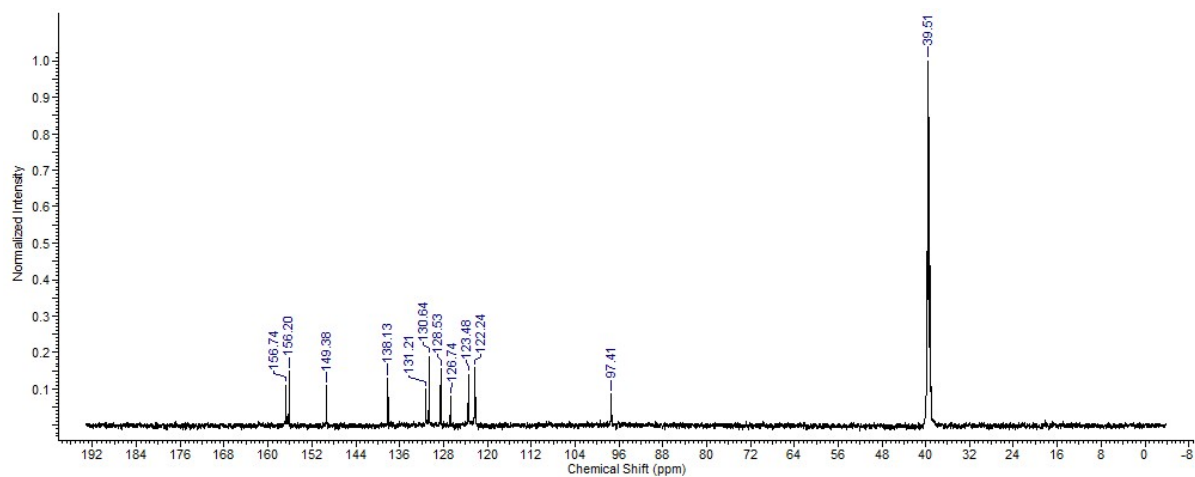
Method Info : X-bridge C18, 50x3.0 mm, 3.5u, 10-97% MeCN 3min,1mL/min, B: MeCN C: NH4HCO3

Sample Info : Walkup method: 'X1097-3'
Target:



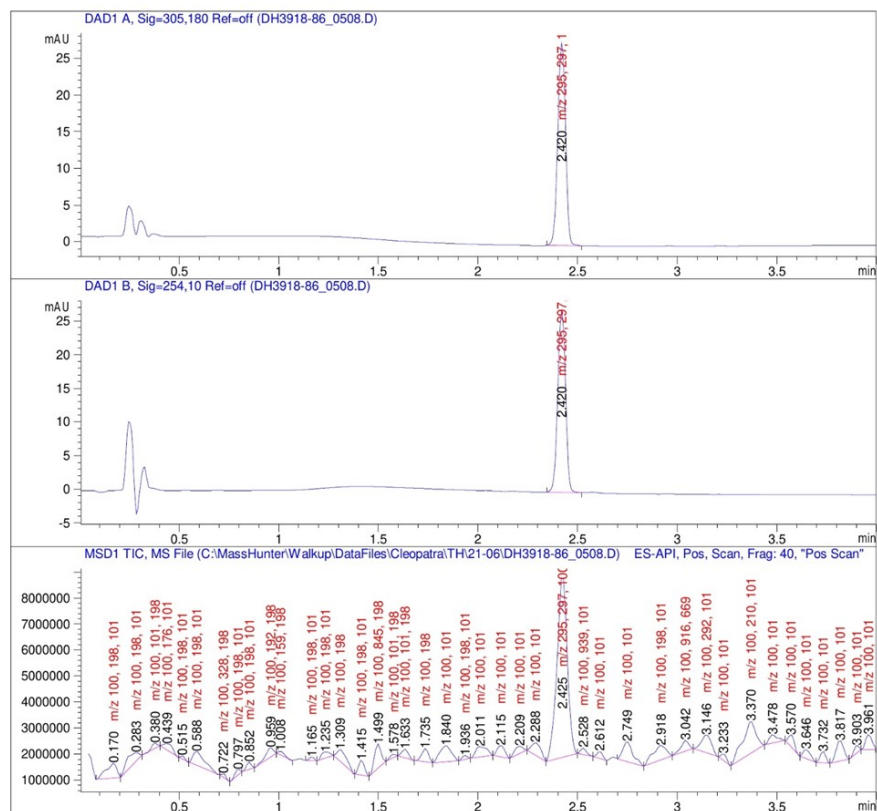
Compound (12):



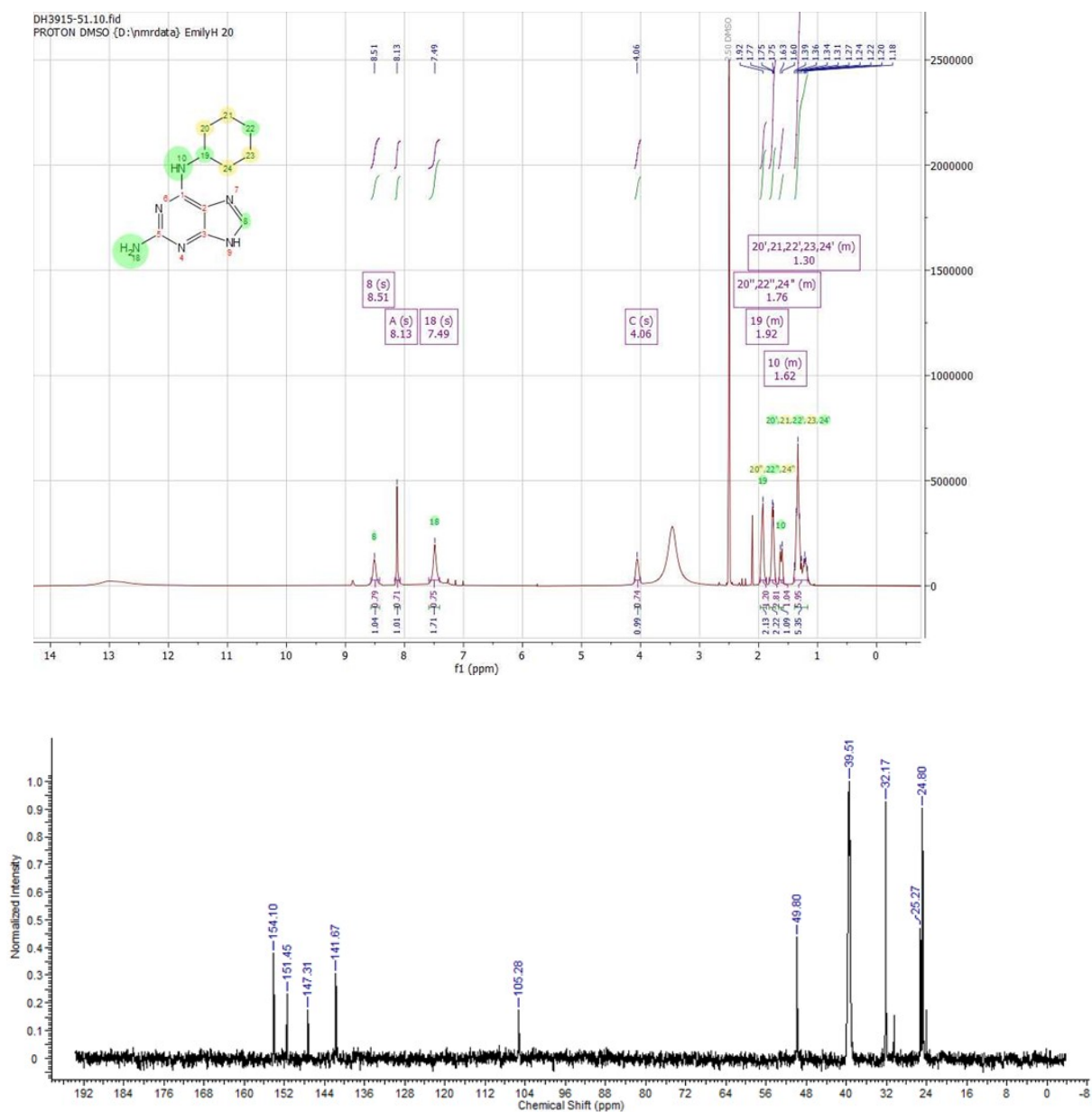


Method Info : X-bridge C18, 50x3.0 mm, 3.5u, 10-97% MeCN 3min,1mL/min, B: MeCN C: NH₄HC03

Sample Info : Walkup method: 'X1097-3'
Target:

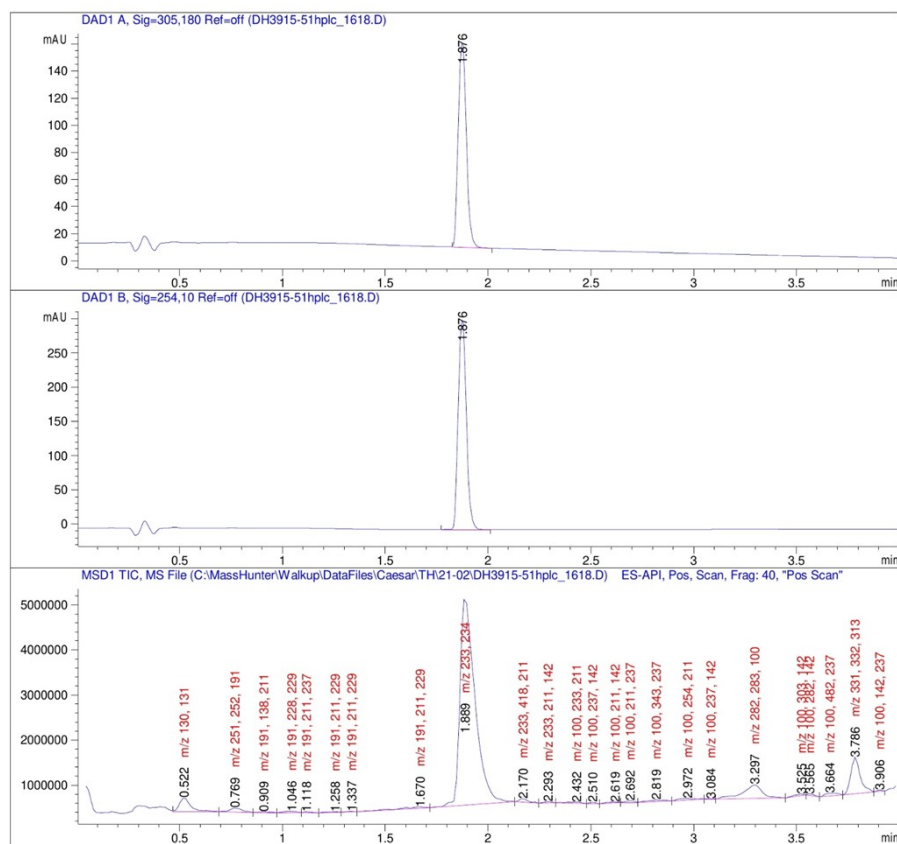


Compound (13):

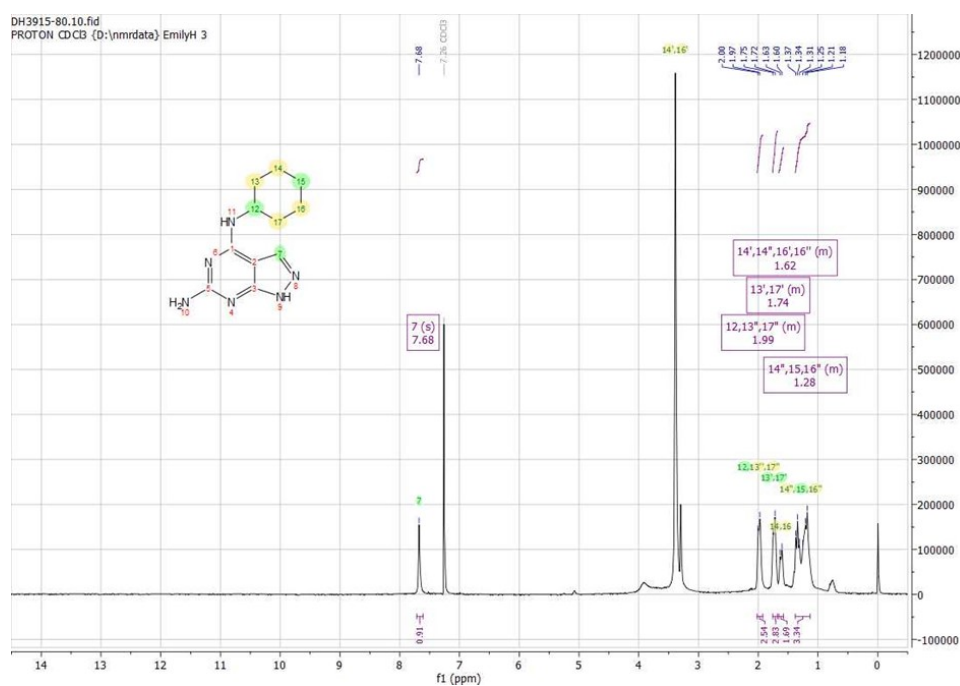


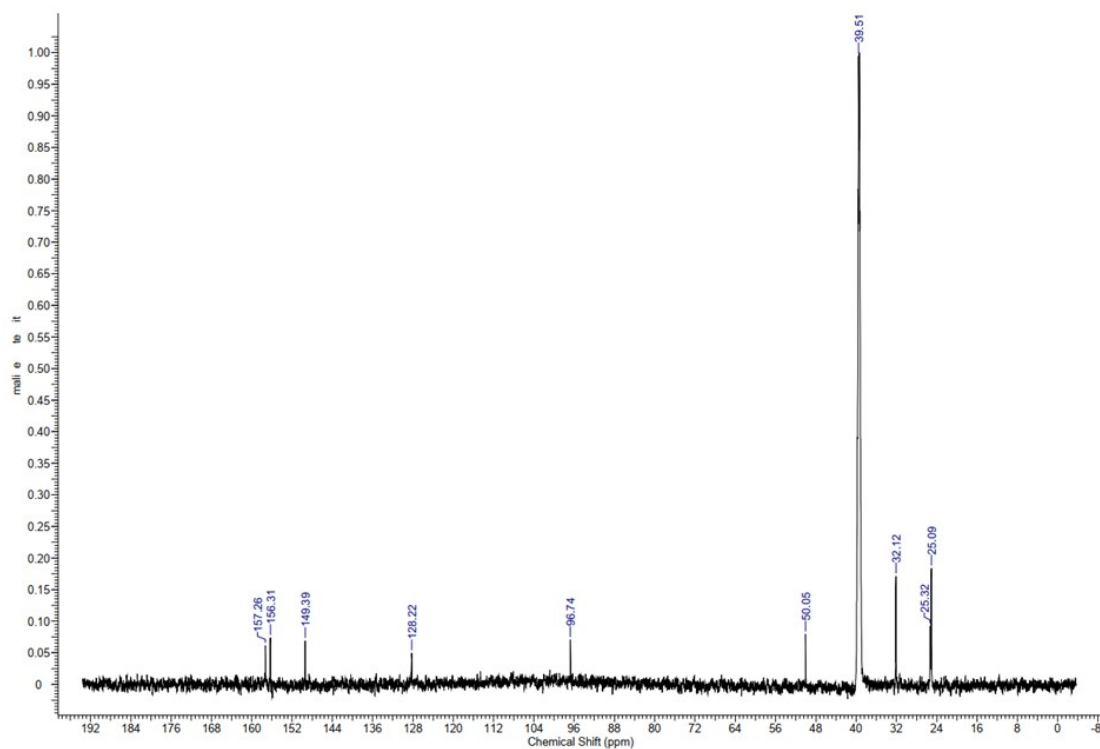
Method Info : ACE C8, 50x3mm, 3μ, 10-97% MeCN, 3min; 1ml/min, A: water 0.1% TFA B MeCN

```
Sample Info      : Walkup method: 'A1097-3'
                  Target:
```



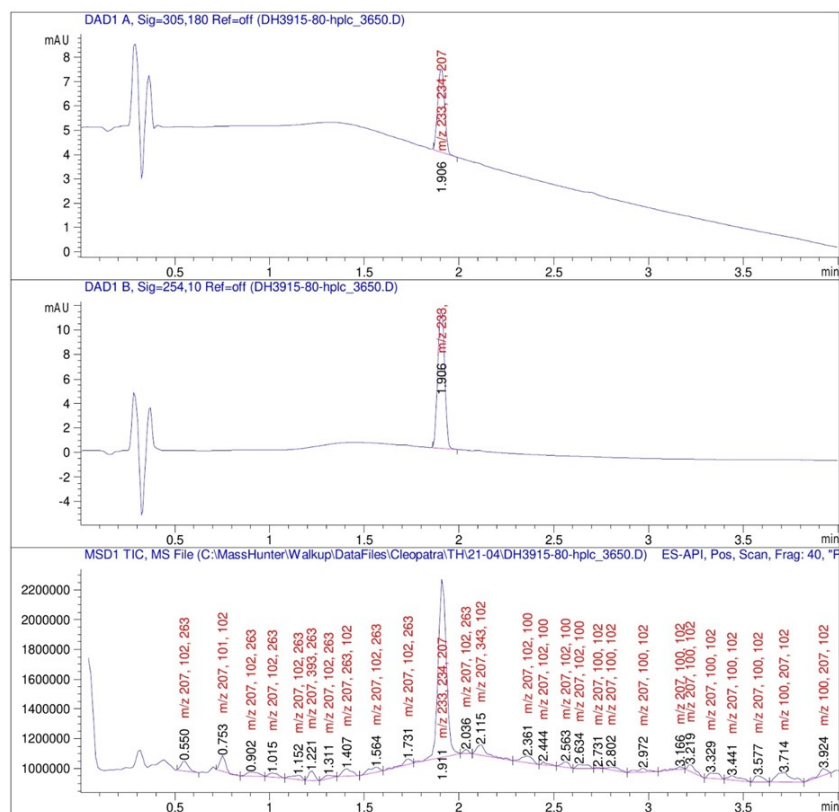
Compound (**14**):



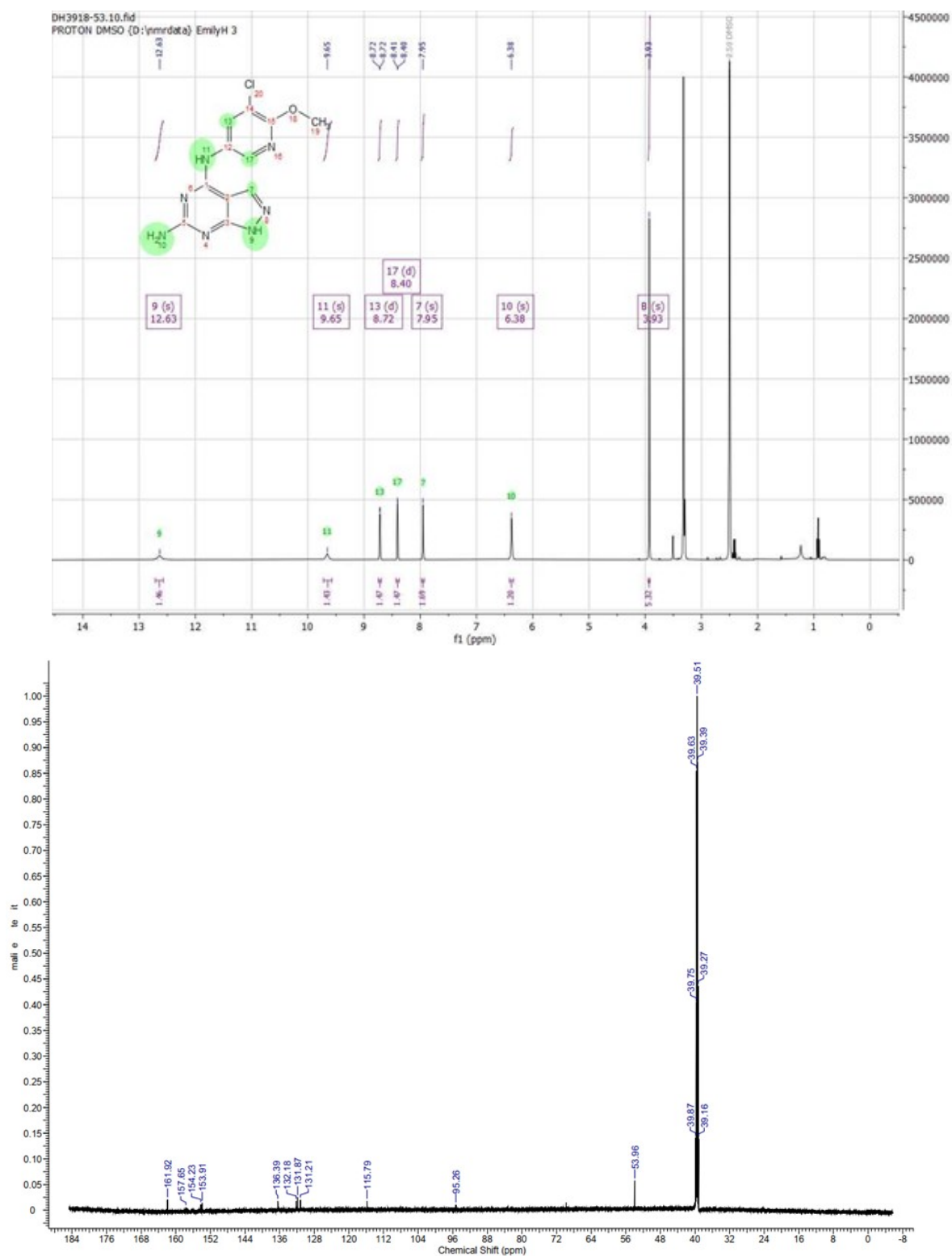


Method Info : ACE C8, 50x3mm, 3μ, 10-97% MeCN, 3min; 1mL/min, A: 0.1% TFA, B:MeCN.

Sample Info : Walkup method: 'A1097-3'
Target:

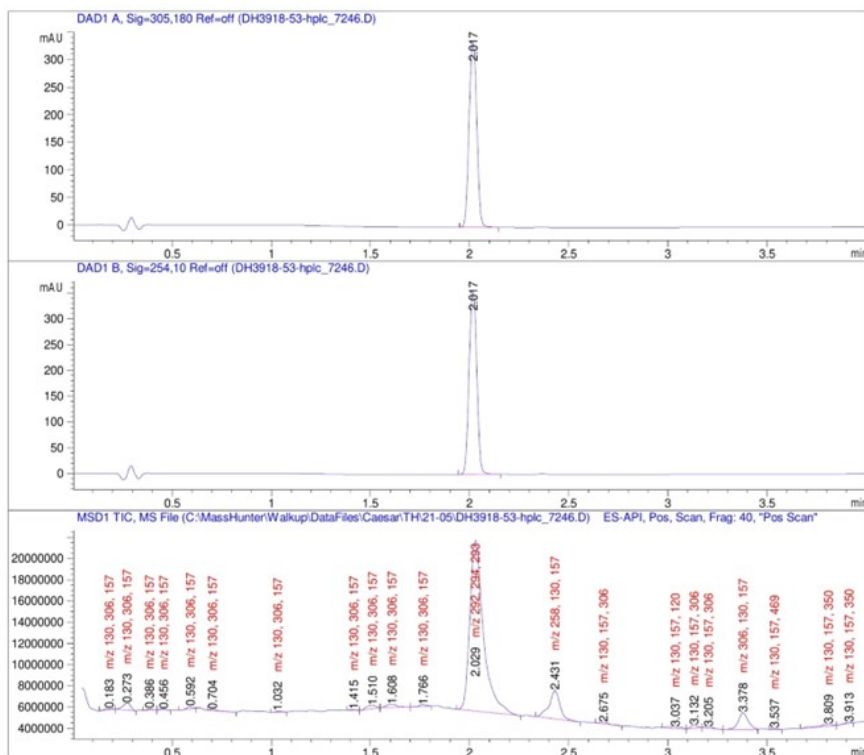


Compound (15):

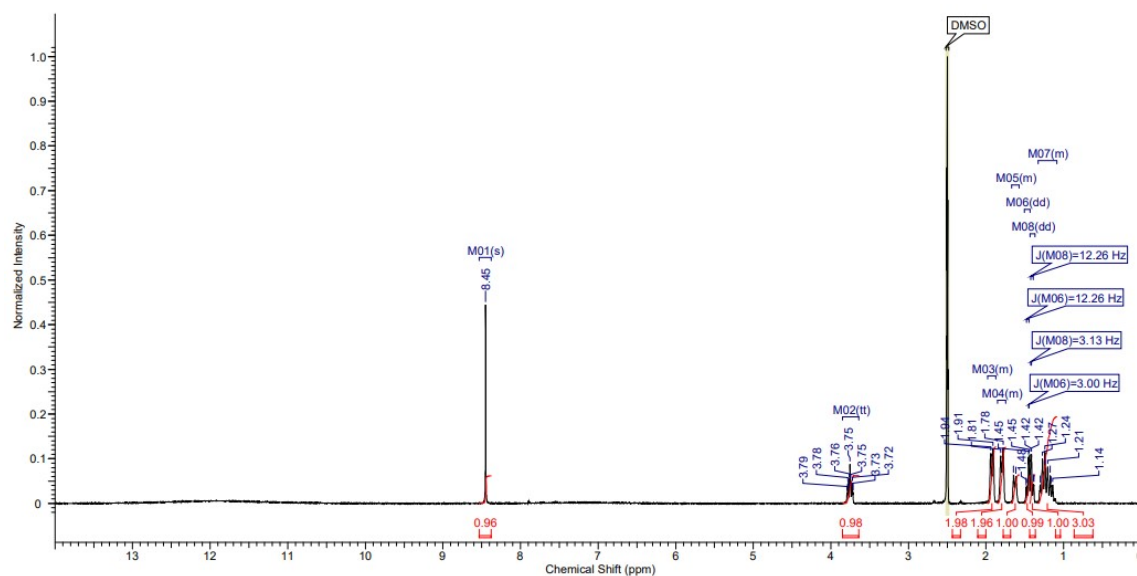


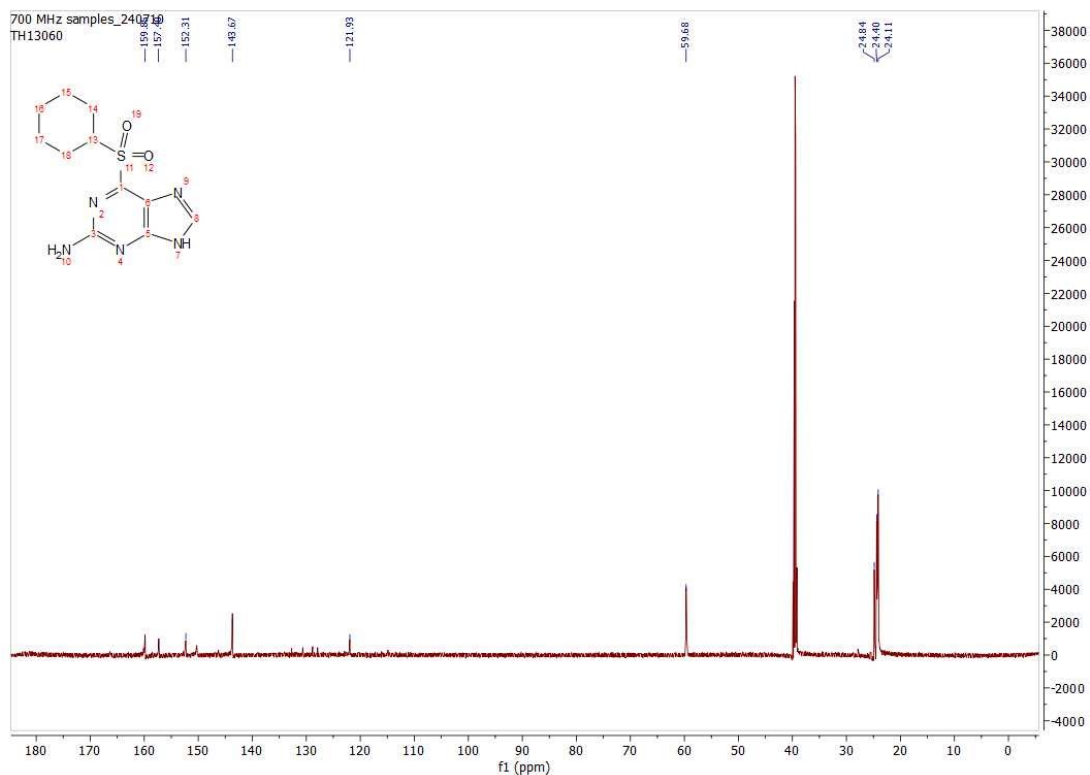
Method Info : X-bridge C18, 50x3.0 mm, 3.5u, 10-97% MeCN 1.5min,1ml/min, B: MeCN C: NH4HCO3

Sample Info : Walkup method: 'X1097'
Target:



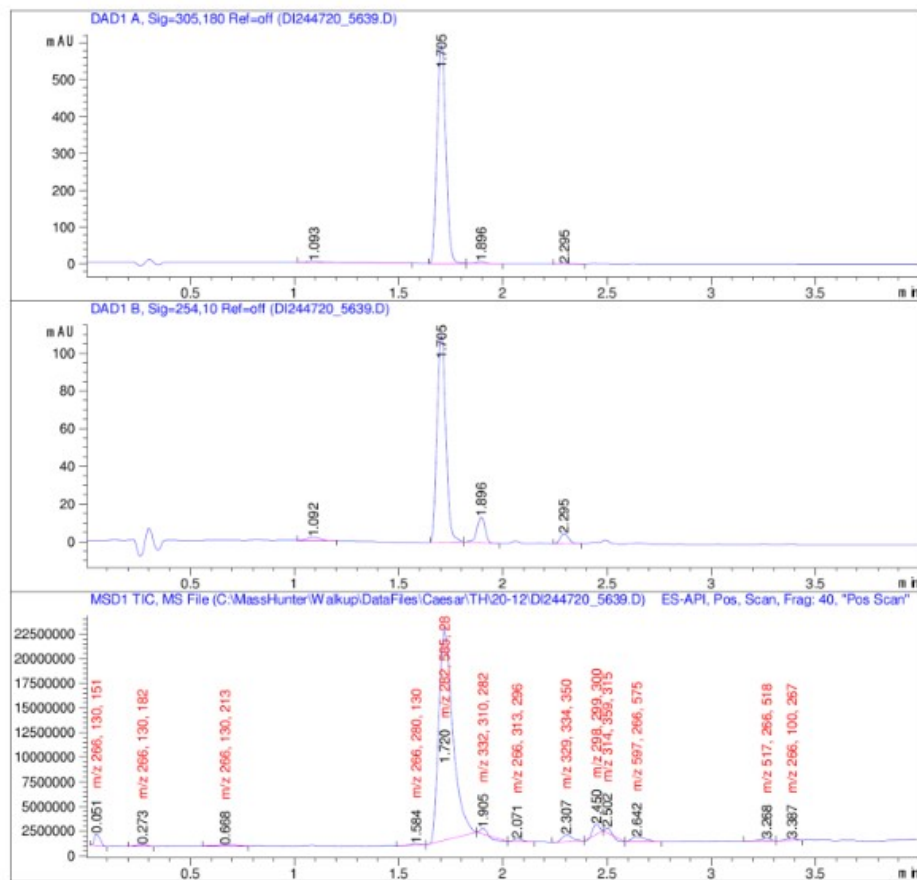
Compound (S15):



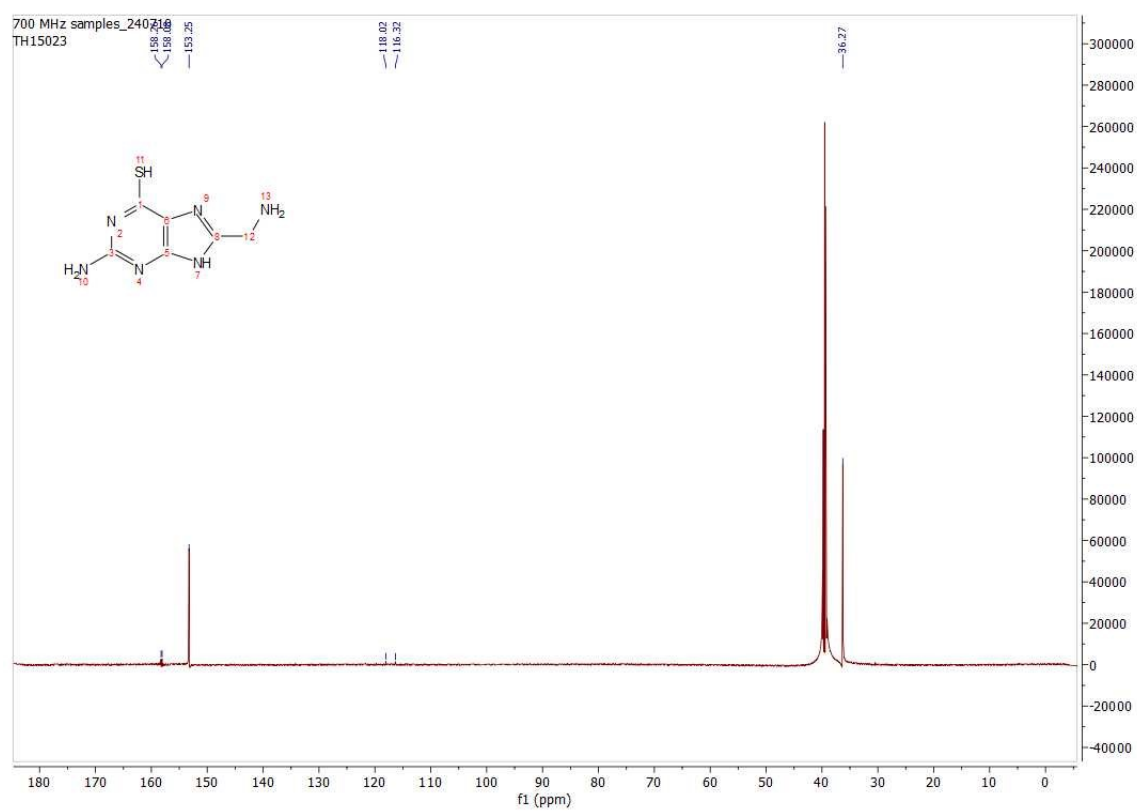
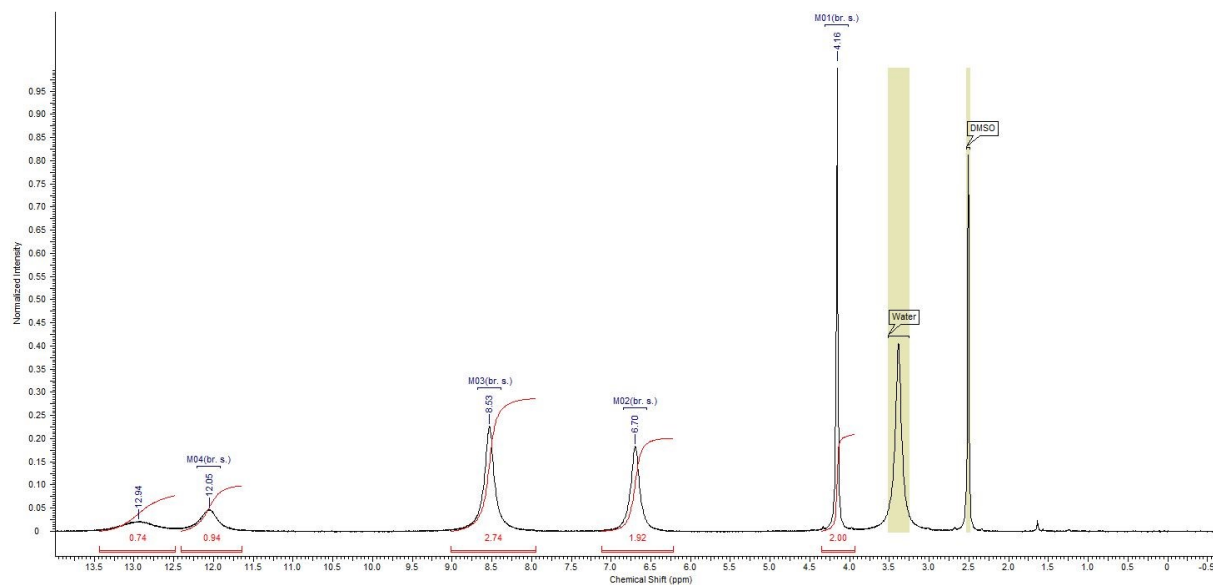


Method Info : X-bridge C18, 50x3.0 mm, 3.5u, 5-60% MeCN 3min,1ml/min, B: MeCN C: NH4HCO3

Sample Info : Walkup method: 'X0560-3'
Target:

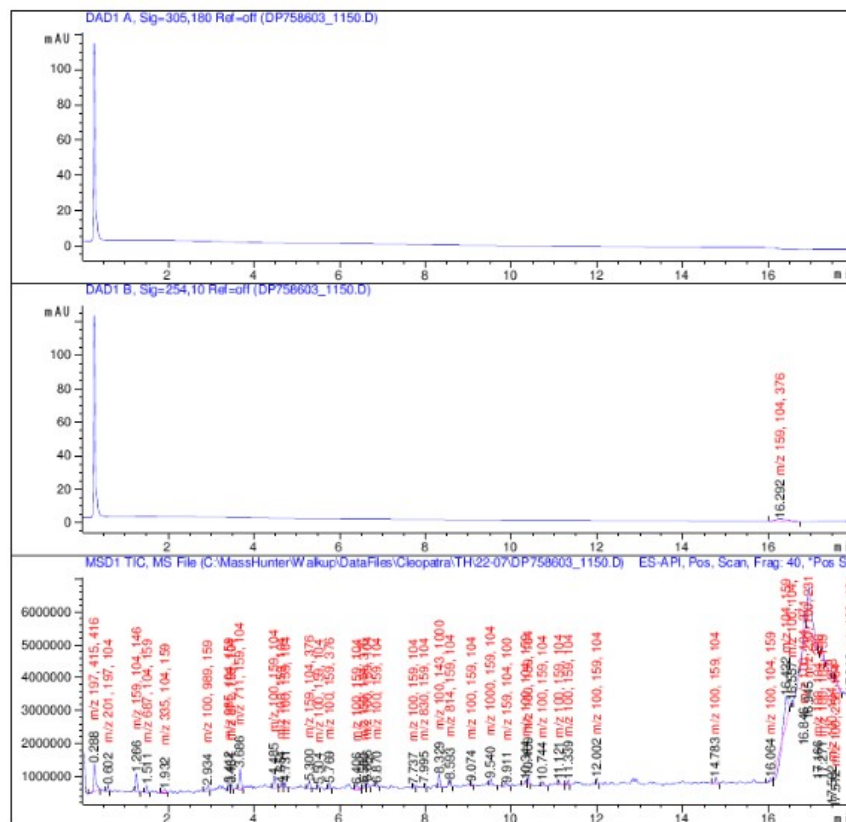


Compound (S25):

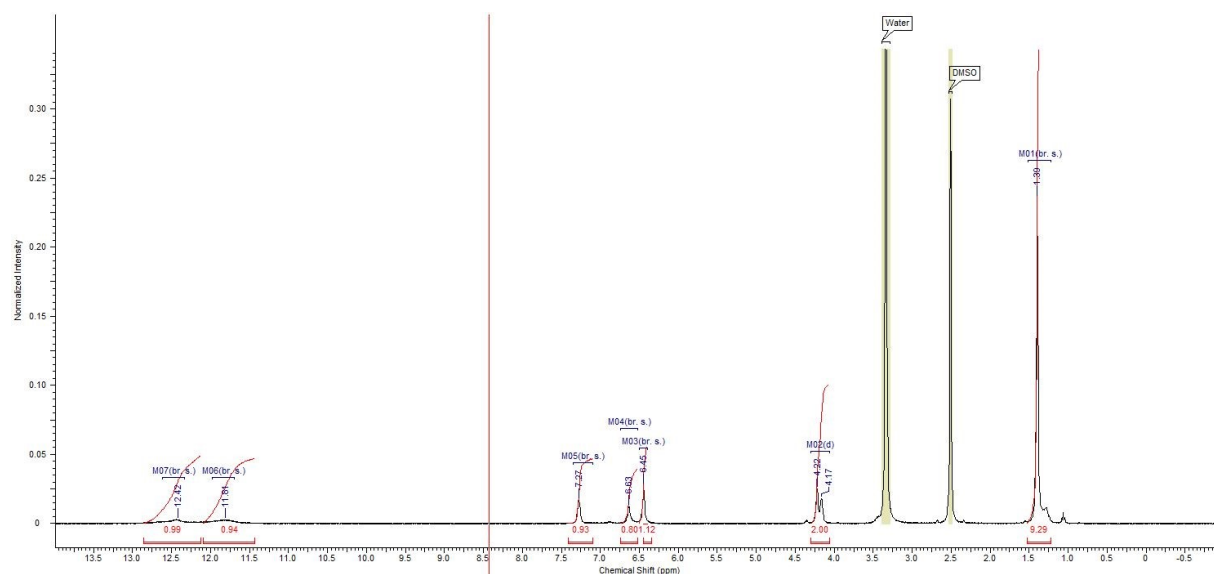


Method Info : X-bridge C18, 50x3.0 mm, 3.5u, 00-10% MeCN 15min, 1ml/min, B: MeCN C: NH4HCO3

Sample Info : Walkup method: 'x0010-15'
Target:

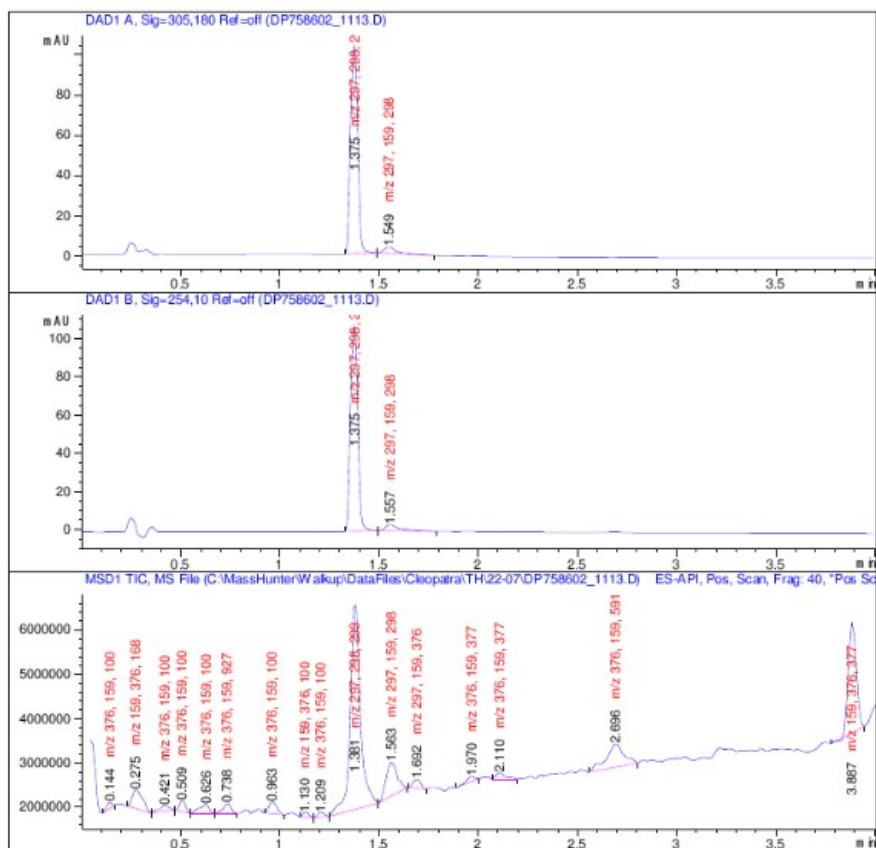


Compound (S26):

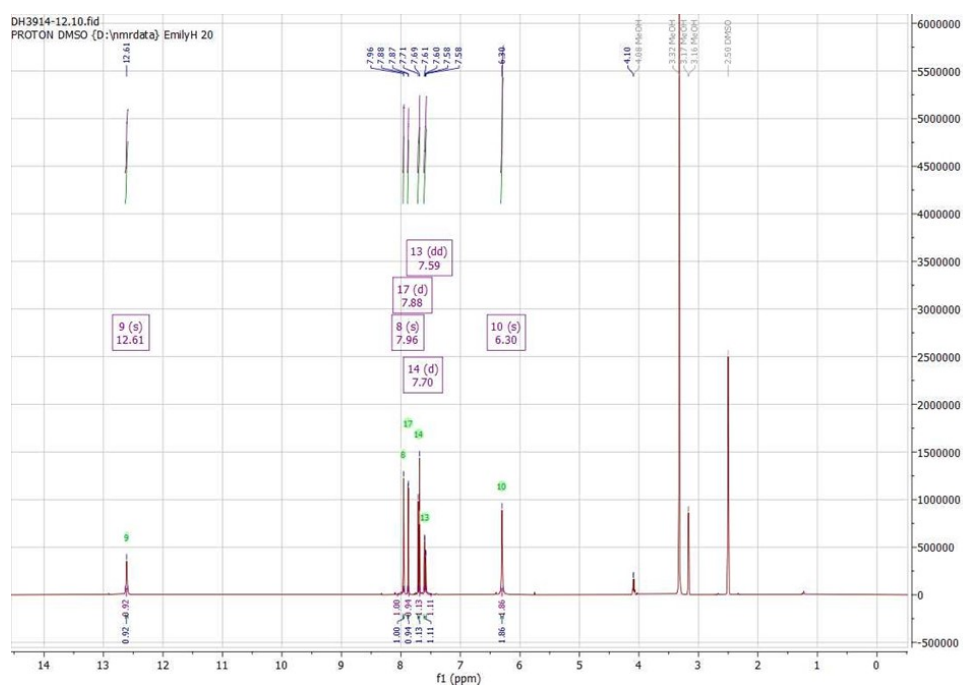


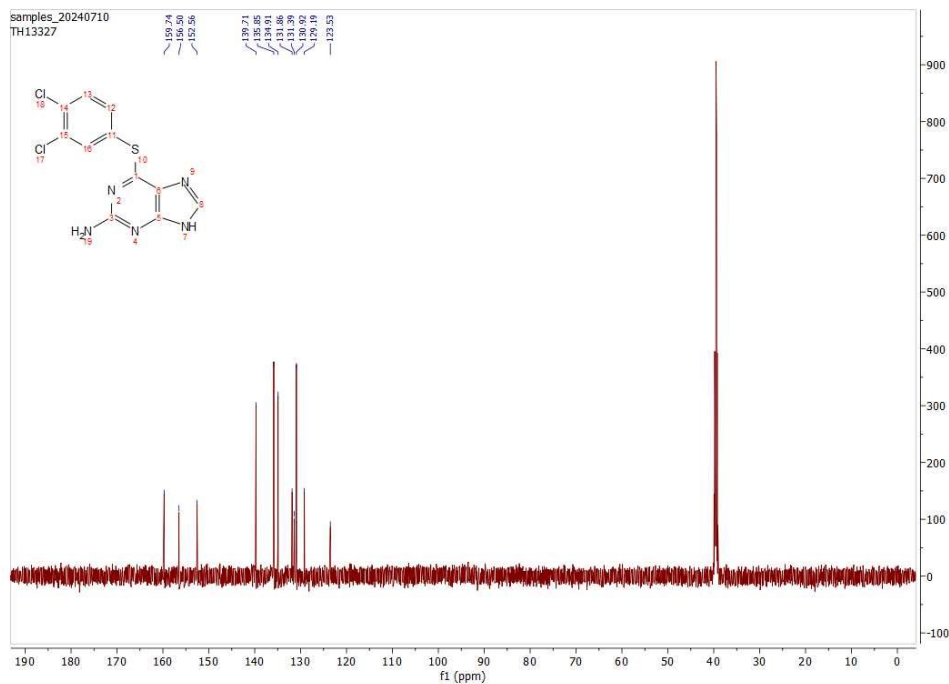
Method Info : X-bridge C18, 50x3.0 mm, 3.5u, 5-60% MeCN 3min, 1ml/min, B: MeCN C: NH4HCO3

```
Sample Info      : Walkup method: 'X0560-3'
                  Target:
```



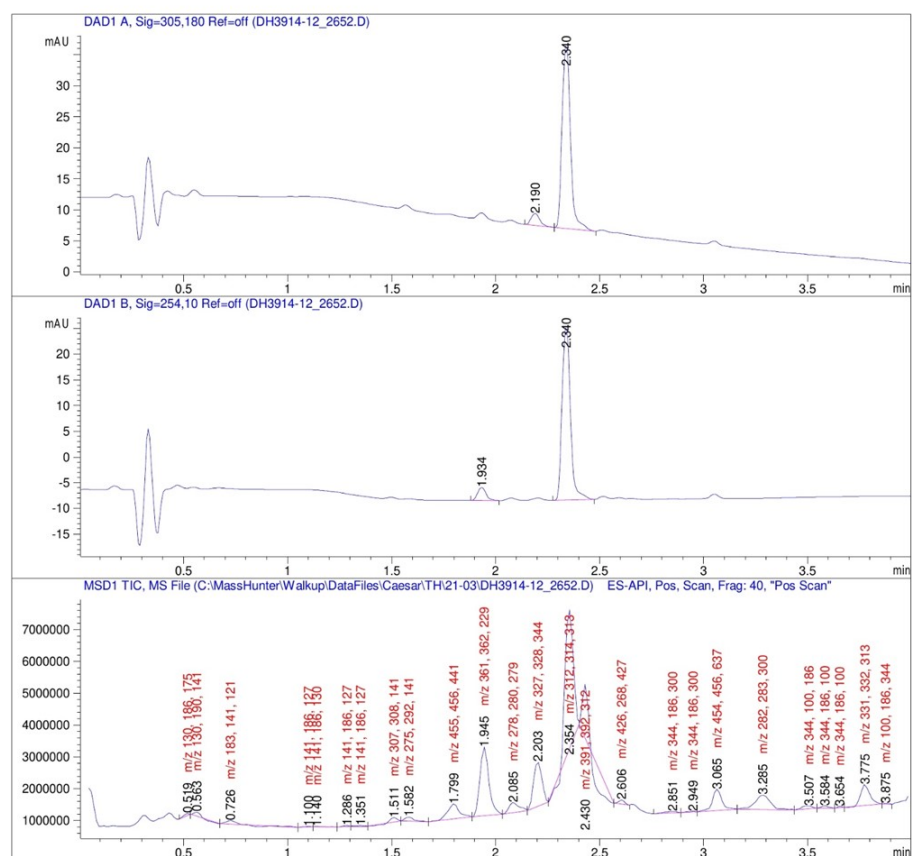
Compound (S39):



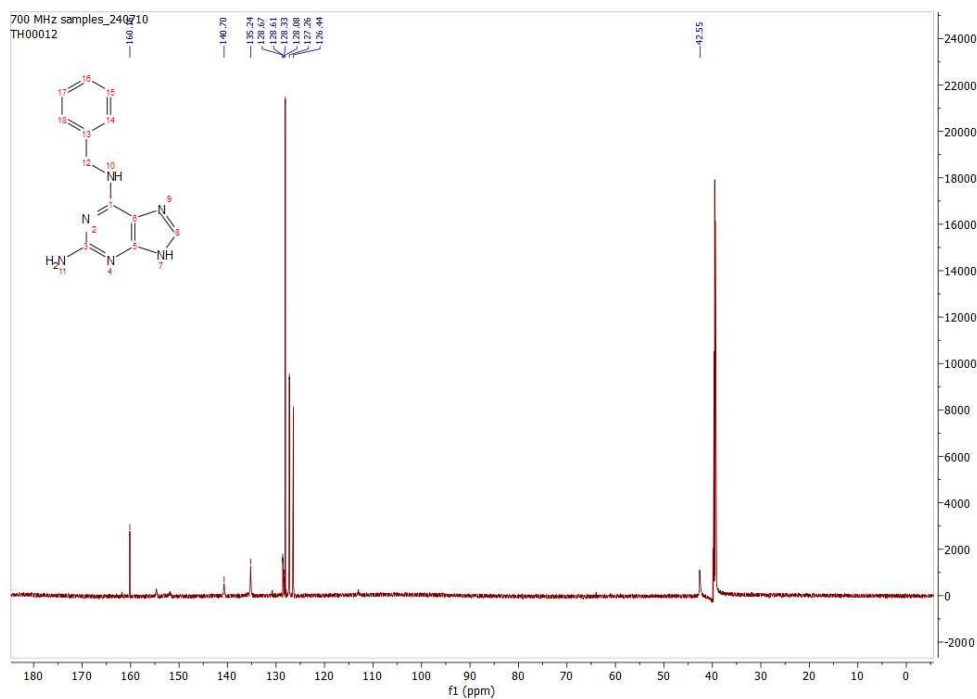
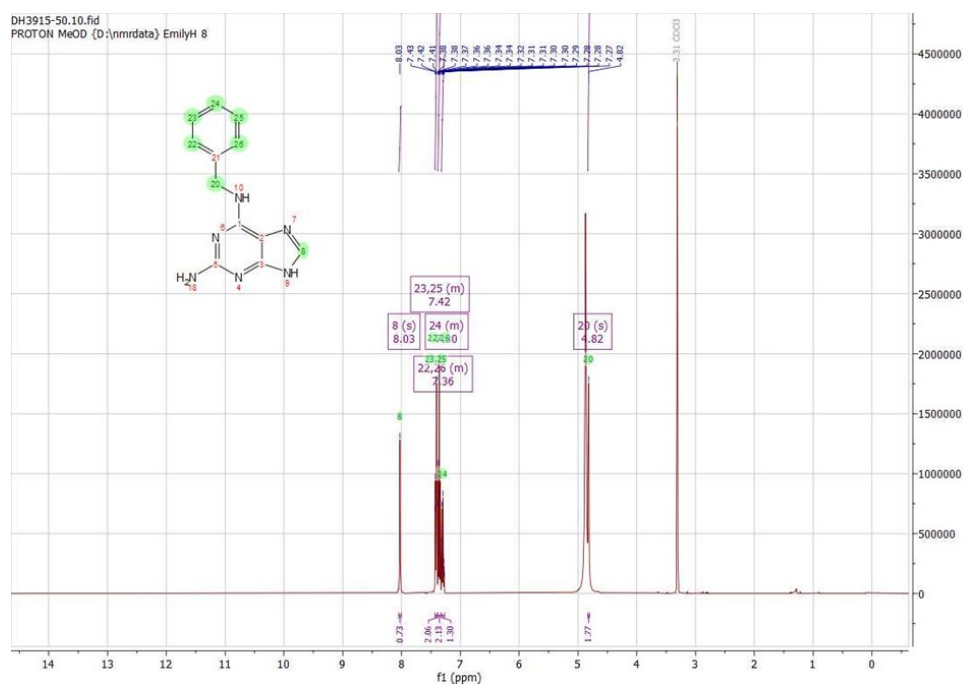


Method Info : ACE C8, 50x3mm, 3 μ , 10-97% MeCN, 3min; 1mL/min, A: water 0.1% TFA B MeCN

Sample Info : Walkup method: 'A1097-3'
Target:

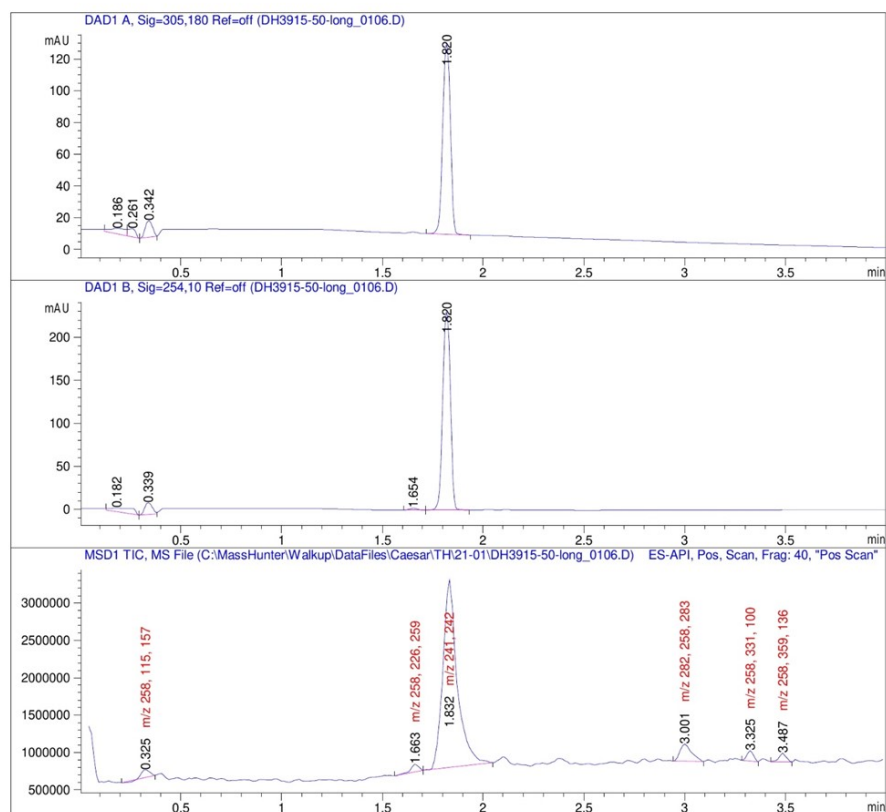


Compound (S40):

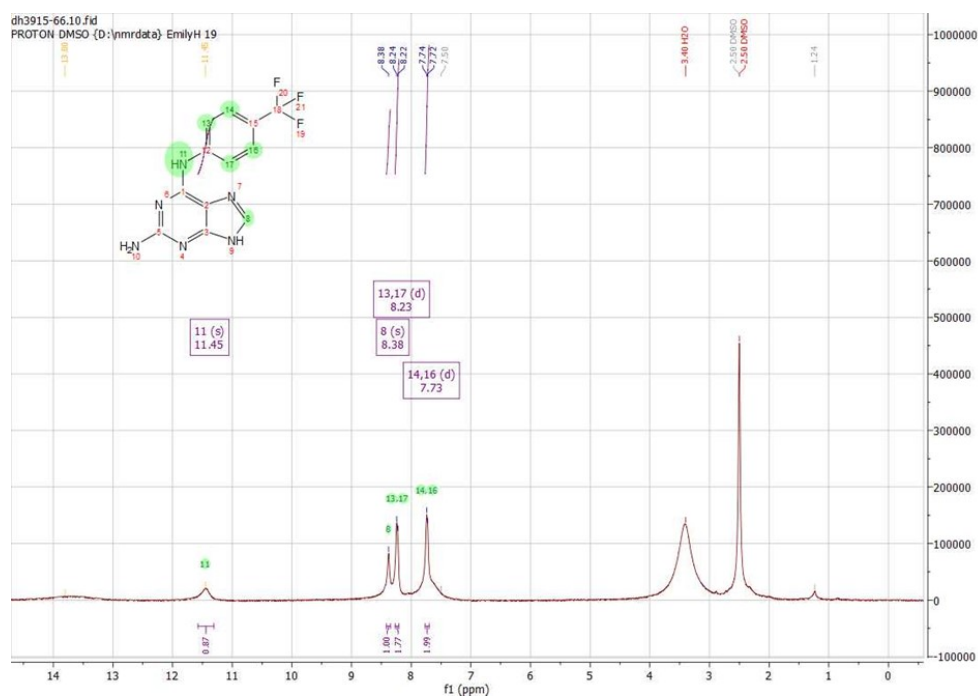


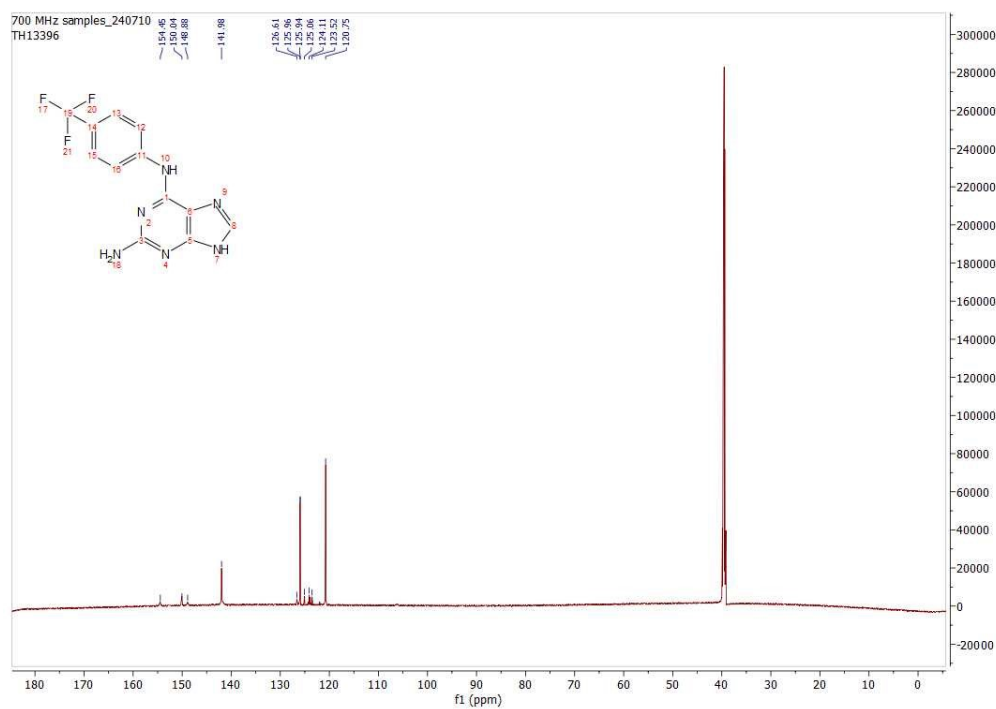
Method Info : ACE Phenyl, 50x3mm, 3 μ ,10-97% MeCN, 3min; 1mL/min, A: 0.1% TFA, B:MeCN.

Sample Info : Walkup method: 'Ph1097-3'
Target:



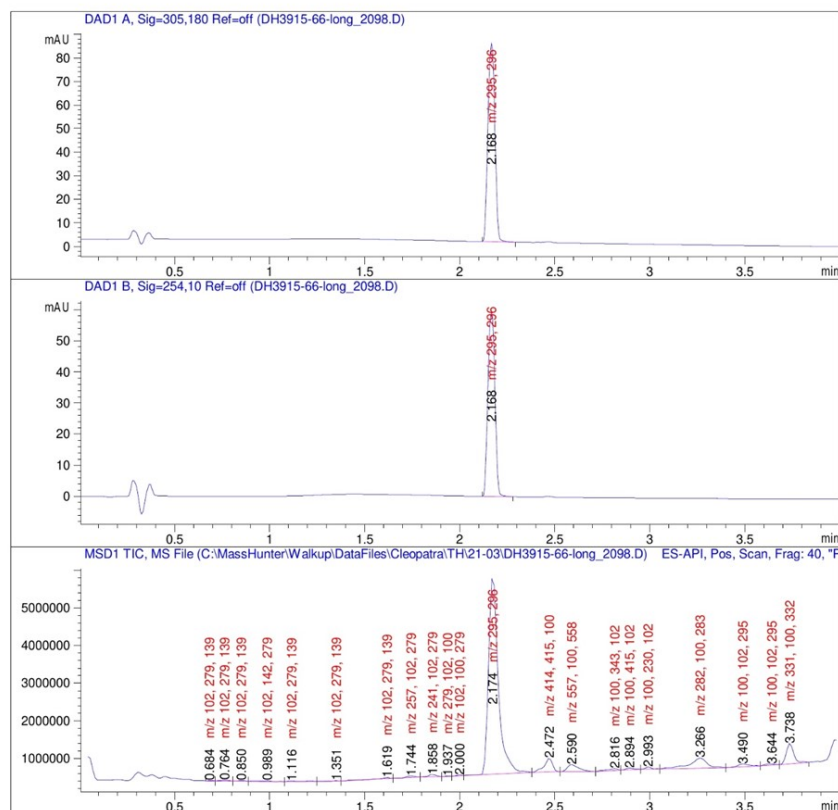
Compound (S44):



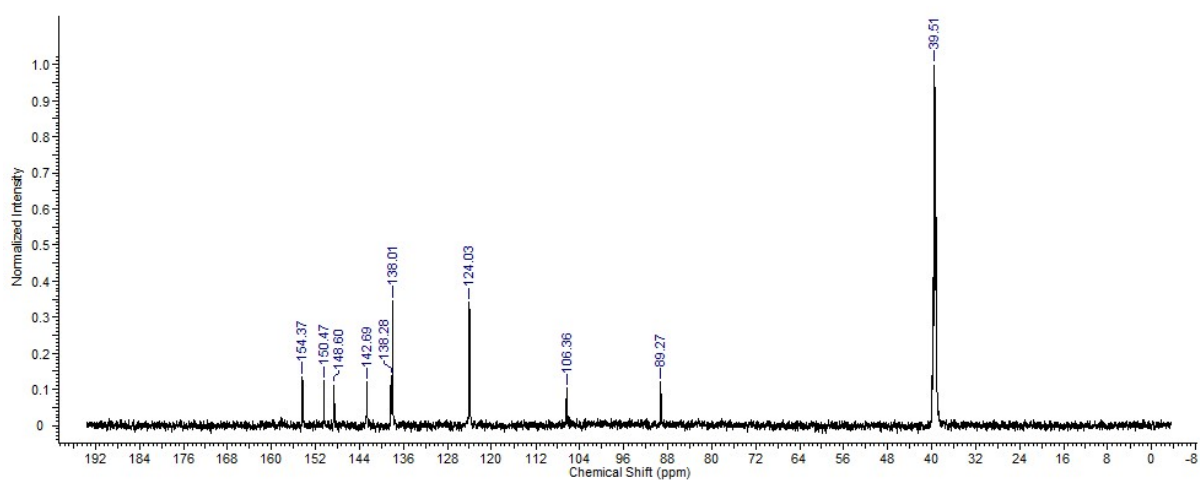
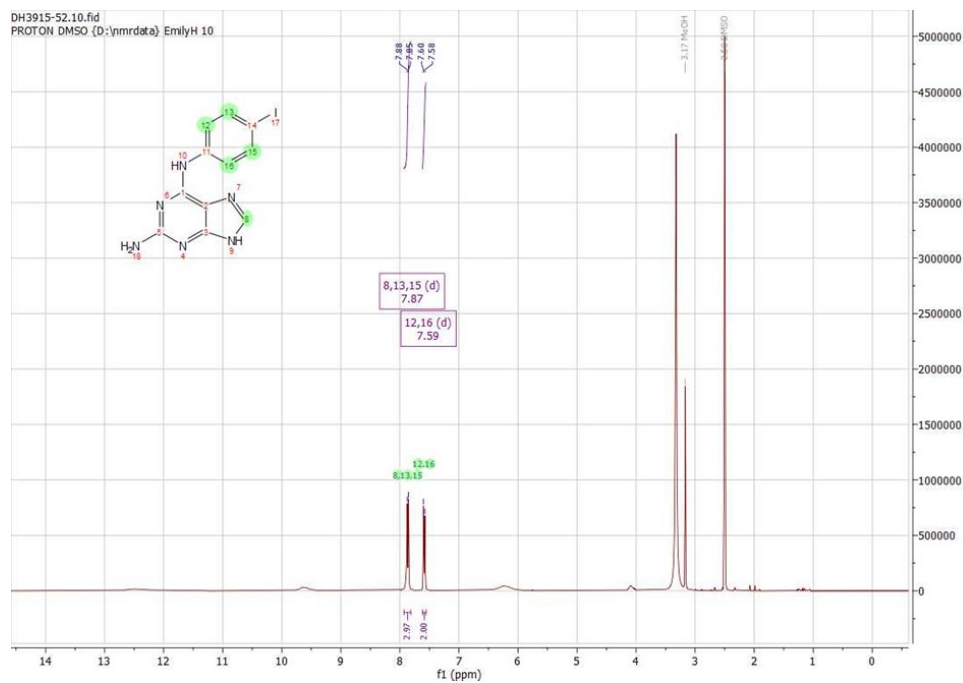


Method Info : ACE C8, 50x3mm, 3μ, 10-97% MeCN, 3min; 1ml/min, A: 0.1% TFA, B:MeCN.

```
Sample Info      : Walkup method: 'A1097-3'
                  Target:
```

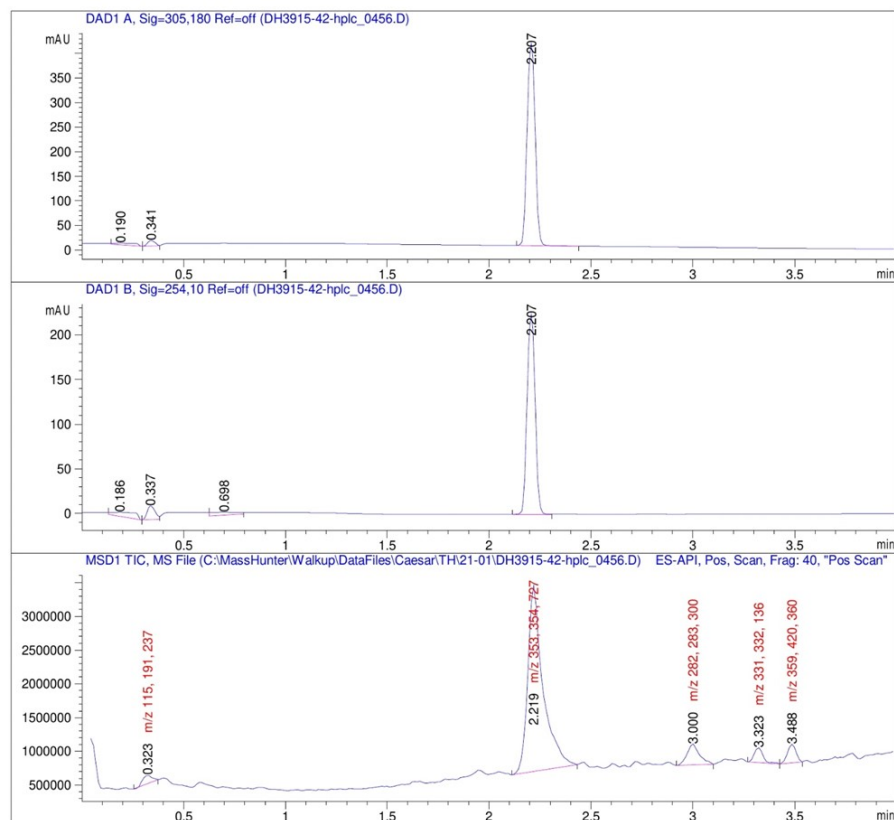


Compound (S45):

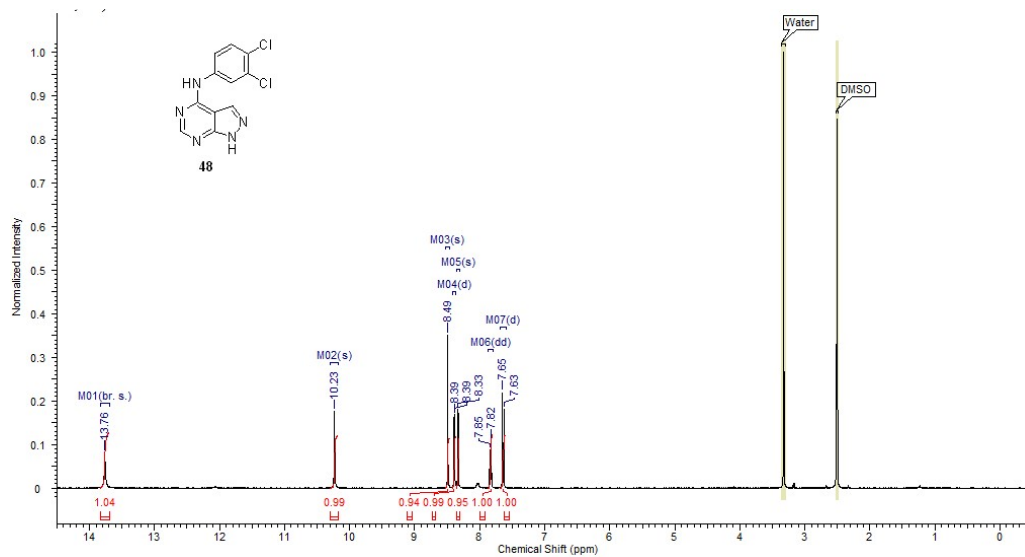


Method Info : ACE Phenyl, 50x3mm, 3 μ , 10-97% MeCN, 3min; 1ml/min, A: 0.1% TFA, B: MeCN.

Sample Info : Walkup method: 'Ph1097-3'
Target:

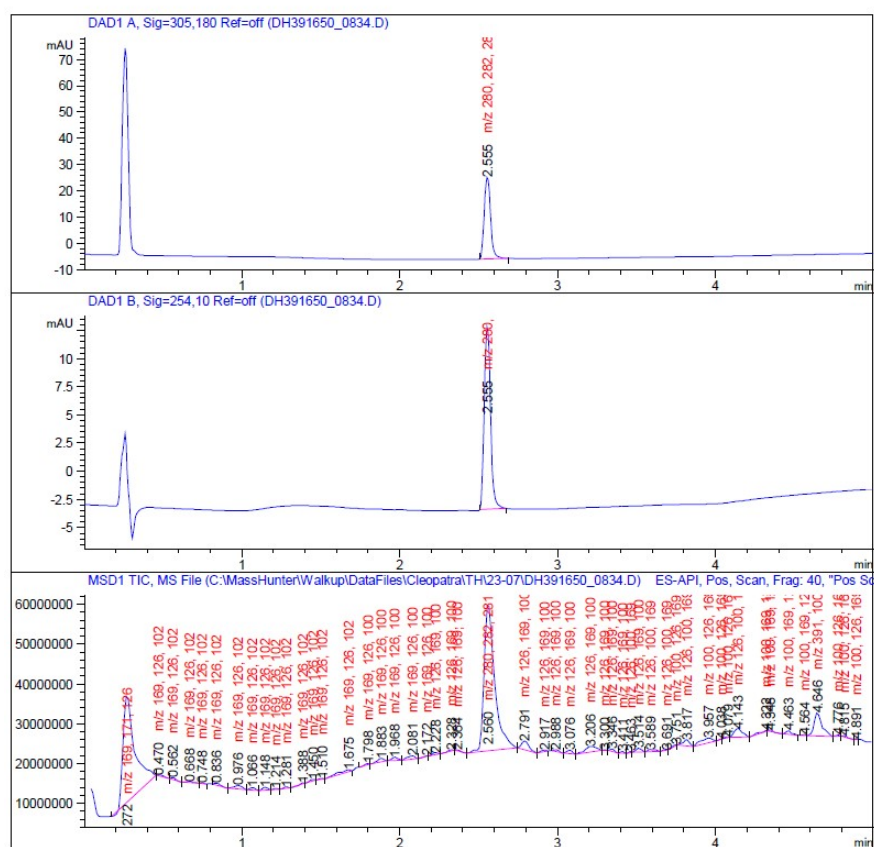


Compound (S46):

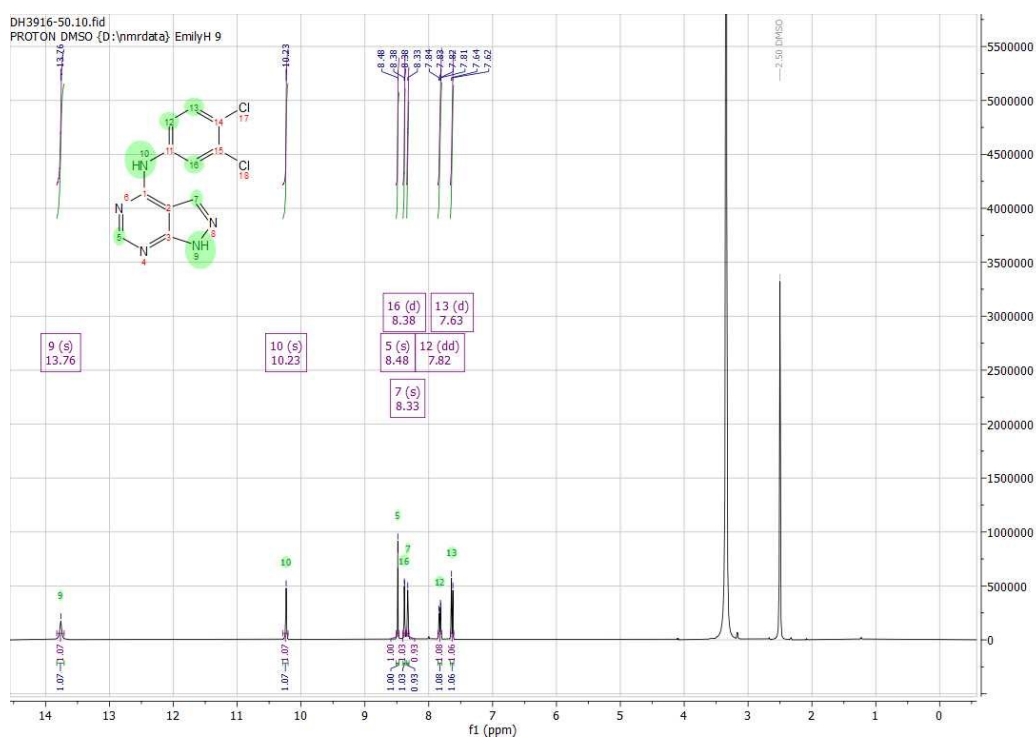


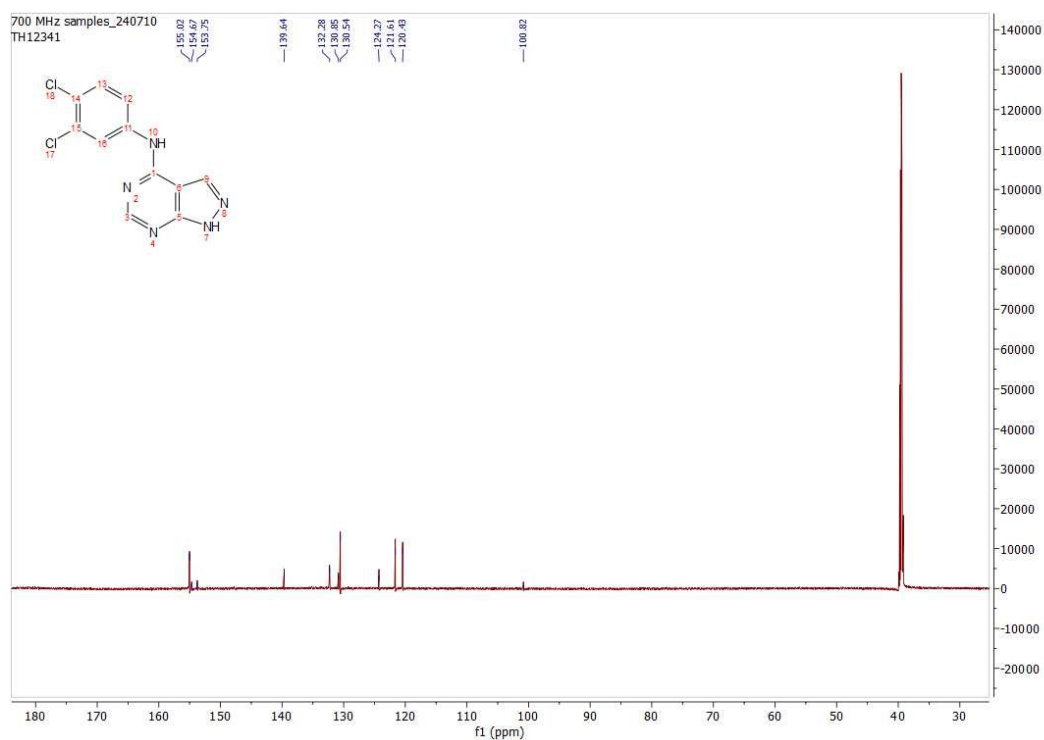
Method Info : X-bridge C18, 50x3.0 mm, 3.5u, 10-97% MeCN 3min, 1ml/min, B: MeCN C: NH4HCO3

```
Sample Info      : Walkup method: 'X1097-3'
                  Target:
```



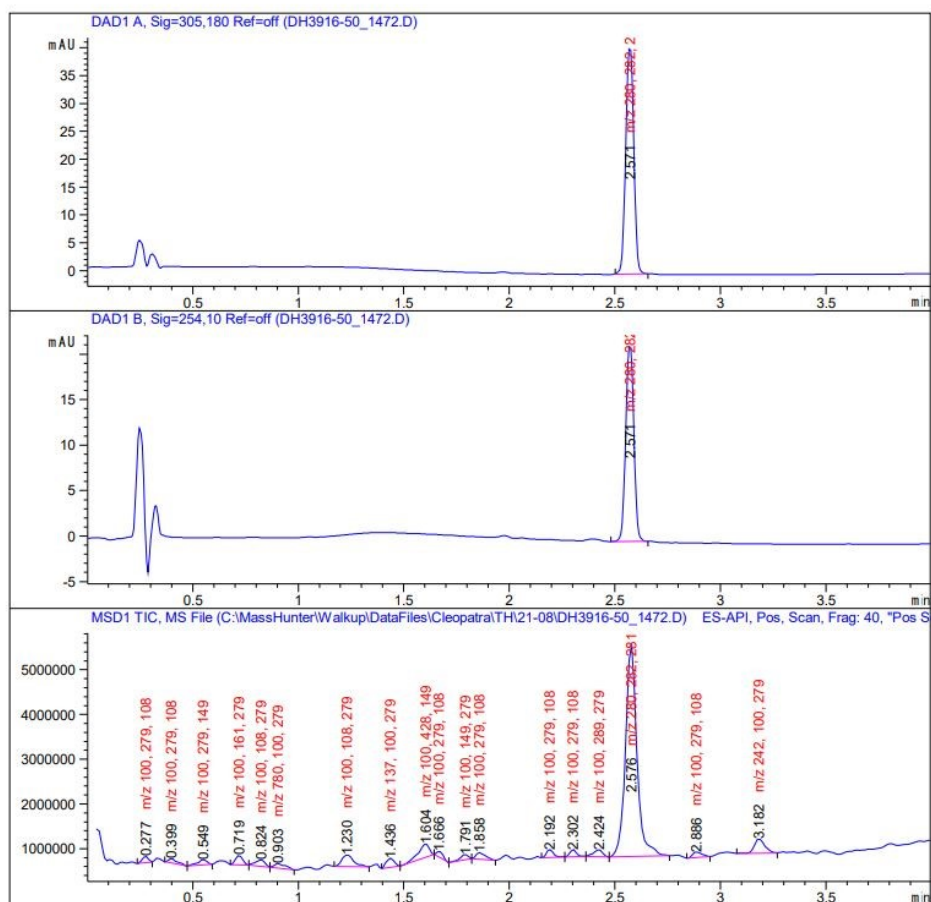
Compound (**S47**):



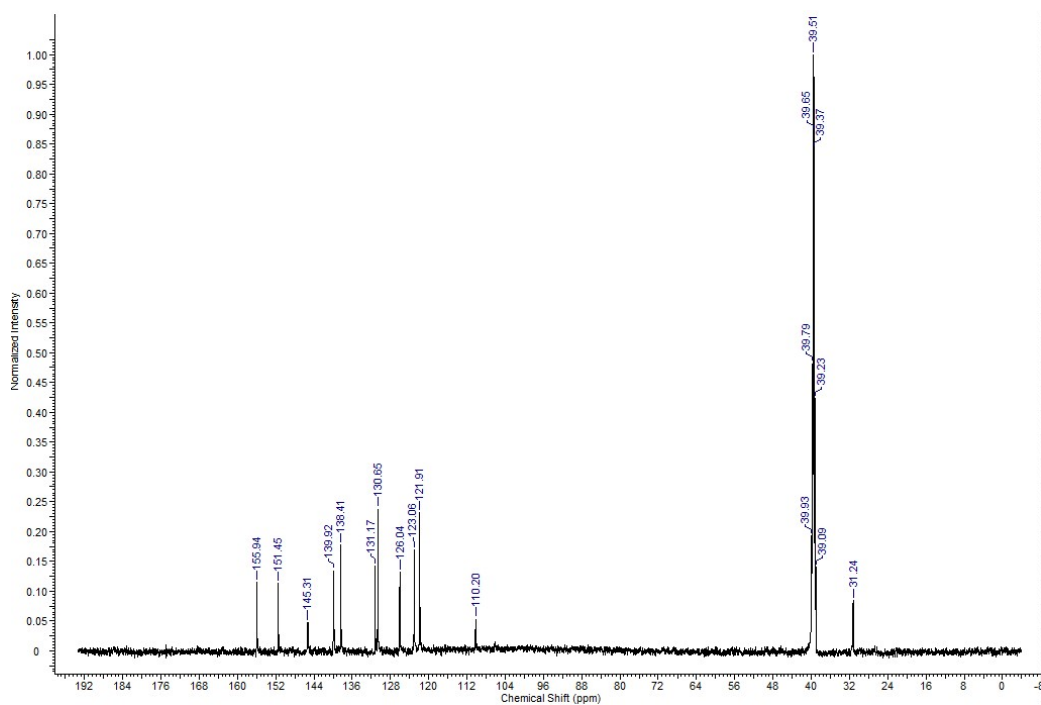
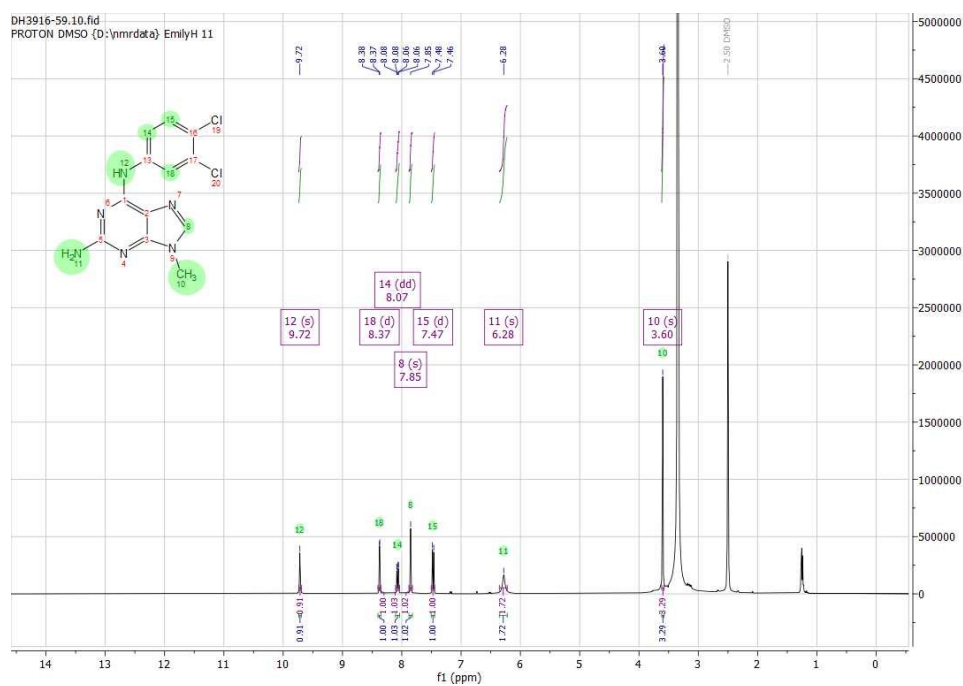


Method Info : X-bridge C18, 50x3.0 mm, 3.5u, 10-97% MeCN 3min, 1ml/min, B: MeCN C: NH4HCO3

Sample Info : Walkup method: 'X1097-3'
Target:



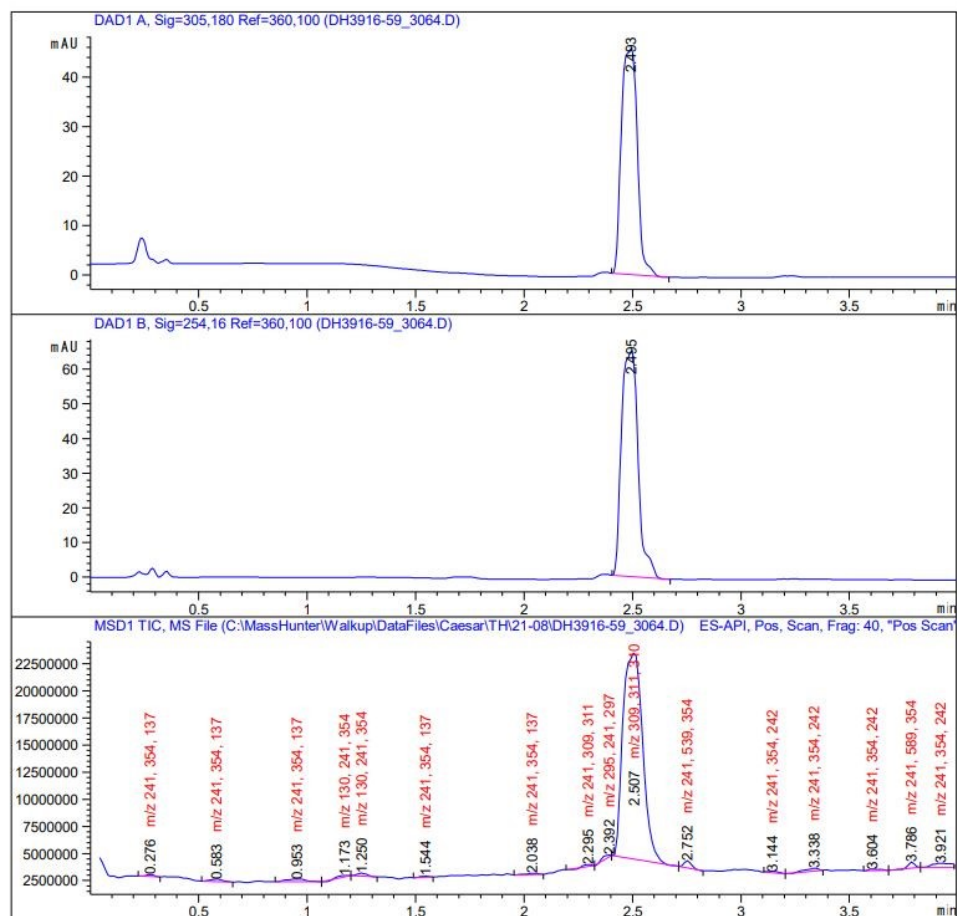
Compound (S49):



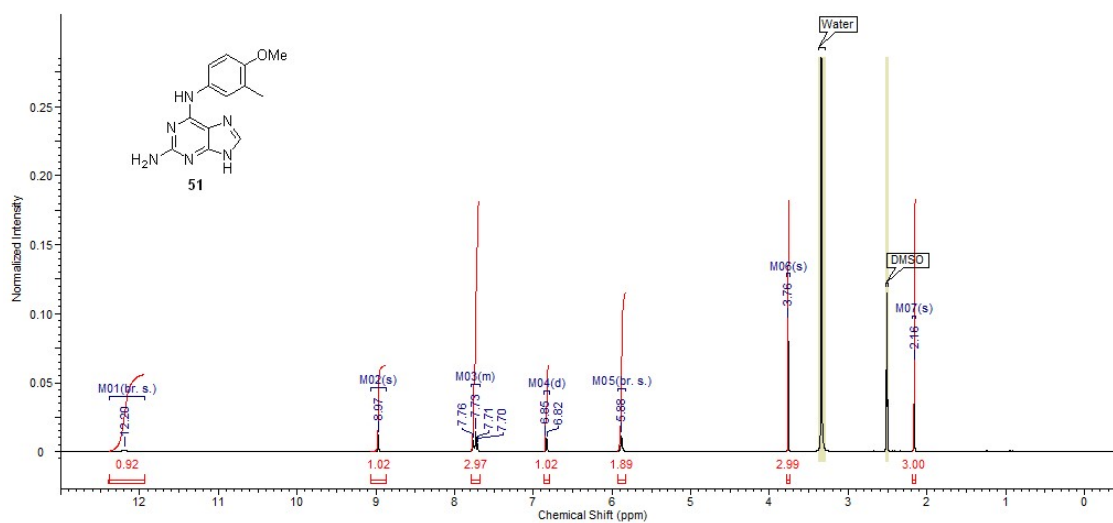
Method Info : X-bridge C18, 50x3.0 mm, 3.5u, 10-97% MeCN 3min,1ml/min, B: MeCN C: NH4HCO3

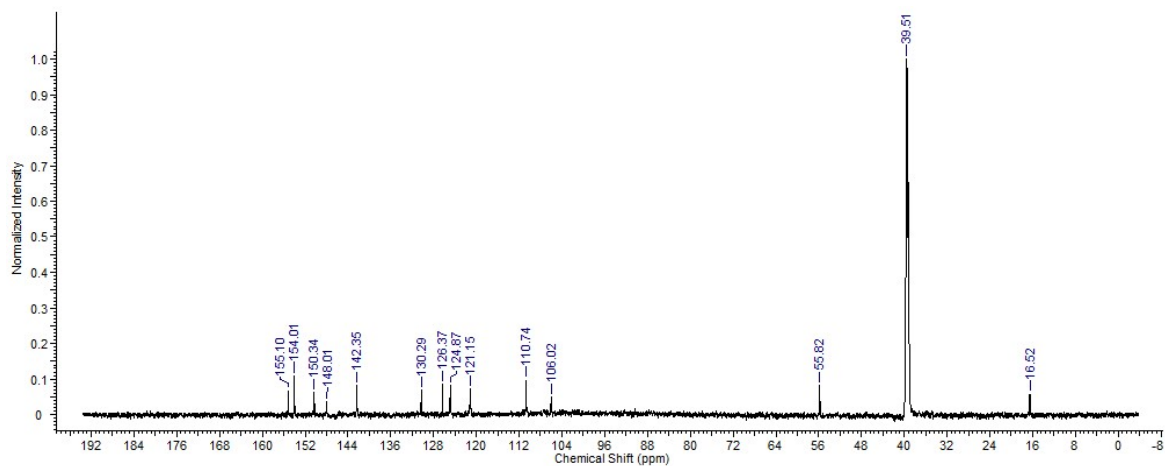
Sample Info : Walkup method: 'X1097-3'

Target:



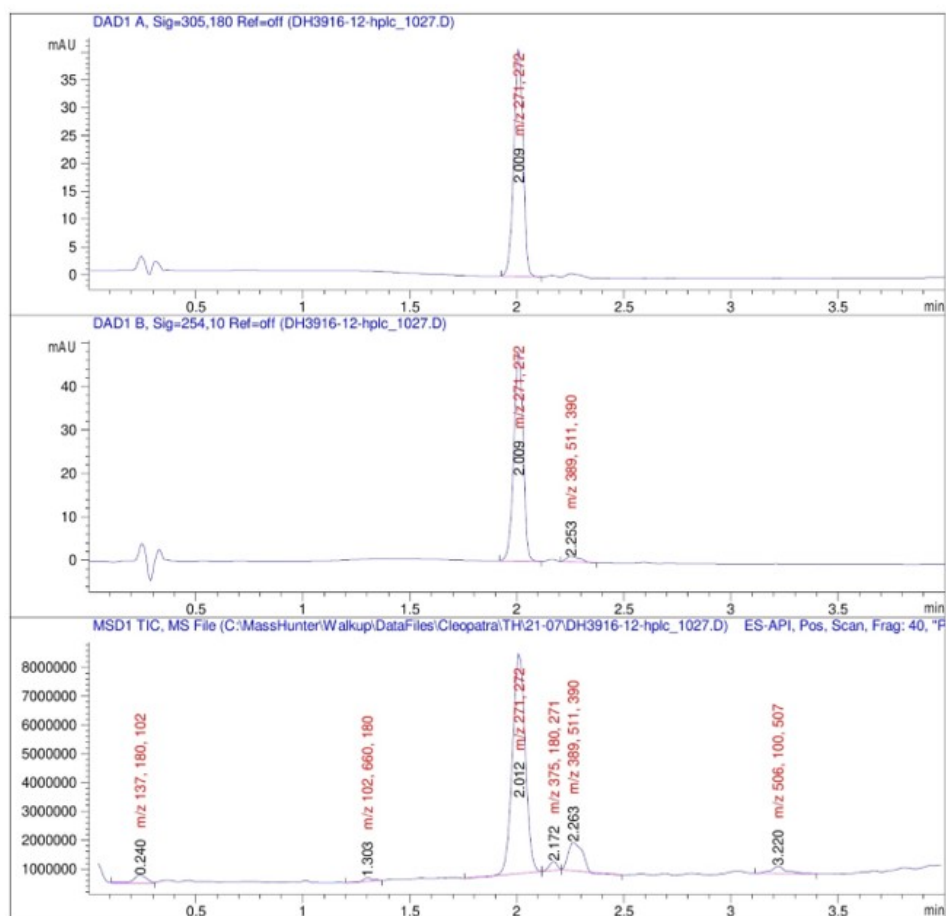
Compound (S50):



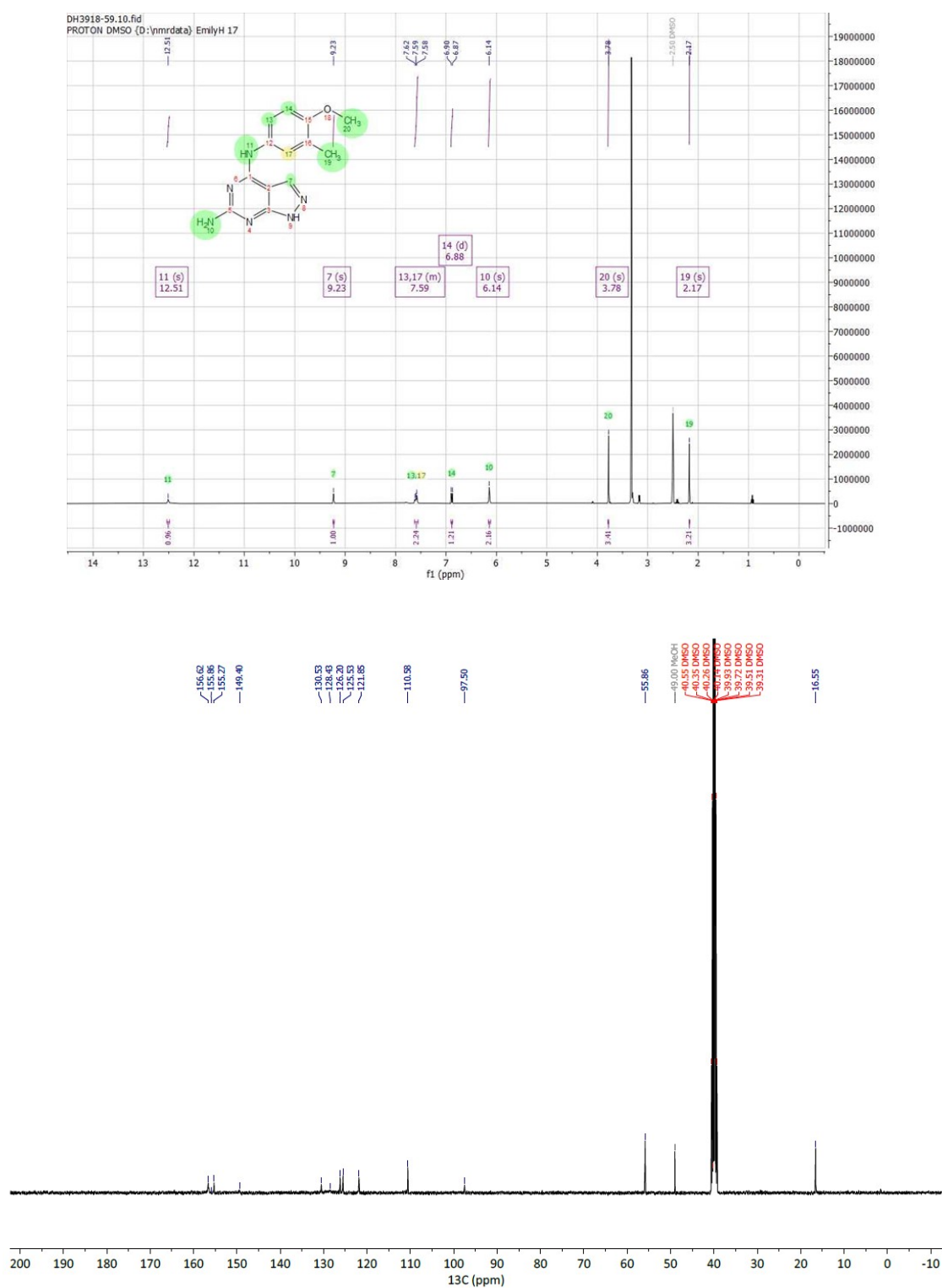


Method Info : X-bridge C18, 50x3.0 mm, 3.5u, 10-97% MeCN 3min,1mL/min, B: MeCN C: NH4HC03

Sample Info : Walkup method: 'X1097-3'
Target:

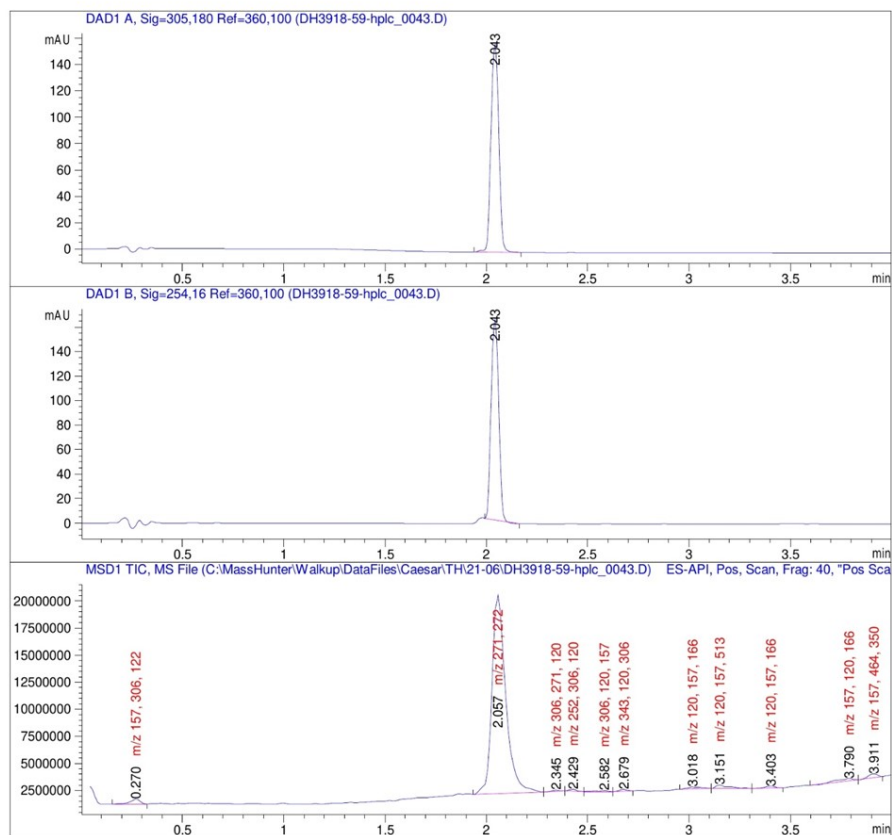


Compound (S51):

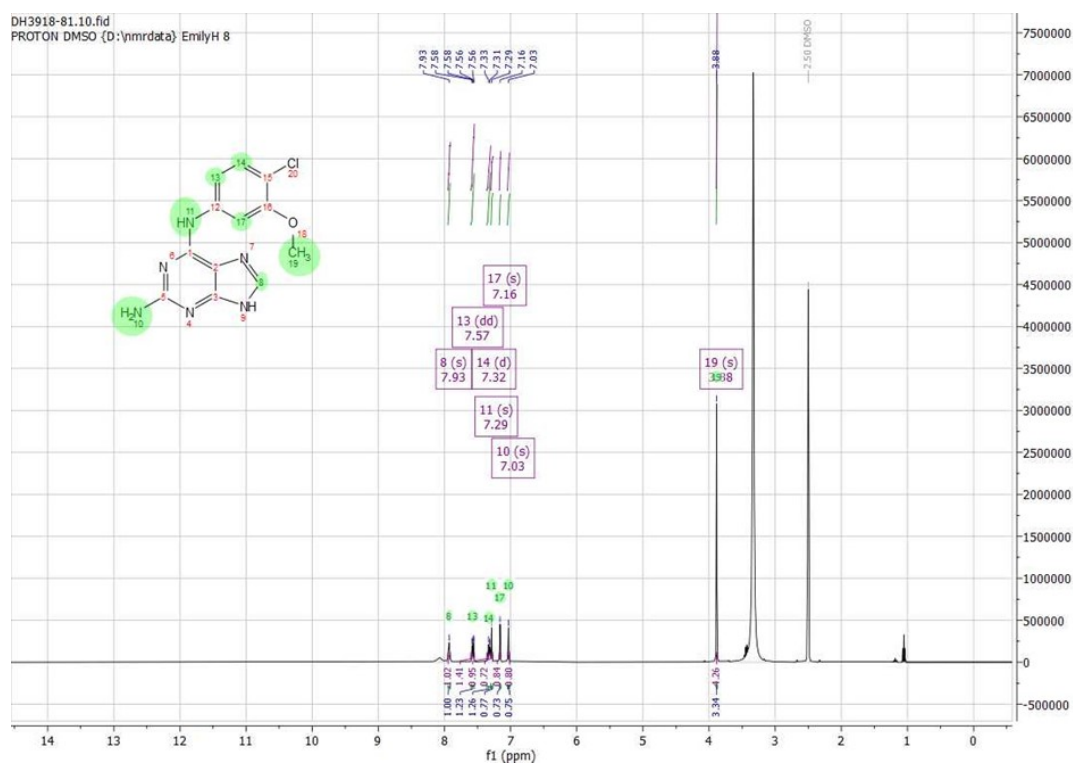


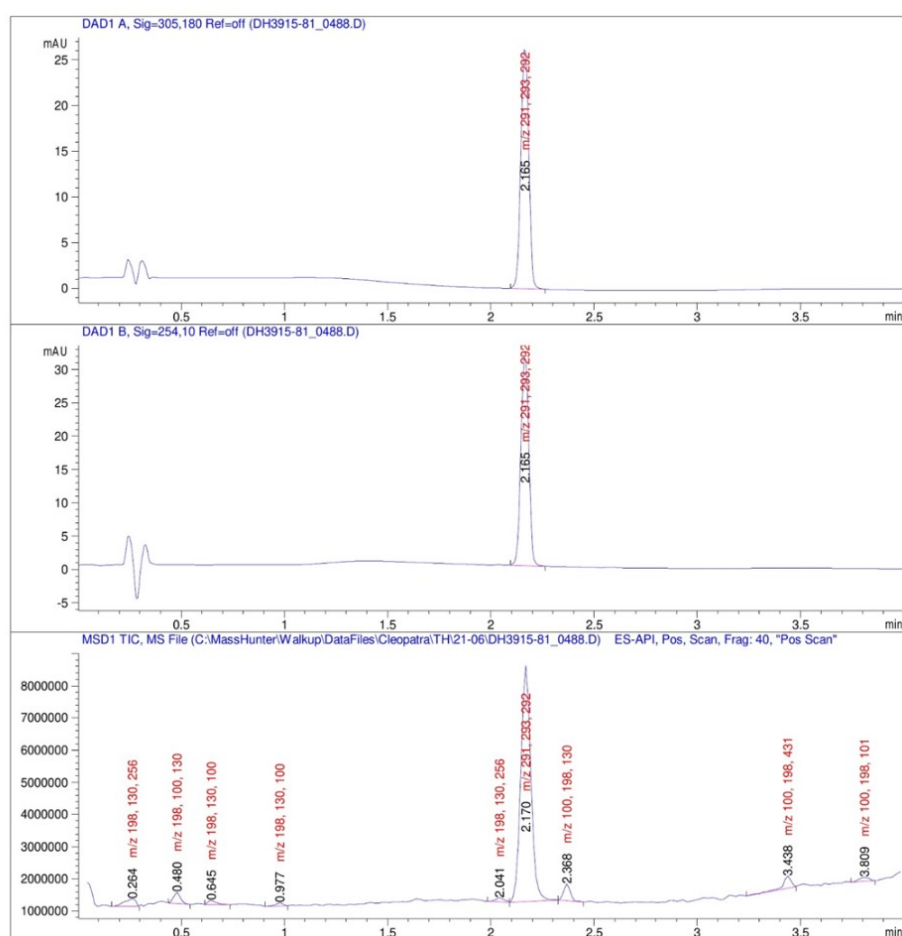
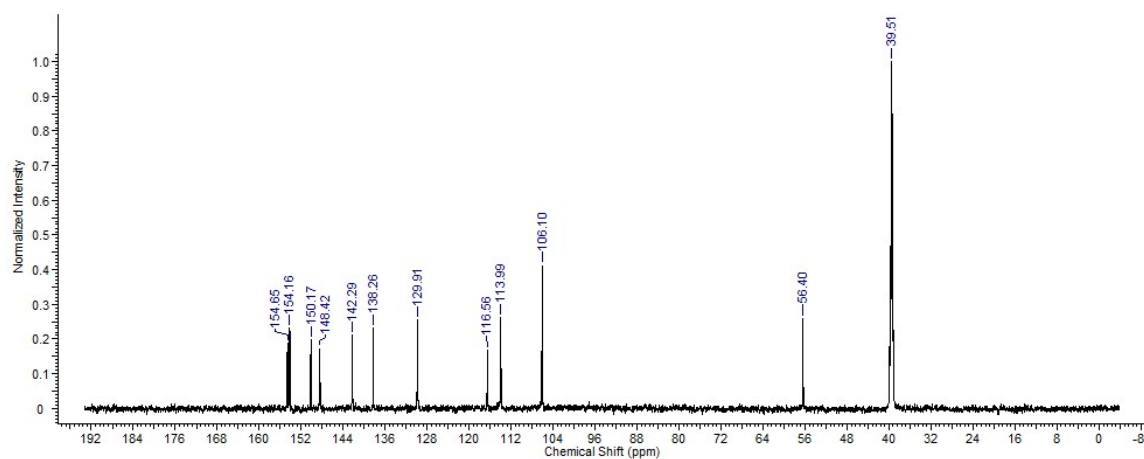
Method Info : X-bridge C18, 50x3.0 mm, 3.5u, 10-97% MeCN 3min,1ml/min, B: MeCN C: NH4HCO3

```
Sample Info      : Walkup method: 'X1097-3'
                  Target:
```

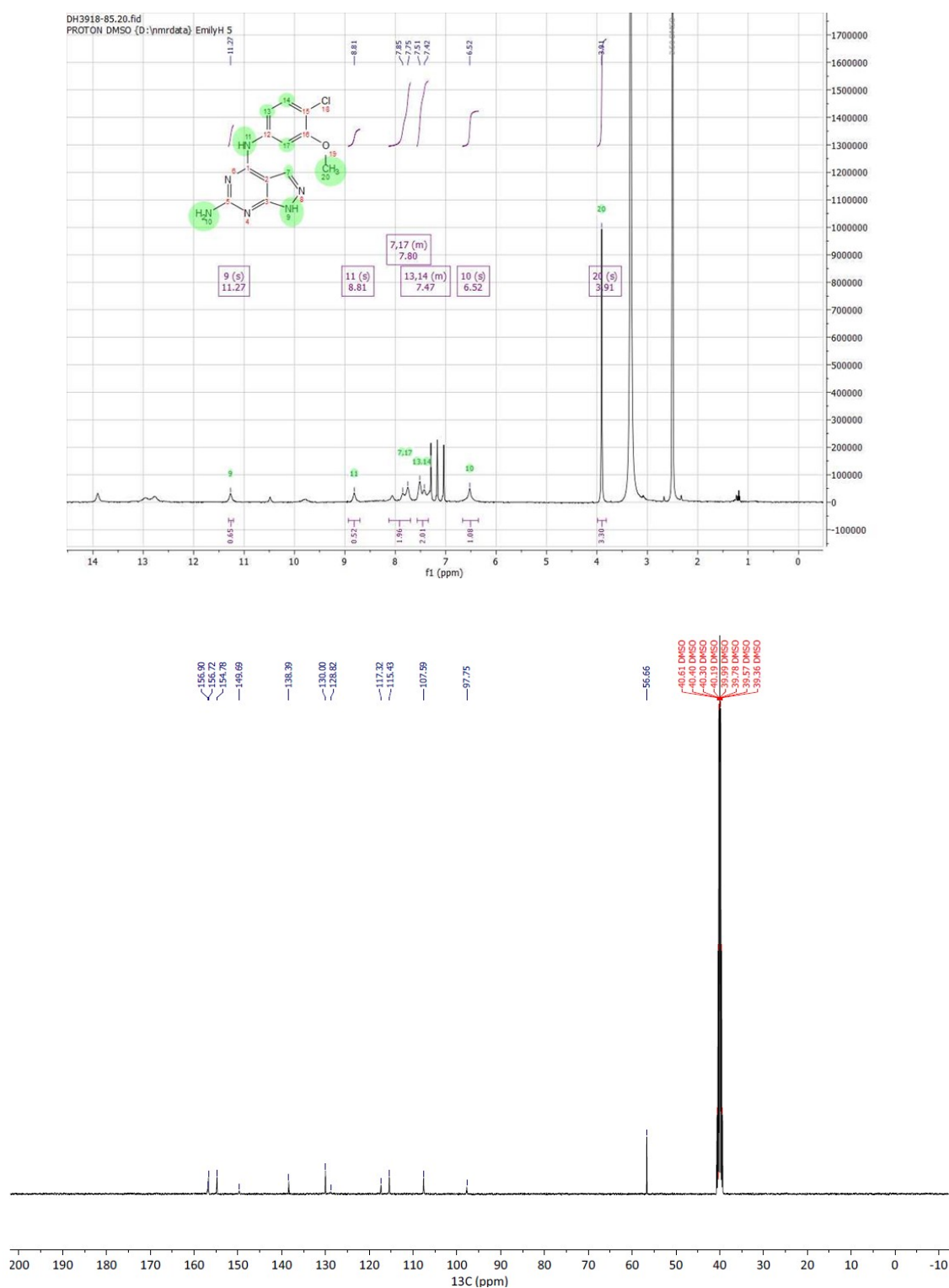


Compound (**S52**):



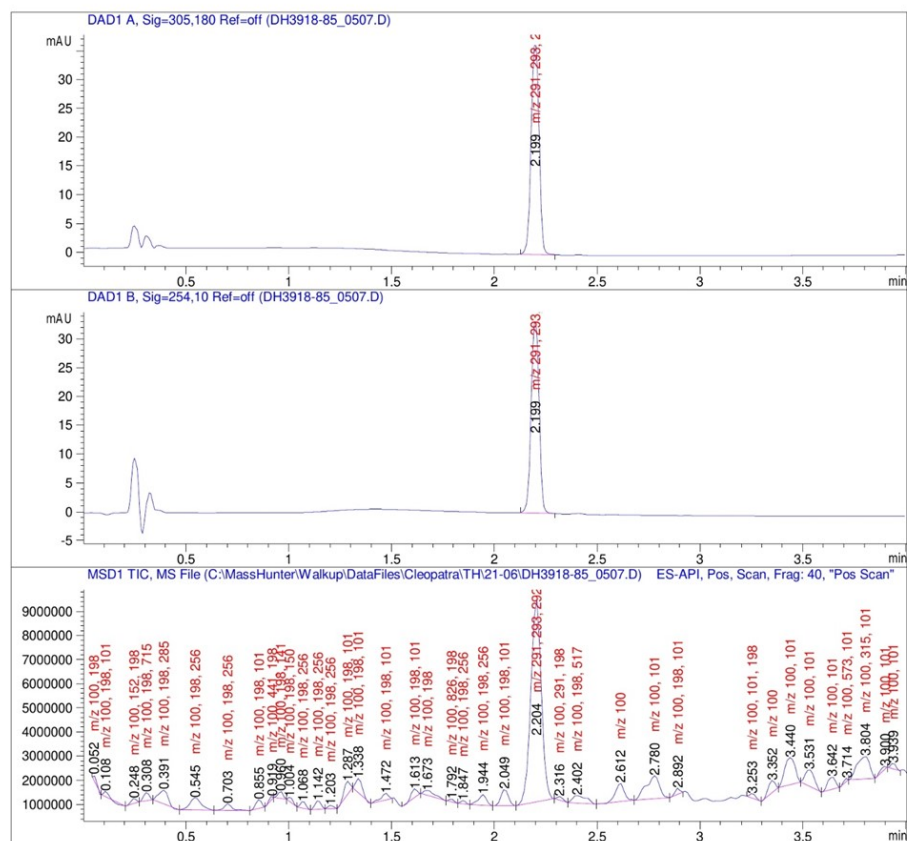


Compound (S53):

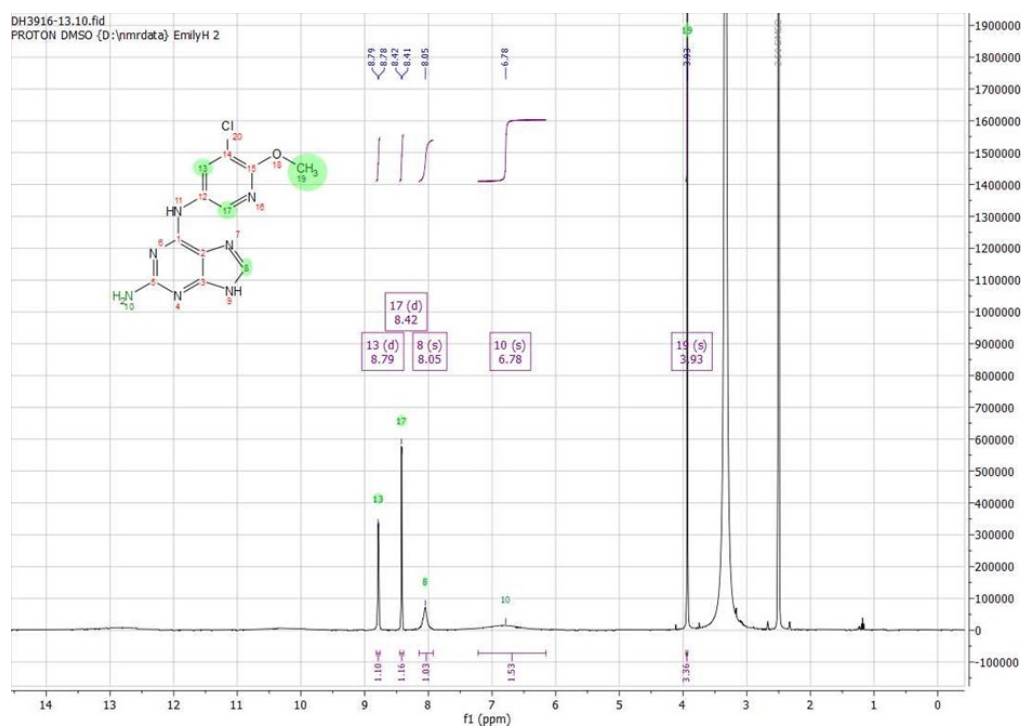


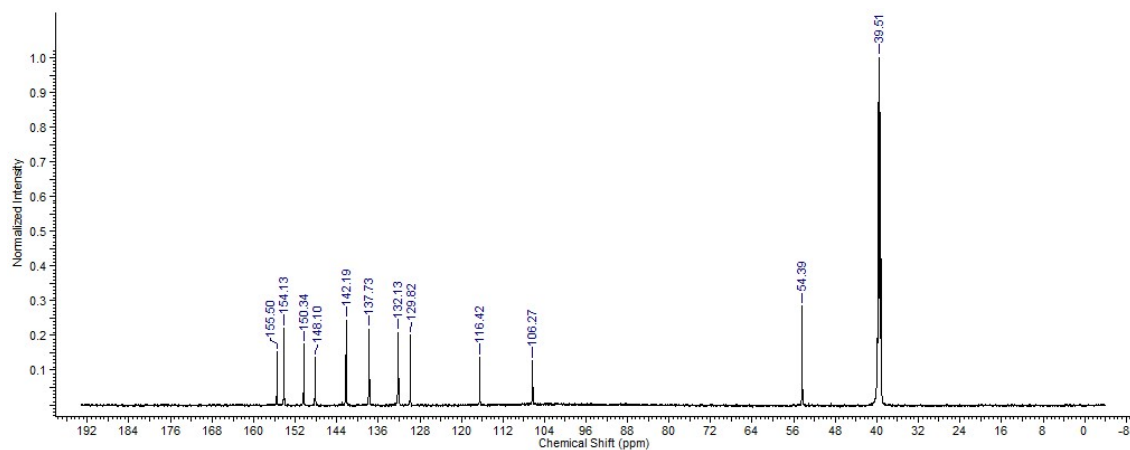
Method Info : X-bridge C18, 50x3.0 mm, 3.5u, 10-97% MeCN 3min, 1ml/min, B: MeCN C: NH4HC03

```
Sample Info      : Walkup method: 'X1097-3'
                  Target:
```



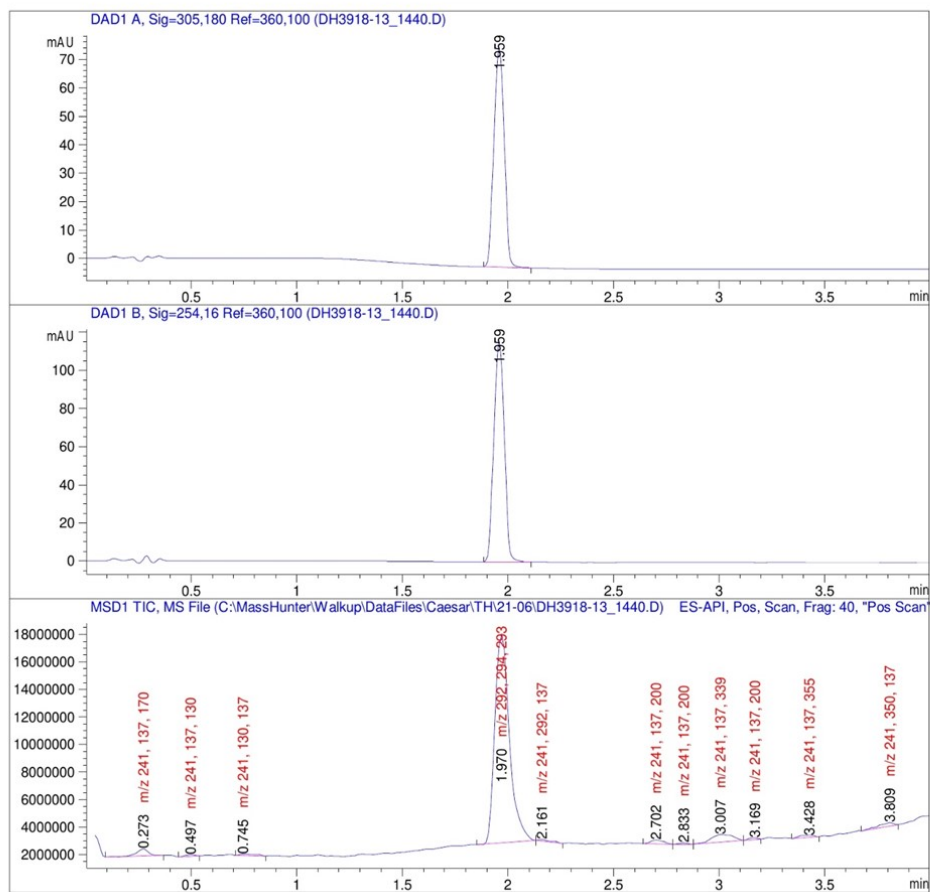
Compound (**S54**):



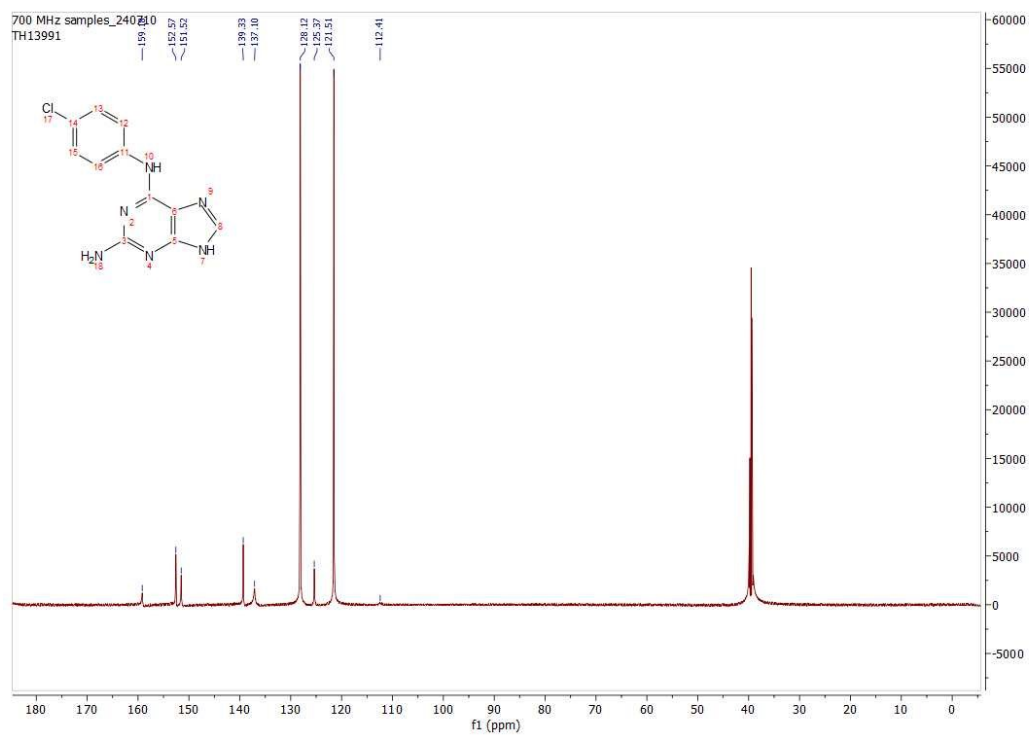
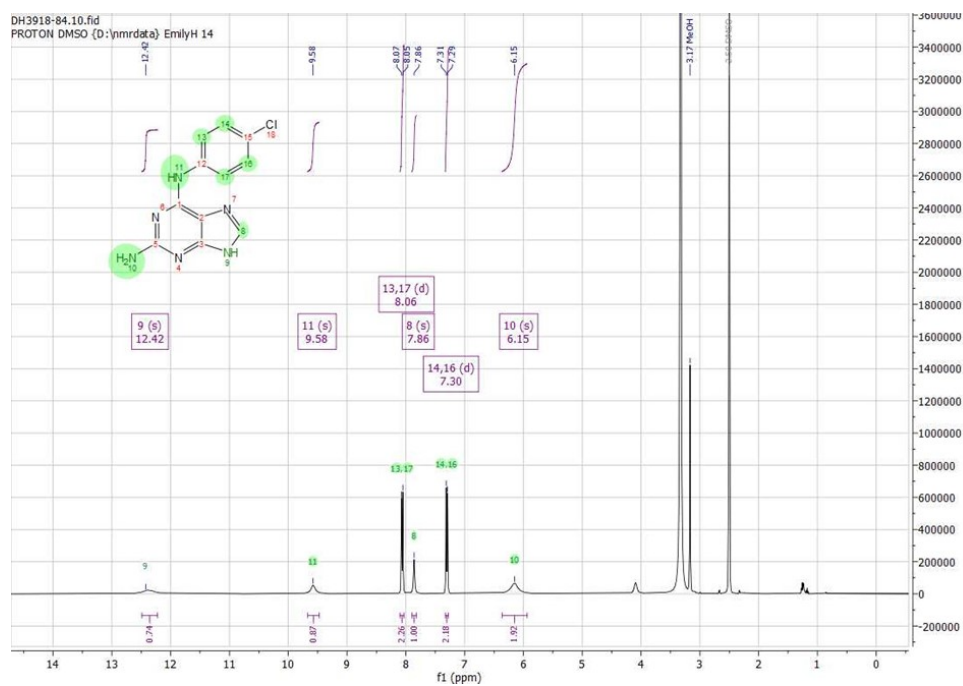


Method Info : X-bridge C18, 50x3.0 mm, 3.5u, 10-97% MeCN 3min,1mL/min, B: MeCN C: NH4HCO3

Sample Info : Walkup method: 'X1097-3'
Target:

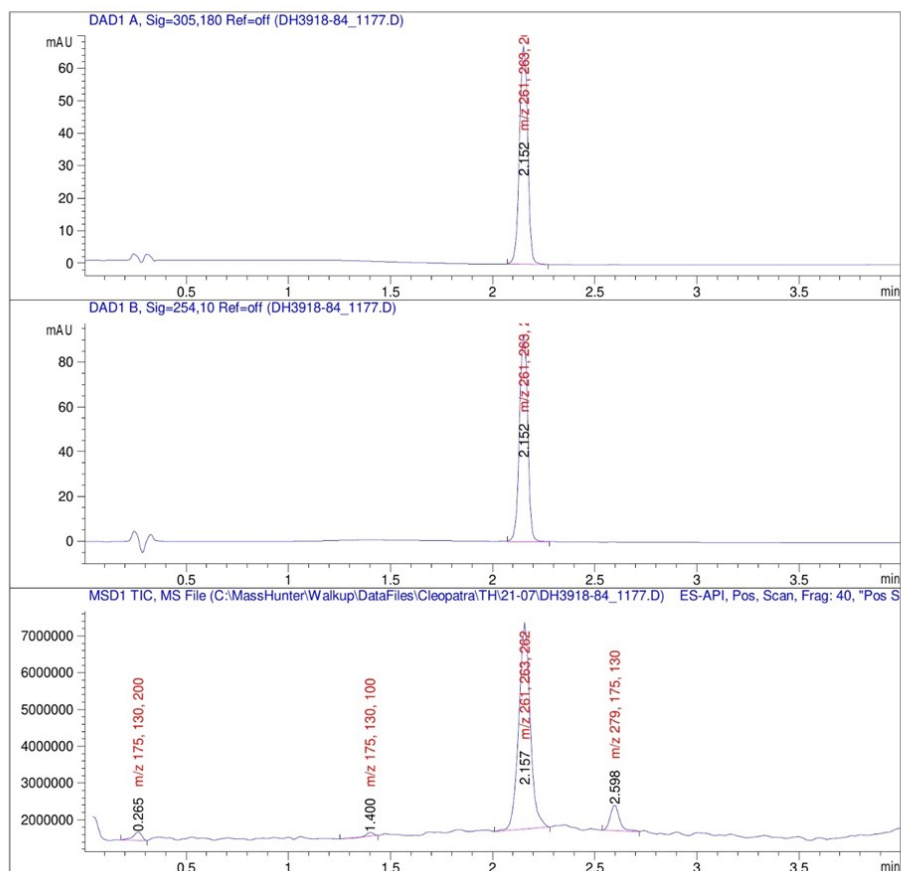


Compound (S55):

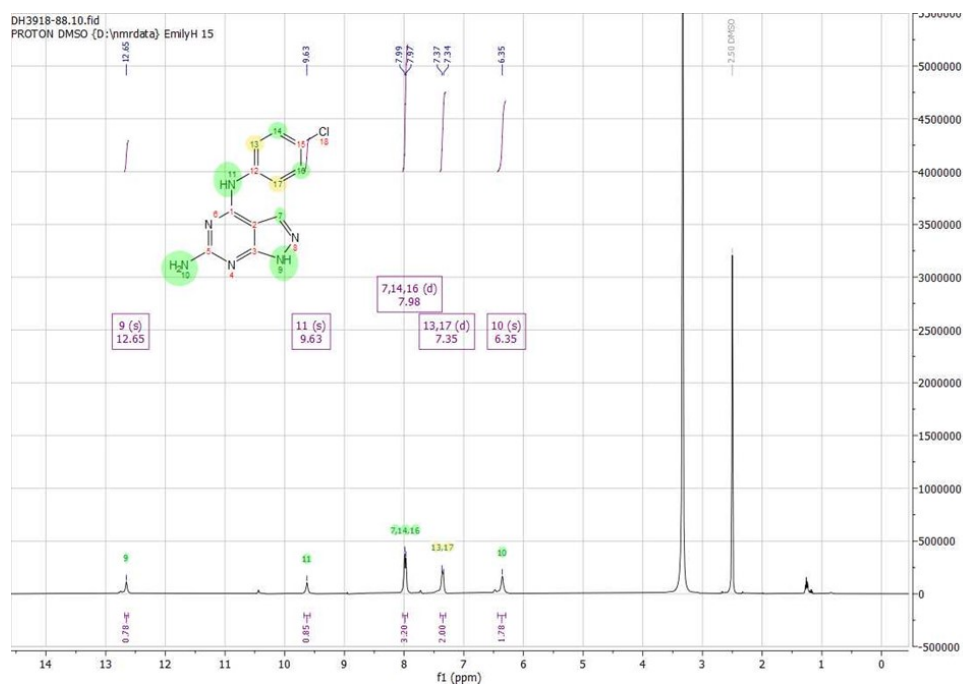


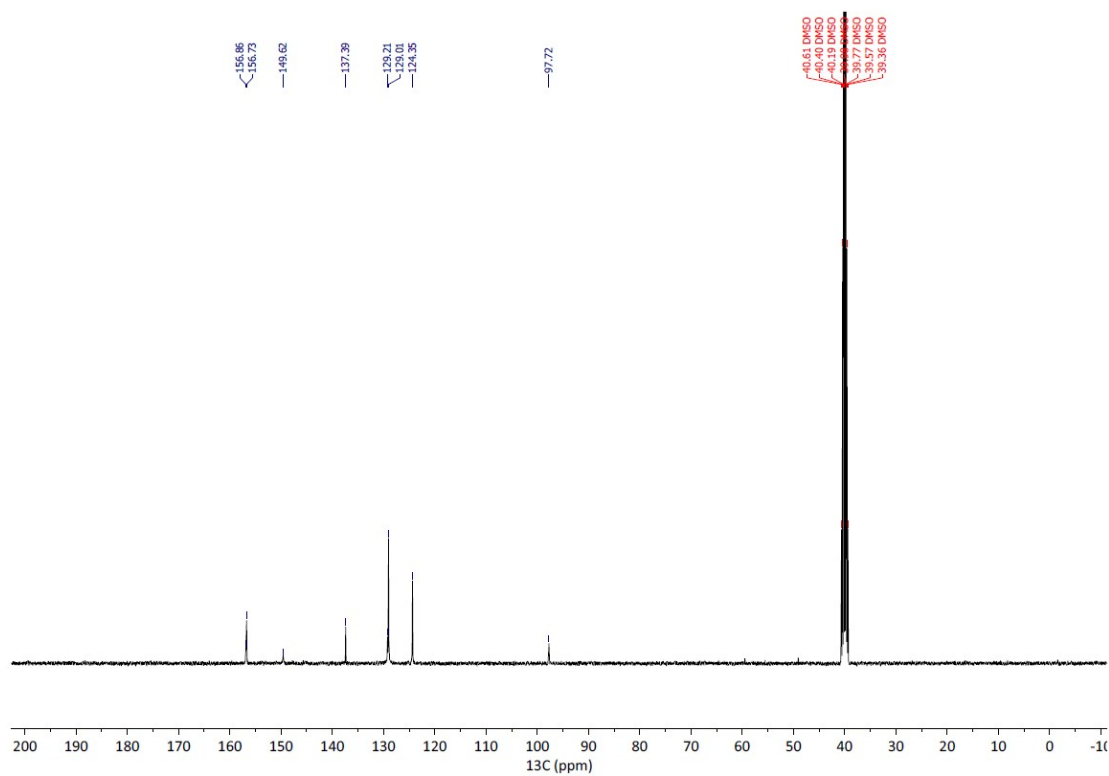
Method Info : X-bridge C18, 50x3.0 mm, 3.5u, 10-97% MeCN 3min,1ml/min, B: MeCN C: NH4HCO3

Sample Info : Walkup method: 'X1097-3'
Target:



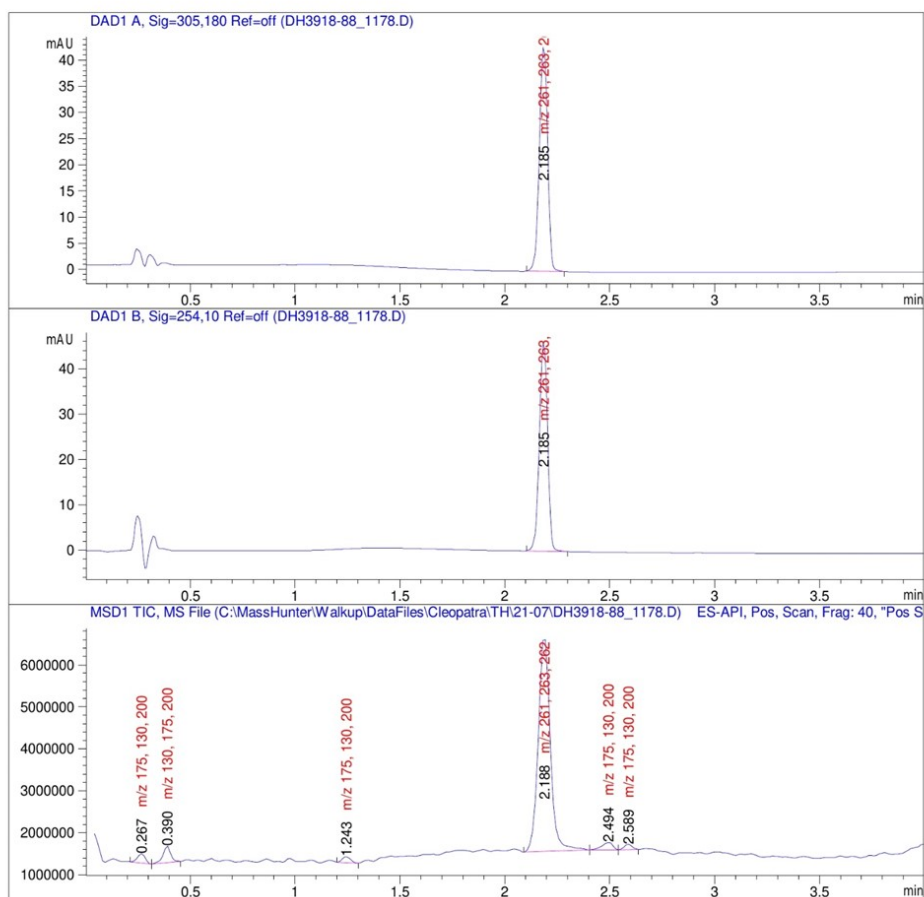
Compound (S56):





Method Info : X-bridge C18, 50x3.0 mm, 3.5u, 10-97% MeCN 3min,1mL/min, B: MeCN C: NH₄HCO₃

Sample Info : Walkup method: 'X1097-3'
Target:



Supplementary References:

- [1] T. Visnes, A. Cázares-Körner, W. Hao, O. Wallner, G. Masuyer, O. Loseva, O. Mortusewicz, E. Wiita, A. Sarno, A. Manoilov, J. Astorga-Wells, A.-S. Jemth, L. Pan, K. Sanjiv, S. Karsten, C. Gokturk, M. Grube, E. J. Homan, B. M. F. Hanna, C. B. J. Paulin, T. Pham, A. Rasti, U. W. Berglund, C. von Nicolai, C. Benitez-Buelga, T. Koolmeister, D. Ivanic, P. Iliev, M. Scobie, H. E. Krokan, P. Baranczewski, P. Artursson, M. Altun, A. J. Jensen, C. Kalderén, X. Ba, R. A. Zubarev, P. Stenmark, I. Boldogh, T. Helleday, *Science* **2018**, 362, 834–839.
- [2] M. Michel, C. Benítez-Buelga, P. A. Calvo, B. M. F. Hanna, O. Mortusewicz, G. Masuyer, J. Davies, O. Wallner, K. Sanjiv, J. J. Albers, S. Castañeda-Zegarra, A.-S. Jemth, T. Visnes, A. Sastre-Perona, A. N. Danda, E. J. Homan, K. Marimuthu, Z. Zhenjun, C. N. Chi, A. Sarno, E. Wiita, C. von Nicolai, A. J. Komor, V. Rajagopal, S. Müller, E. C. Hank, M. Varga, E. R. Scaletti, M. Pandey, S. Karsten, H. Haslene-Hox, S. Loevenich, P. Marttila, A. Rasti, K. Mamonov, F. Ortis, F. Schömberg, O. Loseva, J. Stewart, N. D’Arcy-Evans, T. Koolmeister, M. Henriksson, D. Michel, A. de Ory, L. Acero, O. Calvete, M. Scobie, C. Hertweck, I. Vilotijevic, C. Kalderén, A. Osorio, R. Perona, A. Stolz, P. Stenmark, U. W. Berglund, M. de Vega, T. Helleday, *Science* **2022**, 376, 1471–1476.
- [3] J. Carreras-Puigvert, M. Zitnik, A.-S. Jemth, M. Carter, J. E. Unterlass, B. Hallström, O. Loseva, Z. Karem, J. M. Calderón-Montaño, C. Lindskog, P.-H. Edqvist, D. J. Matuszewski, H. A. Blal, R. P. A. Berntsson, M. Häggblad, U. Martens, M. Studham, B. Lundgren, C. Wählby, E. L. L. Sonnhhammer, E. Lundberg, P. Stenmark, B. Zupan, T. Helleday, *Nature Communications* **2017**, 8, 1541.
- [4] B. L. Carroll, K. E. Zahn, J. P. Hanley, S. S. Wallace, J. A. Dragon, S. Doublie, *Nucleic Acids Research* **2021**, 49, 13165–13178.
- [5] J. M. Parkhurst, G. Winter, D. G. Waterman, L. Fuentes-Montero, R. J. Gildea, G. N. Murshudov, G. Evans, *J Appl Cryst* **2016**, 49, 1912–1921.
- [6] P. Evans, *Acta Crystallogr D Biol Crystallogr* **2006**, 62, 72–82.
- [7] Collaborative Computational Project, Number 4, *Acta Crystallogr D Biol Crystallogr* **1994**, 50, 760–763.
- [8] W. Kabsch, *Acta Crystallogr D Biol Crystallogr* **2010**, 66, 125–132.
- [9] A. J. McCoy, R. W. Grosse-Kunstleve, P. D. Adams, M. D. Winn, L. C. Storoni, R. J. Read, *J Appl Cryst* **2007**, 40, 658–674.
- [10] A. Vagin, A. Teplyakov, *Journal of Applied Crystallography* **1997**, 30, 1022–1025.
- [11] P. Emsley, B. Lohkamp, W. G. Scott, K. Cowtan, *Acta Crystallogr D Biol Crystallogr* **2010**, 66, 486–501.
- [12] G. N. Murshudov, P. Skubák, A. A. Lebedev, N. S. Pannu, R. A. Steiner, R. A. Nicholls, M. D. Winn, F. Long, A. A. Vagin, *Acta Cryst D* **2011**, 67, 355–367.
- [13] A. Krämer, C. G. Kurz, B.-T. Berger, I. E. Celik, A. Tjaden, F. A. Greco, S. Knapp, T. Hanke, *Eur J Med Chem* **2020**, 208, 112770.
- [14] O. Fedorov, F. H. Niesen, S. Knapp, *Methods Mol Biol* **2012**, 795, 109–118.
- [15] M. Michel, T. Visnes, E. J. Homan, B. Seashore-Ludlow, M. Hedenström, E. Wiita, K. Vallin, C. B. J. Paulin, J. Zhang, O. Wallner, M. Scobie, A. Schmidt, A. Jenmalm-Jensen, U. Warpman Berglund, T. Helleday, *ACS Omega* **2019**, 4, 11642–11656.
- [16] M. Michel, E. J. Homan, E. Wiita, K. Pedersen, I. Almlöf, A.-L. Gustavsson, T. Lundbäck, T. Helleday, U. Warpman Berglund, *Front. Chem.* **2020**, 8, DOI 10.3389/fchem.2020.00443.

- [17] S. M. Zhang, M. Desroses, A. Hagenkort, N. C. K. Valerie, D. Rehling, M. Carter, O. Wallner, T. Koolmeister, A. Throup, A.-S. Jemth, I. Almlöf, O. Loseva, T. Lundbäck, H. Axelsson, S. Regmi, A. Sarno, A. Krämer, L. Pudelko, L. Bräutigam, A. Rasti, M. Göttmann, E. Wiita, J. Kutzner, T. Schaller, C. Kalderén, A. Cázares-Körner, B. D. G. Page, R. Krimpenfort, S. Eshtad, M. Altun, S. G. Rudd, S. Knapp, M. Scobie, E. J. Homan, U. W. Berglund, P. Stenmark, T. Helleday, *Nat Chem Biol* **2020**, *16*, 1120–1128.
- [18] B. D. G. Page, N. C. K. Valerie, R. H. G. Wright, O. Wallner, R. Isaksson, M. Carter, S. G. Rudd, O. Loseva, A.-S. Jemth, I. Almlöf, J. Font-Mateu, S. Llona-Minguez, P. Baranczewski, F. Jeppsson, E. Homan, H. Almqvist, H. Axelsson, S. Regmi, A.-L. Gustavsson, T. Lundbäck, M. Scobie, K. Strömberg, P. Stenmark, M. Beato, T. Helleday, *Nature Communications* **2018**, *9*, 250.